

**Comparative characterization and structure-function analyses of the catalase-  
peroxidases of *Escherichia coli* and *Mycobacterium tuberculosis***

by

**Alexander Peter Hillar**

**A thesis**

**submitted to the Faculty of Graduate Studies**

**in partial fulfillment of the requirements for the degree of**

**DOCTOR OF PHILOSOPHY**

**Department of Microbiology**

**University of Manitoba**

**Winnipeg, Manitoba**

**© November, 1999**



**National Library  
of Canada**

**Acquisitions and  
Bibliographic Services**

**395 Wellington Street  
Ottawa ON K1A 0N4  
Canada**

**Bibliothèque nationale  
du Canada**

**Acquisitions et  
services bibliographiques**

**395, rue Wellington  
Ottawa ON K1A 0N4  
Canada**

*Your file Votre référence*

*Our file Notre référence*

**The author has granted a non-exclusive licence allowing the National Library of Canada to reproduce, loan, distribute or sell copies of this thesis in microform, paper or electronic formats.**

**The author retains ownership of the copyright in this thesis. Neither the thesis nor substantial extracts from it may be printed or otherwise reproduced without the author's permission.**

**L'auteur a accordé une licence non exclusive permettant à la Bibliothèque nationale du Canada de reproduire, prêter, distribuer ou vendre des copies de cette thèse sous la forme de microfiche/film, de reproduction sur papier ou sur format électronique.**

**L'auteur conserve la propriété du droit d'auteur qui protège cette thèse. Ni la thèse ni des extraits substantiels de celle-ci ne doivent être imprimés ou autrement reproduits sans son autorisation.**

0-612-51650-4

**Canada**

**THE UNIVERSITY OF MANITOBA**  
**FACULTY OF GRADUATE STUDIES**  
\*\*\*\*\*  
**COPYRIGHT PERMISSION PAGE**

**Comparative characterization and structure-function analyses of the catalase-peroxidases  
of *Escherichia coli* and *Mycobacterium tuberculosis***

**BY**

**Alexander Peter Hillar**

**A Thesis/Practicum submitted to the Faculty of Graduate Studies of The University  
of Manitoba in partial fulfillment of the requirements of the degree**

**of**

**Doctor of Philosophy**

**Alexander Peter Hillar©1999**

**Permission has been granted to the Library of The University of Manitoba to lend or sell  
copies of this thesis/practicum, to the National Library of Canada to microfilm this thesis and  
to lend or sell copies of the film, and to Dissertations Abstracts International to publish an  
abstract of this thesis/practicum.**

**The author reserves other publication rights, and neither this thesis/practicum nor extensive  
extracts from it may be printed or otherwise reproduced without the author's written  
permission.**

**For Larissa and my mother.**

## ABSTRACT

Both *Escherichia coli* and *Mycobacterium tuberculosis* produce catalase-peroxidases encoded by the *katG* structural gene as part of their cellular defence systems against oxidative stress. The *katG* gene products, KatG or HPI (Hydroperoxidase I ; an alternate name for the *E. coli* enzyme) have high catalase activities, as well as low level peroxidase activities utilizing organic electron donors. The catalase-peroxidase from *M. tuberculosis*, KatG or MtHPI, has been implicated in the mode of action of the antitubercular drug isoniazid (isonicotinic acid hydrazide, or INH), whereby MtHPI oxidizes INH to an electrophilic form capable of irreversibly binding enzymes involved in mycolic acid synthesis in the cells. Characterization of certain biochemical and structural properties of recombinant MtHPI and the homologous recombinant *E. coli* catalase-peroxidase (EchPI) was carried out, in order to determine whether differences in the enzymes could be partially responsible for lack of INH susceptibility in *E. coli* compared to *M. tuberculosis*. MtHPI and EchPI were similar with regard to subunit sizes and their intrinsic inhomogeneity estimated by SDS-PAGE analysis and mass spectrometry, affinity for cyanide as a heme ligand, and susceptibility to cyanide and azide as enzyme inhibitors. In contrast, MtHPI had higher peroxidase and lower catalase activity than EchPI, and was more proficient at both INH oxidation ( $k_{\text{cat}}$  of  $8.7 \times 10^4 \text{ s}^{-1}$  compared to  $2.4 \times 10^4 \text{ s}^{-1}$  for EchPI) and INH binding ( $K_d$  of  $17 \mu\text{M}$  INH compared to  $130 \mu\text{M}$  for EchPI), determined using spectrophotometric techniques. The intracellular locale of EchPI in *E. coli* was also determined as a second major part of this study. Assays of catalase and corroborating enzymatic activities in fractions prepared via spheroplasting procedures, as well as in situ immunogold staining followed by microscopic analysis, confirmed that EchPI occurs predominantly in the cytoplasm of *E. coli* cells, contrary to a previous report of EchPI being a periplasmic enzyme. A structure-function study of EchPI via site-directed mutagenesis was carried out as a third principal part of this study, focusing mainly on certain amino acid

residues in the putative active site of the enzyme. Changing the His106, Arg102, Trp105, and His267 residues in EcHPI resulted in significant changes in enzymatic activities as well as changes in absorption spectra, heme content, susceptibility to inhibitors, and cyanide binding in the mutant variant enzymes. Changes to His106 and His267 resulted in drastically decreased catalatic and peroxidatic activities, providing evidence that these residues are critical to enzyme catalysis. Changes to Arg102 resulted in decreased catalatic and peroxidatic activities, however the changes in activity were not as drastic as those for the His106 and His267 variants, suggesting that Arg102 is important but not critical to enzyme catalysis. Changes to Trp105 resulted in catalatic activity decreased by three orders of magnitude, but either an increase (Trp105Phe) or no change (Trp105Leu) in the peroxidatic activity of these mutant variants. Investigation of the Trp105 mutant variants also showed that both are capable of forming a spectral species similar to the compound I intermediate of plant peroxidases, and that this species is rapidly inactivated, in the presence of hydrogen peroxide. A novel catalatic reaction mechanism is proposed for catalase-peroxidases based on active site models of peroxidases and the information derived for the modulation of activities that occurs for the Trp105 mutant variants.

## ACKNOWLEDGEMENTS

I wish to acknowledge Dr. Peter C. Loewen, my supervisor and colleague, for his guidance as well as his financial and personal support during my studies. His breadth of expertise, as well as his dedication to his chosen profession, has made my work under his tutelage exceptionally fulfilling. I could not hope to have found a more capable fellow researcher and friend. I also wish to acknowledge Mr. Jacek Switala, our technician, for the countless times I have called upon his excellent technical expertise. My thanks are extended to the members of my advisory committee, Drs. E. Worobec and I. Suzuki of the department of Microbiology, and Dr. F. Hruska of the department of Chemistry, for their useful suggestions and interest in my research. I also wish to thank Dr. L. Van Caesele and Ms. L. Burton of the department of Botany, for carrying out the immunogold staining procedures forming part of this thesis, as well as Dr. I. Chernushevich and Dr. W. Ens, department of Physics for the electrospray ionization time-of-flight mass spectrometry data that also appears in this thesis. I fondly thank all my fellow graduate students, including those having already completed their course of study during my stay in the department of Microbiology, for all their input, friendship, and occasional wackiness. This salute is also extended to the myriad of project and summer students I have met and interacted with. My thanks and best wishes go out to all the faculty members and support staff in the department of Microbiology as well, for all their encouragement, assistance, and advice over these past five years. Finally, I wish to give my special thanks to my parents, who have always been there for me, and to my dearest Larissa, for the patience, understanding, and support she has continually provided me in striving to reach my goals.

## TABLE OF CONTENTS

	<b>Page</b>
<b>ABSTRACT</b> .....	iii
<b>ACKNOWLEDGEMENTS</b> .....	v
<b>TABLE OF CONTENTS</b> .....	vi
<b>LIST OF FIGURES</b> .....	ix
<b>LIST OF TABLES</b> .....	xii
<b>LIST OF ABBREVIATIONS</b> .....	xiii
<b>PUBLICATIONS ARISING FROM THE THESIS</b> .....	xv
<b>1. GENERAL INTRODUCTION</b> .....	1
1.1. Oxygen toxicity and oxidative stress.....	1
1.2. Removal of reactive oxygen species.....	3
1.3. Catalases and peroxidases.....	6
1.3.1. Properties of catalases.....	6
1.3.2. Properties of peroxidases.....	9
1.4. Catalase-peroxidases.....	13
1.5. Catalases of <i>Escherichia coli</i> and <i>Mycobacterium tuberculosis</i> .....	14
1.5.1. Catalase enzymes of <i>Escherichia coli</i> .....	14
1.5.1a. Catalase hydroperoxidase II of <i>E. coli</i> .....	14
1.5.1b. Catalase-peroxidase hydroperoxidase I of <i>E. coli</i> .....	15
1.5.1c. Catalase-peroxidase KatG (MtHPI) of <i>Mycobacterium tuberculosis</i> ...	16
1.6. Role of MtHPI in cytotoxicity of isoniazid.....	18
1.7. Object of the thesis.....	22
<b>2. MATERIALS AND METHODS</b> .....	25
2.1. <i>Escherichia coli</i> strains, plasmids and bacteriophage.....	25
2.2. Biochemicals and common reagents.....	28
2.3. Media, growth conditions and storage of cultures.....	28
2.4. DNA manipulation.....	29
2.4.1. Preparation of synthetic oligonucleotides.....	29
2.4.2. DNA isolation and purification.....	29
2.4.3. Restriction nuclease digestion.....	30
2.4.4. Agarose gel electrophoresis.....	31
2.4.5. Ligation.....	31
2.4.6. Transformation.....	32
2.4.7. DNA sequencing.....	32

## Table of contents (continued)

2.4.8. In vitro mutagenesis strategy.....	33
2.5. Purification of HPI catalase-peroxidases.....	40
2.6. Polyacrylamide gel electrophoresis of proteins and staining.....	42
2.7. Enzymatic assays and protein quantitation.....	44
2.8. Absorption spectrophotometry.....	45
2.9. Spheroplasting procedures and fraction analysis.....	46
2.9.1. Spheroplasting procedures.....	46
2.9.2. Enzymatic assays of the spheroplasting fractions.....	46
2.10. In situ immunogold staining.....	47
2.11. Effects of inhibitors.....	48
2.12. Determination of sulfhydryl groups.....	48
2.13. Electrospray ionization time-of-flight mass spectrometry.....	48
<b>3. RESULTS.....</b>	<b>50</b>
3.1. Purification of MtHPI and comparison with EcHPI.....	50
3.1.1. Introduction.....	50
3.1.2. Purification of MtHPI.....	50
3.1.3. Physical characterization of EcHPI and MtHPI.....	52
3.1.3a. Optical absorption spectrophotometry of the HPI enzymes.....	52
3.1.3b. Polyacrylamide gel electrophoresis of the HPI enzymes.....	52
3.1.3c. Mass spectrometry of the HPI enzymes.....	56
3.1.4. Biochemical characterization of EcHPI and MtHPI.....	62
3.1.4a. Specific activities and kinetics of the HPI enzymes.....	62
3.1.4b. Effects of KCN and NaN <sub>3</sub> as enzyme inhibitors.....	62
3.1.4c. Effect of KCN on HPI enzymes as a heme ligand.....	67
3.1.4d. Determination of free sulfhydryl groups in the HPI enzymes.....	67
3.2. Isoniazid oxidation catalyzed by EcHPI and MtHPI.....	74
3.2.1. Introduction.....	74
3.2.2. Peroxidase staining of non-denaturing polyacrylamide gels.....	75
3.2.3. Isoniazid / H <sub>2</sub> O <sub>2</sub> dependent generation of free radicals by HRP.....	77
3.2.4. Comparison of isoniazid/ H <sub>2</sub> O <sub>2</sub> dependent generation of free radicals by HRP, EcHPI, and MtHPI.....	80
3.2.5. Spectral evaluation of EcHPI and MtHPI interaction with isoniazid.....	82
3.3. Intracellular location of EcHPI.....	87
3.3.1. Introduction.....	87
3.3.2. Catalase levels in spheroplast fractions.....	87
3.3.3. In situ localization of EcHPI by immunogold staining.....	93
3.4. Construction and characterization of EcHPI mutants.....	93
3.4.1. Introduction.....	93
3.4.2. Structural characterization of EcHPI mutants.....	98
3.4.3. Biochemical characterization of EcHPI mutants.....	104
3.4.3a. Specific activities and kinetics of EcHPI mutants.....	104

## Table of Contents (continued)

3.4.3b. Effect of inhibitors on catalytic activities of EcHPI mutants.....	106
3.4.3c. Effect of KCN on EcHPI mutants as a heme ligand.....	118
3.4.3d. Determination of sulfhydryl groups in H106C and R102C mutants.....	119
3.4.4. Further characterization of W105 mutants.....	123
3.5. Construction and characterization of other EcHPI variants.....	126
3.5.1. Introduction.....	126
3.5.2. Characterization of the EcHPI variants.....	128
<b>4. DISCUSSION.....</b>	<b>133</b>
4.1. Purification of MtHPI.....	133
4.2. Biochemical and structural comparison between EcHPI and MtHPI.....	133
4.3. Inhomogeneity of EcHPI and MtHPI preparations.....	135
4.4. Differential oxidation and binding of isoniazid by EcHPI and MtHPI.....	135
4.5. EcHPI is predominantly cytoplasmic.....	136
4.6. Identification of amino acids critical to catalysis of EcHPI.....	137
4.7. Modulation of catalase versus peroxidase activities in W105 mutants.....	140
4.8. Failure in improving purification and homogeneity by His-tag EcHPI.....	142
4.9. Future directions.....	144
<b>5. REFERENCES.....</b>	<b>155</b>
<b>6. APPENDIX.....</b>	<b>163</b>

## LIST OF FIGURES

<b>Figure</b>	<b>Page</b>
1.1. Cartoon representation of the mode of action of isoniazid (INH) in <i>Mycobacterium tuberculosis</i> and <i>M. smegmatis</i> .....	23
2.1. Simplified restriction maps of the chromosomal inserts containing the <i>E. coli katG</i> gene in plasmids pBT22/pAH6/pAH8 and the <i>M. tuberculosis</i> gene in plasmid pAH1.....	27
2.2. Nucleotide sequence of <i>E. coli katG</i> in the chromosomal insert of pBT22, pAH6, and pAH8 plasmids.....	34
3.1.1. Optical absorbance spectra of purified EchPI and MthPI.....	54
3.1.2. SDS-polyacrylamide gel electrophoresis analysis of purified EchPI, MthPI, and MthPI partially digested with trypsin.....	55
3.1.3. Electrospray ionization time-of-flight mass spectroscopic analysis of EchPI.....	58
3.1.4. Electrospray ionization time-of-flight mass spectroscopic analysis of MthPI.....	60
3.1.5. Effect of hydrogen peroxide concentrations on the initial catalytic velocities of purified EchPI and MthPI.....	64
3.1.6. Inhibition of catalase activity of EchPI and MthPI by KCN and NaN <sub>3</sub> ...	66
3.1.7. Spectral titrations of EchPI and MthPI with KCN.....	69
3.1.8. Equilibrium spectrophotometric cyanide binding titrations of EchPI and MthPI: primary and secondary plots.....	71
3.2.1. <i>In situ</i> enzymatic activity staining following non-denaturing polyacrylamide gel electrophoresis of EchPI, MthPI, and horseradish peroxidase.....	76
3.2.2. Time courses for horseradish peroxidase mediated oxidation of isoniazid followed by NBT reduction.....	79

## List of Figures (continued)

<b>3.2.3.</b> Comparison of INH oxidation rates of catalase-peroxidases and horseradish peroxidase.....	81
<b>3.2.4.</b> Effect of isoniazid concentrations on the initial rate of peroxidatic oxidation as detected by nitroblue tetrazolium reduction of purified MtHPI and EcHPI.....	83
<b>3.2.5.</b> Spectral titrations of EcHPI and MtHPI with INH.....	85
<b>3.2.6.</b> Equilibrium spectrophotometric isoniazid binding titrations of EcHPI and MtHPI: primary and secondary plots.....	86
<b>3.3.1.</b> Hydrophobicity plots for EcHPI and MtHPI.....	89
<b>3.3.2.</b> Recovery of catalase and glucose-6-phosphate dehydrogenase activities from spheroplast fractions.....	91
<b>3.3.3.</b> Recovery of catalase and glucose-6-phosphate dehydrogenase activities from spheroplast fractions of <i>E. coli</i> strain UM262, harboring plasmid pBT22.....	92
<b>3.3.4.</b> Immunogold staining to visualize the intracellular location of EcHPI in <i>E. coli</i> strains.....	94
<b>3.4.1.</b> Representation of the relative positions of key active site residues in EcHPI based on the structure of cytochrome c peroxidase.....	96
<b>3.4.2.</b> SDS-polyacrylamide gel electrophoresis analysis of EcHPI and the putative active site mutants of EcHPI following purification.....	99
<b>3.4.3.</b> Non-denaturing polyacrylamide gel electrophoresis analysis of EcHPI and the putative active site mutants of EcHPI following purification.....	100
<b>3.4.4.</b> Absorption spectra of EcHPI mutant enzymes compared to EcHPI wild type.....	101
<b>3.4.5.</b> Effect of H <sub>2</sub> O <sub>2</sub> on the initial catalytic velocities of EcHPI mutants: Michaelis-Menten plots.....	108

## List of Figures (continued)

<b>3.4.6.</b> Effect of 2,2-azinobis(3-ethylbenzothiazolinesulfonic acid) on the initial peroxidatic velocities of EcHPI mutants: Michaelis-Menten plots.....	109
<b>3.4.7.</b> Effect of H <sub>2</sub> O <sub>2</sub> concentrations on the rate of catalase reaction of EcHPI mutants: Lineweaver-Burk plots.....	110
<b>3.4.8.</b> Effect of 2,2-azinobis(3-ethylbenzothiazolinesulfonic acid) on the initial peroxidatic velocities of EcHPI mutants: Lineweaver-Burk plots.....	112
<b>3.4.9.</b> Inhibition of catalase activity of EcHPI mutants by KCN and NaN <sub>3</sub> ..	115
<b>3.4.10.</b> Inhibition of ABTS peroxidase activity of EcHPI mutants by KCN and NaN <sub>3</sub> .....	117
<b>3.4.11.</b> Primary plots of equilibrium spectrophotometric cyanide binding titrations of EcHPI mutants.....	121
<b>3.4.12.</b> Effect of H <sub>2</sub> O <sub>2</sub> on the spectra of EcHPI, horseradish peroxidase, and W105 mutants.....	124
<b>3.4.13.</b> ABTS peroxidatic activity of W105 mutants primed by H <sub>2</sub> O <sub>2</sub> .....	125
<b>3.4.14.</b> Effect of H <sub>2</sub> O <sub>2</sub> preincubation on the ABTS peroxidase activity of W105 mutant.....	127
<b>3.5.1.</b> SDS-polyacrylamide gel electrophoresis analysis of purified EcHPI loop deletion and polyhistidine tagged variants.....	130
<b>3.5.2.</b> Optical absorbance spectrum of purified EcHPI loop deletion variant.	131
<b>4.1.</b> Hypothetical scheme for the mechanism of compound I formation and reduction during the catalytic turnover of catalase peroxidases.....	143
<b>6.1.</b> Alignment of amino acid sequences of <i>E. coli</i> and <i>M. tuberculosis</i> catalase-peroxidases, cytochrome <i>c</i> peroxidase, and horseradish peroxidase.....	163

## LIST OF TABLES

<b>Table</b>	<b>Page</b>
2.1. Summary of <i>Escherichia coli</i> strains, plasmids and bacteriophage used in this study.....	26
2.2. Sequences of the oligonucleotides used for site-directed mutagenesis of <i>E. coli katG</i> .....	39
3.1.1. Comparison of the effect of supplementing growth medium with FeCl <sub>3</sub> and $\delta$ -aminolevulinic acid on the expression of catalase activity of EcHPI and MtHPI.....	51
3.1.2. Purification of MtHPI and EcHPI from <i>E. coli</i> strain UM262 harboring either plasmid pAH1 ( <i>M. tuberculosis katG</i> ) or pBT22 ( <i>E. coli katG</i> ).....	53
3.1.3. Comparison of the specific activities and kinetic parameters of purified EcHPI and MtHPI enzymes.....	65
3.1.4. Quantitation of free sulfhydryl groups of purified EcHPI and MtHPI with 5,5'-dithiobis-(2-nitrobenzoic acid).....	73
3.4.1. Summary of EcHPI mutants constructed.....	97
3.4.2. Summary of observed optical absorbance maxima and heme/protein ratios for purified EcHPI and mutants.....	103
3.4.3. Specific enzymatic activities of EcHPI mutants.....	105
3.4.4. Kinetic parameters of EcHPI mutants.....	113
3.4.5. Estimated equilibrium dissociation constants for EcHPI mutant-cyanide complexes.....	122

## LIST OF ABBREVIATIONS

A	Absorbance
ABTS	2,2-azinobis(3-ethylbenzothiazolinesulfonic acid)
ACP	Acyl carrier protein
ALA	$\delta$ -aminolevulinic acid
Amp <sup>r</sup>	Ampicillin resistant
ATP	Adenosine triphosphate
bp	Base pair(s)
BSA	Bovine serum albumin
CCP	Cytochrome <i>c</i> peroxidase
Ci	Curie
Da	Dalton
DAB	3,3'-diaminobenzidine
DEAE	Diethylaminoethyl
DMSO	Dimethylsulfoxide
DNA	Deoxyribonucleic acid
DTNB	5,5'-dithiobis-(2-nitrobenzoic acid)
EchPI	<i>Escherichia coli</i> Hydroperoxidase I
EDTA	Ethylenediaminetetraacetic acid
ESI-TOF	Electrospray ionization time-of-flight
GDH	Glucose-6-phosphate dehydrogenase
HPI	Hydroperoxidase I
HPII	Hydroperoxidase II
HPLC	High performance liquid chromatography
HRP	Horseradish peroxidase
IgG	Immunoglobulin G
INH	Isonicotinic acid hydrazide (isoniazid)
$k_{cat}$	Turnover number
kDa	kiloDalton
$K_m$	Michaelis-Menten constant
MDR	Multi-drug resistant
MtHPI	<i>Mycobacterium tuberculosis</i> Hydroperoxidase I
NADH	Nicotinamide adenine dinucleotide (reduced)
NADP <sup>+</sup>	Nicotinamide adenine dinucleotide phosphate (oxidized)
NADPH	Nicotinamide adenine dinucleotide phosphate (reduced)
NBT	Nitroblue tetrazolium
OD	Optical density
PAGE	Polyacrylamide gel electrophoresis
PBS	Phosphate buffered saline
PEG	Polyethylene glycol
PMSF	Phenylmethylsulfonyl fluoride
RNAse	Ribonuclease
ROS	Reactive oxygen species

**List of Abbreviations (continued)**

<b>ROM</b>	<b>Reactive oxygen metabolites</b>
<b>SDS</b>	<b>Sodium dodecyl sulfate</b>
<b>SOD</b>	<b>Superoxide dismutase</b>
<b>TPCK</b>	<b>N-tosyl-L-phenylalanine chloromethyl ketone</b>
<b>Tris</b>	<b>Tris(hydroxymethyl)aminomethane</b>
<b>V</b>	<b>Volts</b>
<b>V<sub>max</sub></b>	<b>Maximum velocity</b>
<b>w/v</b>	<b>Weight per unit volume</b>

**PUBLICATIONS ARISING FROM THE THESIS**

**Powers, L., Hillar, A., and Loewen, P.C.** (1999) Active site structure of the catalase-peroxidases from *Mycobacterium tuberculosis* and *Escherichia coli* by extended X-ray absorption fine structure analysis (EXAFS). (in preparation)

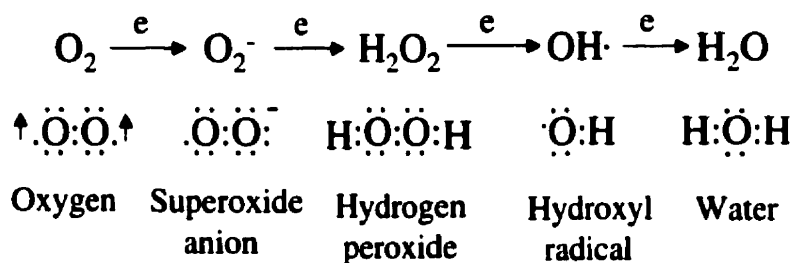
**Hillar, A., Van Caesele, L., and Loewen, P.C.** (1999) Intracellular location of catalase-peroxidase hydroperoxidase I of *Escherichia coli*. *FEMS Lett.* **170**: 307-312.

**Hillar, A. and Loewen, P.C.** (1995) Comparison of isoniazid oxidation catalyzed by bacterial catalase-peroxidases and horseradish peroxidase. *Arch. Biochem. Biophys.* **323**: 438-446.

## 1. General Introduction

### 1.1. Oxygen toxicity and oxidative stress

Oxygen, though essential to aerobically respiring organisms as an electron acceptor, poses a significant risk due to the production of partially reduced forms of  $O_2$  during normal metabolism. While the complete four-electron equivalent reduction of oxygen to water is thermodynamically favoured, carrying out full reduction without forming free, partially reduced species as a one-step process is mechanistically difficult (Jones and Wilson, 1978). Ground state molecular  $O_2$  is a biradical (called triplet oxygen) containing two unpaired electrons. While radicals in general are very reactive species, the paramagnetic nature of  $O_2$  forbids direct reaction of a ground-state triplet oxygen molecule with species in which all electrons are paired, according to the Pauli exclusion principle (Grisham, 1992). The spin restriction that oxygen imposes allows its reduction in one of three ways: 1) via energy input to "flip" the spin of one electron and convert  $O_2$  from the triplet to a highly reactive singlet form,  $^1O_2$ ; 2) via ligation or binding to a transition metal which contains unpaired electrons; or 3) by adding electrons to  $O_2$  one at a time, producing partially reduced  $O_2$  species or related oxidants and oxygen-derived free radicals (Grisham, 1992). Partially reduced  $O_2$  species are generally termed reactive oxygen species (ROS), or reactive oxygen metabolites (ROM) if they are derived from normal aerobic metabolism. Oxygen derived free radicals include superoxide anion ( $O_2^-$ ), hydroperoxyl ( $HOO\cdot$ ), hydroxyl ( $OH\cdot$ ), peroxy ( $ROO\cdot$ ), and alkoxy ( $RO\cdot$ ) free radicals. Other ROS which contain even numbers of electrons include hydrogen peroxide ( $H_2O_2$ ) and hypohalous acids (HOX) (Grisham, 1992). The products of partial and full reduction of  $O_2$  are shown schematically below, including their electronic configurations (modified from Grisham, 1992):



The presence of an excess of reactive oxygen species (pro-oxidants) in the cell is the operational definition of oxidative stress, and oxygen toxicity occurs when the degree of oxidative stress exceeds the capacity of the cell's antioxidant defense systems (Farr and Kogoma, 1991).

Sources of reactive oxygen species occur both within and extraneous to the cell. Within mammalian cells, mitochondria have been shown to produce  $\text{O}_2^-$  and  $\text{H}_2\text{O}_2$  (Dionisi *et al.*, 1975) as a consequence of "leaks" in electron flow onto  $\text{O}_2$  during respiration. It has been estimated that such leaks represent 1-2% of the total electron flow through the electron transport chain (Grisham, 1992; Chance *et al.*, 1979). Other sources of reactive oxygen species within the cell include enzymatic catalysis by a number of different oxidases, some dehydrogenases, and redox enzymes such as peroxidases and P-450 oxygenases. Non-enzymatic sources of ROS in the cell include autoxidation of catecholamines, reduced flavins, hydroquinone, and reaction with transition metal ions in reduced form (Farr and Kogoma, 1991).

Extraneous sources of oxidants are numerous, with most exerting their toxic effects as a result of being metabolized to free radicals. Various toxic chemicals and antibiotics including the herbicide paraquat, azo dyes, the anthracycline anticancer drugs doxorubicin and daunorubicin, and nitroaryl/ nitroheterocyclic antibiotics such as metronidazole, have all been shown to form free radical metabolites that can react with  $\text{O}_2$  to generate ROS (Mason, 1992). Environmental and other sources of oxidants include such diverse factors as air pollution, cigarette smoking, natural radiation

sources (radioactive gases and ultraviolet), and macrophage response to bacterial infections (Ames, 1983; Cerutti, 1991; Babior, 1981).

In the absence of cellular defenses against ROS, various types of toxic effects can be exerted on the cell. Oxidants may react with DNA to produce base modifications or strand breaks (Ames and Shigenaga, 1992; Farr and Kogoma, 1991). ROS have also been shown capable of oxidizing proteins and enzymes (Weser, 1983; Gardner and Fridovich, 1991), and initiating lipid peroxidation by oxidizing membrane fatty acids to radical species (Chance *et al.*, 1979; Cadenas and Sies, 1984; Koster *et al.*, 1984). The end results of oxidant-induced modifications or damage to cellular macromolecules may be cell death and tissue damage potentially leading to various categories of pathophysiology such as gastrointestinal inflammation, arthritis, disorders of the retina, neurodegenerative disorders, and various conditions associated with aging (Grisham, 1992; Markesbery and Carney, 1999; Stadtman and Berlett, 1998).

## **1.2. Removal of reactive oxygen species**

In order to protect themselves from oxidative stress and its toxic effects, cells contain a number of different enzymatic and nonenzymatic antioxidants that serve to prevent or limit oxidative damage. The enzymatic antioxidants are comprised of superoxide dismutase, catalase, and in mammalian cells, glutathione peroxidase. The nonenzymatic antioxidants include various low molecular weight scavengers and reductants and some iron binding proteins.

Superoxide dismutase and hydroperoxidases such as catalase have been referred to as a "defensive team" that prevents the less reactive species  $O_2^-$  and  $H_2O_2$  from forming the highly reactive hydroxyl radical,  $OH\cdot$  (Liochev and Fridovich, 1992). Superoxide dismutase enzymes (SODs) catalyze the reduction of two molecules of  $O_2^-$  to yield  $H_2O_2$  and  $O_2$ . All SODs have reaction centres containing either copper-zinc,

manganese, or iron atoms (Stallings *et al.*, 1992). The bacterium *Escherichia coli* is known to produce four SOD isoenzymes: a manganese containing SOD (Keele *et al.*, 1970); an iron containing SOD (Yost and Fridovich, 1973), an iron-manganese containing hybrid SOD (Clare *et al.*, 1984), and a copper-zinc containing SOD (Battistoni and Rotilio, 1995) The dismutation reaction for mammalian Cu-Zn SOD has a rate constant of  $1.6 \times 10^9 \text{ M}^{-1}\text{s}^{-1}$ , about four orders of magnitude higher than the spontaneous dismutation reaction, ensuring that steady state levels of  $\text{O}_2^-$  in vivo are extremely low (Grisham, 1992).

Catalase enzymes are hemoproteins that catalyze the decomposition of  $\text{H}_2\text{O}_2$  in a two step reaction cycle as shown below, whereby the enzyme first reacts with one molecule of  $\text{H}_2\text{O}_2$  and becomes oxidized to an oxoferryl intermediate with a formal oxidation state of five on the heme iron, also referred to as compound I. To complete the reaction cycle, the compound I species reacts with a second  $\text{H}_2\text{O}_2$  that reduces the enzyme back to its resting state. Two  $\text{H}_2\text{O}$  and one  $\text{O}_2$  molecule are the net products of the two steps of the reaction cycle. The affinity of catalases for  $\text{H}_2\text{O}_2$  is relatively low, ( $K_m$ s in the mM to M range), raising the question as to whether the enzyme plays any significant role in eliminating  $\text{H}_2\text{O}_2$  at physiological concentrations. Peroxidase enzymes also undergo initial oxidation by reaction with  $\text{H}_2\text{O}_2$  to form compound I species, and this property has lead to the conception that these enzymes may be functionally similar to catalases and have a protective effect while using hydrogen donors other than  $\text{H}_2\text{O}_2$ . Such candidates include the alkyl hydroperoxidase reductase (alkyl hydroperoxidase) AhpC of *E. coli* and *Salmonella typhimurium* (Storz and Tartaglia, 1992; Sherman *et al.*, 1996; Jacobson *et al.*, 1989), which is capable of reducing organic peroxides such as cumene hydroperoxide, and the di-heme cytochrome *c* peroxidase from *Pseudomonas aeruginosa*, a periplasmic enzyme believed to provide protection against toxic peroxides (Fülöp *et al.*, 1995). It should be pointed out, however, that peroxidases are also known to catalyze the formation of

cytotoxic oxidants such as hypohalous acids, as well as undergo oxidative modes of redox cycling that can generate  $O_2^-$  (Grisham, 1992; Saikumar *et al.*, 1994, Nakajima and Yamazaki, 1987). *E. coli* produces two enzymes having catalase activity: a monofunctional catalase (hydroperoxidase II or HPII)(Claiborne *et al.*, 1979), and a bifunctional catalase-peroxidase (hydroperoxidase I or HPI) (Claiborne and Fridovich, 1979). Characteristics of both enzymes will be discussed in detail below.

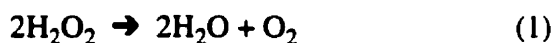
Glutathione peroxidase is a selenoenzyme which decomposes peroxides using reduced glutathione as the hydrogen donor ( Ren *et al.*, 1997), the reaction products being oxidized glutathione and water. Oxidized glutathione is then reduced via the enzyme glutathione reductase, which utilizes the dinucleotide cofactor NADPH. Levels of intracellular glutathione are normally maintained high relative to the oxidized form (Grisham, 1992), allowing efficient interception of ROS. *E. coli* contains glutathione reductase (Storz and Tartaglia, 1992), but no glutathione peroxidase system for direct removal of peroxides (Smith and Schrif, 1979).

In addition to the various enzymatic antioxidants described, there are a number of small molecule antioxidants as well as antioxidant proteins that contribute to the mediation of ROS both intracellularly and extracellularly. Examples that are found in human blood plasma, in which there are virtually no antioxidant enzymes include small molecules such as ascorbic acid, uric acid, glutathione,  $\alpha$ -tocopherol, lycopene, and  $\beta$ -carotene, and proteins such as albumin (which may act as a sacrificial antioxidant (Halliwell and Gutteridge, 1986)), ferritin, lactoferrin, transferrin, and metallothioneines (Frei *et al.*, 1992).

### 1.3. Catalases and peroxidases

#### 1.3.1. Properties of catalases

Catalases are predominantly heme containing proteins which catalyze the overall reaction (1):

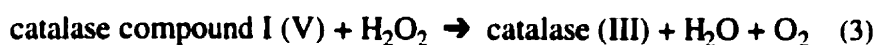


Typical properties of catalases mentioned here derive mainly from early investigations of the purified enzyme from mammalian blood or liver tissues. Generally, most catalases are homotetramers having subunit sizes of approximately 60 kDa (Tanford and Lovrien, 1962). Each subunit contains a non-covalently bound heme prosthetic group characterized as protoferriheme (protoporphyrin IX) (Stern, 1936) in the high-spin Fe(III) state (Maeda *et al.*, 1973). High resolution crystal structures of various catalases (Reid *et al.*, 1981; Murthy *et al.*, 1981; Fita and Rossmann, 1985; Vainshtein *et al.*, 1986; Murshudov *et al.*, 1992; Bravo *et al.*, 1995) have shown that the axial ligand at the fifth coordination position of the heme iron is a tyrosine residue, while the sixth coordination position of the iron is probably occupied by a water molecule (Oakes, 1986; Schonbaum and Chance, 1976).

Catalases show pseudo-first order saturation kinetics (Michaelis-Menten kinetics) with a kinetic constant for the overall reaction being independent of pH in the range of 4.7- 10.5, with mammalian enzymes having reported specific rate constants in the range 0.01 to  $6 \times 10^7 \text{ M}^{-1}\text{s}^{-1}$ , and having an apparent  $K_m$  of  $\approx 1.0 \text{ M}$  (Sevinc *et al.*, 1999, Jones and Wilson, 1978). The reliability of the reported kinetic parameters however, may be questionable, as it has been amply demonstrated that  $\text{H}_2\text{O}_2$  causes inactivation of the enzyme at concentrations of less than 1 M (Sevinc *et al.*, 1999; DeLuca *et al.*, 1995), probably making it impossible to achieve true saturation conditions for the enzyme with hydrogen peroxide. Inhibitors of catalase activity include classical inhibitors such as cyanide, azide, and hydroxylamine (Nicholls and

Schonbaum, 1963; Maj *et al.*, 1996), which bind reversibly to the heme iron; 3-amino 1,2,4-triazole, which irreversibly inhibits catalase by forming a covalent bond with a histidine residue on the oxidized catalytic intermediate of catalase (compound I) (Chang and Schroeder, 1972); t-butyl hydroperoxide, which causes suicide inhibition through formation of an inactive catalytic intermediate (Pichorner *et al.*, 1993); and thiol reagents,  $O_2^-$ , and  $H_2O_2$ , which may either directly or indirectly lead to oxidation of amino acid residues on the enzyme (Takeda *et al.*, 1980; Kono and Fridovich, 1982; DeLuca *et al.*, 1995). Catalases from various eukaryotic and prokaryotic organisms have also been shown to contain one tightly bound NADPH molecule per enzyme subunit (Kirkman and Gaetani, 1984; Gouet *et al.*, 1995; Yusifov *et al.*, 1989; Hillar *et al.*, 1994). The bound NADPH has been postulated to prevent the enzyme from accumulating an inactive catalytic intermediate known as compound II (Kirkman *et al.*, 1987), or a compound II- like species in which a tyrosinate based radical is present (Hillar and Nicholls, 1992; Ivancich *et al.*, 1997; Kirkman *et al.*, 1999).

As discussed briefly above, the catalase reaction mechanism proceeds in two sequential steps as shown below:



In reaction (2), the resting (ferric) enzyme reacts with one molecule of  $H_2O_2$  via a two-electron oxidation to produce an oxoferryl heme species known as compound I.

Compound I is a short-lived catalytic intermediate with a distinct absorption spectrum characterized by a reduction in absorbance intensity of the Sorêt band ( $\approx 400\text{nm}$ ; a band which is diagnostic of all hemoproteins). Considerable evidence indicates that the compound I structure is  $Fe^{IV}=\text{O}$  having a formal oxidation state of (V), in which the second electron is delocalized on the porphyrin ring of the heme as a  $\pi$ -cation

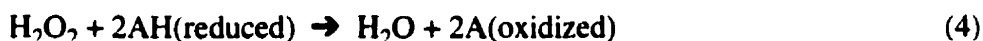
radical (Dolphin *et al.*, 1971). The reaction is believed to be initiated by a histidine side chain in the active site above (distal to) the plane of the heme. The histidine acts as a general base by donating electrons to the  $\text{H}_2\text{O}_2$  molecule coordinated to the heme iron, forming a transition complex which is stabilized by additional charge interactions provided by other residues in the active site, most likely an asparagine residue in the bovine liver enzyme. This allows scission of the peroxide O-O bond, to form compound I and one molecule of water (Fita and Rossmann, 1985).

In reaction (3) shown above, a molecule of  $\text{H}_2\text{O}_2$  reacts with compound I as a two-electron reductant to produce one molecule of  $\text{O}_2$  and one water molecule. In this case, the second  $\text{H}_2\text{O}_2$  molecule enters the active site and is preoriented for reaction by hydrogen bonding and charge interactions with the side chains of the active site histidine and asparagine residues. As the charge density on the  $\text{H}_2\text{O}_2$  molecule shifts due to interaction with the two amino acid side chains, it is believed that the O-O bond takes on double bond character while the oxygen-iron bond is broken. The active site histidine side chain then acquires greater nucleophilic character, allowing a rearrangement in the relative positions of the hydroxyl group closest to the active site side chains, while a hydroxyl is simultaneously formed on the heme iron. Water is then thought to be formed through transfer of a hydrogen and electron to the OH group still coordinated to the iron, as the  $\text{O}_2$  molecule is released from coordination with the histidine residue (Fita and Rossmann, 1985).

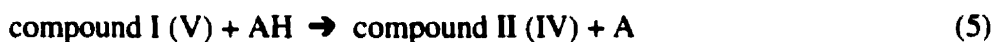
Catalases have also been shown to be able to react with other hydrogen donors as well as  $\text{H}_2\text{O}_2$  to produce distinct spectral species (Nicholls and Schonbaum, 1963). An example of this is the reaction of catalase compound I with ferrocyanide or ascorbate, a reaction which produces compound II, an inactive intermediate of catalase that is one oxidizing equivalent above that of the ferric enzyme. Addition of large excesses of hydrogen peroxide to catalases leads to formation of inactive catalase compound III or oxycatalase form of the enzyme.

### 1.3.2. Properties of peroxidases

Like catalases, peroxidases are predominantly heme containing enzymes which catalyze overall reaction (4), where AH represents reduced substrate hydrogen donor, and A represents the oxidized hydrogen donor, which may be a free radical species :



The reaction proceeds in three steps. Reaction (2) above, is the first step, common to both catalases and peroxidases. Reduction of compound I then occurs as shown in reactions (5) and (6) below:



Unlike the catalases however, there is a great deal of variability in peroxidases in regard to their structural properties. This is probably a consequence of the many different roles that individual peroxidases play in the organisms from which they are derived. While the majority of peroxidases are hemoproteins, such as horseradish peroxidase (HRP), cytochrome *c* peroxidase (CCP), and other mammalian, plant and fungal peroxidases, there are also non-heme peroxidases, such as the vanadium containing chloroperoxidase enzyme from the fungus *Curvularia inaequalis* (Messerschmidt and Wever, 1996), the FAD cysteine redox centre NADH peroxidase from *Streptococcus faecalis* (Stehle *et al.*, 1991), and the recently identified human peroxiredoxin (peroxidase) (Choi *et al.*, 1998).

Multiple amino acid sequence alignments carried out by Welinder (1992) using data for a number of hemoprotein peroxidases allowed their classification into three distinct structural families or classes. Class I enzymes are identified as bacterial

peroxidases, and include the sequences of *E. coli* catalase-peroxidase HPI and yeast cytochrome *c* peroxidase. Class II enzymes are the fungal peroxidases, exemplified by lignin peroxidase from *Phanerochaete chrysosporium*. Class III enzymes are the plant peroxidases, exemplified by horseradish peroxidase isoenzyme C. It should be noted that the structural classes identified do not imply degrees of evolutionary relatedness, simply structural variation. Among class I enzymes, for example, the yeast cytochrome *c* peroxidase has been shown to be evolutionarily distinct from bacterial peroxidases (catalase-peroxidases) by phylogenetic analyses (Loewen, 1997).

Historically, the most intensively studied hemoprotein peroxidases have been yeast cytochrome *c* peroxidase (CCP) and horseradish peroxidase C isoenzyme (neutral or slightly basic isoenzyme form) (HRP). The former is a protein that occurs as a single polypeptide chain of 294 amino acids with a single protoporphyrin IX prosthetic group bound to it non-covalently, having a molecular weight of 35.4 kDa (Bosshard *et al.*, 1991). The latter is a protein that occurs as a single polypeptide chain of 308 amino acids, having a blocked amino terminal, a protoporphyrin IX prosthetic group bound non-covalently, eight neutral carbohydrate side chains attached through Asn residues, four disulphide bridges, and two Ca<sup>2+</sup> ions per HRP molecule. The molecular weight of HRP is 34.5 kDa if the carbohydrate content is excluded, but 42.1 kDa if the contribution by the carbohydrate groups are taken into account (Dunford, 1991). Both enzymes can be readily expressed in *E. coli* as apoenzymes, and then reconstituted with heme (Fishel *et al.*, 1987; Smith *et al.*, 1990). The crystal structure of CCP was first to be solved (Poulos *et al.*, 1980; Finzel *et al.*, 1984), with that of recombinantly expressed HRP having been solved only very recently (Gajhede *et al.*, 1997). Unlike catalases (excepting the catalase-peroxidases), the proximal axial ligands to the heme iron in these peroxidases are histidine side chains (His 175 in CCP, His 170 in HRP). Similar to catalases, the substrate accessible distal heme pocket is occupied by several amino acid residues which are highly conserved and are

considered critical to catalysis. These residues include the distal histidine (His 52 in CCP, His 42 in HRP), arginine (Arg 48 in CCP, Arg 38 in HRP), and either a tryptophan (Trp 51 or CCP) or more usually, a phenylalanine (Phe 41 in HRP) (Welinder *et al.*, 1992).

CCP and HRP react rapidly with  $\text{H}_2\text{O}_2$  to form very stable compound I species (two oxidizing equivalents above the ferric resting enzyme) similar to those of catalases. The compound I species have absorption spectra distinct from those of the resting (ferric) enzymes, and the compound I absorption spectra of both CCP and HRP are distinct from each other. In HRP, the compound I structure is also an oxoferryl ( $\text{Fe}^{\text{IV}}=\text{O}$ ) species having a  $\pi$ -cation radical delocalized on the porphyrin ring (Dolphin *et al.*, 1970). In CCP however, the compound I structure is an oxoferryl species with a protein radical localized onto the Trp 191 side chain, on the proximal side of the heme (Sivaraja *et al.*, 1989). Specific rate constants for the reaction of  $\text{H}_2\text{O}_2$  with CCP are extremely high ( $10^7$ - $10^8 \text{ M}^{-1}\text{s}^{-1}$ ) (Ohlsson *et al.*, 1986), being very similar in magnitude to those reported for catalases (Nicholls and Schonbaum, 1963)

Although there is evidence that peroxidases can occasionally act to oxidize substrates in a catalytic fashion, through a one-step, two electron transfer, as in the case of HRP compound I with iodide, one key distinguishing feature between the two types of enzymes is that peroxidase compounds I are preferentially reduced in two one electron transfer steps. In CCP the reductants are thus two molecules of ferrocyanide, while in HRP, the possible reductants comprise a wide range of compounds such as aromatic phenols, anilines, amines, and even NADH/NADPH (Smith *et al.*, 1995; Dunford, 1991; Halliwell, 1978). Reduction of CCP compound I is extremely rapid, with a maximum steady state turnover number reported to be  $1.4 \times 10^4 \text{ s}^{-1}$  (Yonetani and Ray, 1966). The kinetics of the reduction are very complex, as each reduction step requires the formation of a CCP-cytochrome *c* complex followed by intramolecular electron transfer to effect electron donation to the CCP active site.

A recently proposed model for the mechanism proposes a two binding site model, where the affinity of the two sites for cytochrome c differs by 1,000 fold and rapid electron transfer occurs only at the high affinity site (Miller, 1996). Reduction of HRP has been described as following a type of ping-pong (ordered two-substrate, two-product) reaction (Dunford, 1991), which proceeds through sequential one electron reductions of the enzyme, and yielding an optically observable second HRP reaction intermediate known as compound II, which is one oxidizing equivalent above that of resting (ferric) enzyme. Reduction of HRP compounds I and II usually generates radical products. This feature, in combination with the involvement of mediating molecules such as scopoletin and oxygen, allows HRP to carry out peroxidatic as well as oxidatic reactions (Saikumar *et al.*, 1994; DeSandro *et al.*, 1991), and can often lead to mechanism based inactivation of the enzyme by formation of substrate radical adducts (Gilfoyle *et al.*, 1996) or other types of substrate inhibition (Baynton *et al.*, 1994). The most parsimonious mechanisms for HRP compound I and II reduction propose that the hydrogen donor donates an electron to reduce the porphyrin radical and simultaneously donates its hydrogen to the distal basic histidine chain in reducing compound I to compound II, and then a second donor molecule donates both its hydrogen and one electron to the oxoferryl group which is hydrogen bonded to the protonated distal histidine, resulting in reduction of the iron and formation of the water leaving group (Dunford, 1991).

Like catalases, HRP can undergo other reactions *in vitro*, such as superoxide anion mediated production of yet another spectral intermediate, an inactive form of the enzyme termed compound III or oxyperoxidase (Nakajima and Yamazaki, 1987), and formation of compound IV, a similar but irreversibly inactivated species (Baynton *et al.*, 1994). However, these types of reactions, like those for catalases, may not be physiologically relevant.

#### **1.4. Catalase-peroxidases**

Investigations of mammalian catalases have provided ample evidence that these enzymes can occasionally function as peroxidases under specific conditions, with a limited number of small hydrogen donors such as formate, ethanol, nitrite, or elemental mercury (Sichak and Dounce, 1986). The reactions catalyzed are two-electron oxidations of the donor substrates by compound I under conditions of low steady state levels of  $H_2O_2$ , achieved by continual enzymic generation or gradual infusion (Keilin and Hartree, 1955; Chance, 1950). The peroxidatic activity of these catalases, however, is regarded primarily as a catalytic artifact, because unlike true peroxidases, there is little evidence that the enzymes can oxidize large organic molecules under physiological conditions (Sichak and Dounce, 1986). In fact, the crystal structures of monofunctional catalases indicate that their hemes are too deeply buried and have very narrow access channels, which would restrict to reaction with only relatively small molecules (Sevinc *et al.*, 1999).

Enzymes having both catalase and organic peroxidase activity have been isolated from various species of bacteria (Loewen, 1997) and fungi (Fraaije *et al.*, 1996; Levy *et al.*, 1992). Biochemical and phylogenetic analysis of bacterial representatives of this group of enzymes has ascertained that they are more closely allied to true peroxidases rather than to eukaryotic-type monofunctional catalases (Welinder, 1992; Loewen, 1997). This has led to their classification as catalase-peroxidases, although some confusion regarding the naming of these enzymes arises from their possessing either the only catalatic or peroxidatic activity characterized from a specific organism. Most catalase-peroxidases have been shown to be homotetrameric enzymes with protoporphyrin IX (heme b or protoheme) prosthetic groups, with subunit sizes of about 80 kDa (Loewen, 1997), although some occur as homodimers. To date, there have been no reports in the literature of the successful crystallization of any catalase-peroxidase.

## **1.5. Catalases of *Escherichia coli* and *Mycobacterium sp.***

### **1.5.1 Catalase enzymes of *Escherichia coli***

Three enzymes having catalase activity have been identified in *E. coli*. Catalase hydroperoxidases I (Claiborne and Fridovich, 1979) and II (Claiborne *et al.*, 1979) are the best known of these enzymes, and their characteristics will be detailed below. More recently, a novel catalase-peroxidase encoded by the large plasmid of enterohaemorrhagic *E. coli* strain O157:H7 and termed KatP, has been described (Brunner *et al.*, 1996). The *katP* gene predicts a polypeptide with a molecular mass of 81.8 kDa, and sequence and biochemical analyses suggest that the enzyme is exported to, and functions in the periplasm (Brunner *et al.*, 1996).

#### **1.5.1a. Catalase Hydroperoxidase II of *E. coli***

The *E. coli* genome encodes two enzymes having catalase activity. One enzyme, known as catalase hydroperoxidase II (HPHII) is a monofunctional catalase. This enzyme has been extensively investigated, and its high-resolution crystal structure has been solved (Bravo *et al.*, 1995; Bravo *et al.*, 1999). It is a homotetrameric enzyme with 84 kDa subunits, each containing a non-covalently associated heme  $d_{cis}$  prosthetic group, and lacks the NADPH binding site found in other catalases. The enzyme has a high catalase specific activity ( $\approx 15,000$  U/ mg; Loewen and Switala, 1986), and is found in the cytoplasm. HPHII maintains full catalytic activity over a pH range of 5-11 (Loewen and Switala, 1986) and is extremely thermotolerant, with a temperature inactivation midpoint of 83°C (Switala *et al.*, 1999). The enzyme is expressed at low levels during exponential growth phase of *E. coli* from the *katE* gene, but is expressed at up to ten times higher levels as cells enter stationary phase. Synthesis of HPHII is regulated predominantly by the alternate sigma factor  $\sigma^S$  of the

DNA dependent RNA polymerase (Ivanova *et al.*, 1994) as a consequence of starvation and potentially, oxygen levels in the cell (Loewen, 1997).

#### **1.5.1b. Catalase-peroxidase Hydroperoxidase I of *E. coli***

A second enzyme having catalase activity in *E. coli* is known as catalase-peroxidase hydroperoxidase I (EcHPI or EcKatG), a bifunctional catalase with an associated organic peroxidase activity. The enzyme was first purified and described by Claiborne and Fridovich (1979) as a tetrameric enzyme of identical 80 kDa subunits containing two protoporphyrin IX prosthetic groups per tetramer. The amino acid sequence of the enzyme subunits has been deduced from the DNA sequence (Triggs-Raine *et al.*, 1988) of the cloned structural gene *katG* (Loewen *et al.*, 1983) to consist of 726 amino acids. The cloned, plasmid expressed enzyme has a relatively high catalase specific activity ( $\approx 2,000$  U/ mg; Loewen *et al.*, 1990), although this activity is approximately one-sixth that reported for the HP II enzyme (Loewen and Switala, 1986). The enzyme also has a low level peroxidase activity (1.9 U/ mg with *o*-dianisidine substrate; Loewen *et al.*, 1990), exhibiting the ability to oxidize the aromatic hydrogen donors *o*-dianisidine, guaiacol, pyrogallol, *p*-phenyldiamine (Claiborne and Fridovich, 1979), and 3-diaminobenzidine used for *in situ* localization of peroxidase activity in polyacrylamide gels (Loewen and Switala, 1986). By comparison commercially available horseradish peroxidase enzyme has specific activity at least three orders of magnitude higher than EcHPI when *o*-dianisidine is employed as the donor substrate (Worthington Enzyme Catalog, 1968). The enzyme is not as robust as HP II, showing a relatively sharp pH optimum for both catalase and peroxidase activities at 6.5-7.0 (Loewen *et al.*, 1990), and a much lower temperature inactivation midpoint of 53° (Switala *et al.*, 1999). The enzyme's intracellular location was initially demonstrated to be periplasmic (Heimberger and Eisenstark, 1988), however, more recent studies have suggested that EcHPI may in fact be located in the

cytoplasm (Brunder *et al.*, 1996). EchPI is expressed primarily in exponentially growing cells, with synthesis of the enzyme being responsive to oxidative stress as part of the *oxyR* regulon (Loewen *et al.*, 1985; Christman *et al.*, 1989).

### **1.5.1c. Catalase-peroxidase KatG of *Mycobacterium tuberculosis***

Correlation between acquisition of resistance in *Mycobacterium tuberculosis* strains to the antitubercular drug isoniazid, and loss of catalase and peroxidase activities present in the cells (Winder, 1982), was the initial impetus for earlier reports of the purification of catalase also noted to have peroxidase activity, from *M. tuberculosis* cells. The enzyme was first purified and described by Diaz and Wayne (1974) as a 160 kDa enzyme containing heme with a reported heme/protein ratio (407nm/280nm) of 0.37. This study also determined that the enzyme was thermally inactivated at about 60°C, and lost up to 35% initial activity after freezing at -70°C for only 24h. The authors also found that the enzyme functioned as a peroxidase with a pH optimum of 7.5, in the presence of catechol, guaiacol, and pyrogallol as hydrogen donors. A subsequent purification of peroxidase from *M. tuberculosis* also showed concomitant purification of catalase activity and what was termed Y enzyme activity (probably a type of isoniazid coupled oxidation) (Gayathri Devi *et al.*, 1978). These workers, however, estimated the enzyme's molecular weight to be 240 kDa, though the spectrum for the enzyme was characteristic of a hemoprotein, and the preparations had both o-dianisidine activity and also carried out isoniazid oxidation via the Y-enzyme activity.

Following the characterization and cloning of the structural gene for the *M. tuberculosis* KatG (MtKatG or MtHPI) (Zhang *et al.*, 1992), purifications of the recombinant form of the catalase-peroxidase have been reported by a number of groups (Nagy *et al.*, 1995; Johnsson *et al.*, 1997; Nagy *et al.*, 1997a; Saint-Joanis *et al.*, 1999), and purification of the catalase-peroxidases from *M. intracellulare* (Morris

*et al.*, 1992), *M. smegmatis* (Marcinkeviciene *et al.*, 1995) and *Mycobacterium* sp. Pyrl (Rafii *et al.*, 1999) have also been carried out. The former studies have shown that the MtHPI enzyme is a homodimer made up of two 80 kDa subunits, and that the heme content is one molecule of protoporphyrin IX per dimer. The catalase activity of MtHPI is quite high, having reported values of between 1,000 and 2,000 U/mg enzyme (Johnsson *et al.*, 1997; Saint-Joanis *et al.*, 1999). The enzyme has peroxidase activity with a number of tested organic hydrogen donors, including o-dianisidine, pyrogallol, p-phenyldiamine, NADH, NADPH, isoniazid (Johnsson *et al.*, 1997) and ABTS (Nagy *et al.*, 1997a), utilizing both H<sub>2</sub>O<sub>2</sub> and t-buty hydroperoxide as oxidants for the peroxidatic reactions. In comparison to the commercial horseradish peroxidase enzyme, the  $k_{cat}/K_m$  ratio for MtHPI is about two orders of magnitude lower (Nagy *et al.*, 1997a). The enzyme also shows sharp pH optima for both catalase and o-dianisidine peroxidase activities of 7.0 and 5.5, respectively (Johnsson *et al.*, 1997). Small-angle X-ray scattering experiments have indicated that the purified enzyme has a radius of gyration of 3.8nm and an excluded volume of 306 nm<sup>3</sup> (Nagy *et al.*, 1997b). These data have been used to determine a molecular envelope for the enzyme using a shape determination algorithm in order to guide construction of a homology based model.

Similar to EcHPI, MtHPI expression in *M. tuberculosis* cells is peroxide inducible, albeit to a level which is insufficient to protect against H<sub>2</sub>O<sub>2</sub> induced stress (Sherman *et al.*, 1995). Unlike other enteric bacteria, such as *E. coli*, whose oxidative stress responsive element is the OxyR transcription factor, the *oxyR* gene of *M. tuberculosis* is inactive, as all contemporary strains of the organism have multiple lesions such as frameshifts and deletions (Deretic *et al.*, 1995). Loss of *oxyR* in *M. tuberculosis* is related to altered expression of the closely linked and divergently transcribed *ahpC* gene, which encodes the *M. tuberculosis* homolog of alkyl hydroperoxide reductase (AhpC)(Jacobson *et al.*, 1989). Mutations that eliminate the

*M. tuberculosis* KatG (MtHPI) activity in clinical isolates have been found that compensate for this loss of a protective enzyme by increasing the expression of AhpC through promoter mutations, allowing sufficient levels of AhpC expression to partially protect cells against cumene hydroperoxide (Sherman *et al.*, 1996). More recently, studies of both the *oxyR-ahpC* and *katG* loci of *M. marinum* have led to the discovery that a homolog of the ferric uptake regulator Fur was identified immediately 5' from the start of *M. marinum katG*, and that homologs occurring in similar arrangements exist in *M. tuberculosis*, *M. smegmatis*, and *M. leprae* (Pagán-Ramos *et al.*, 1998), and these sequences have been found to be cotranscribed. Thus the possibility of the involvement of other regulatory elements in the expression of MtHPI exists.

#### **1.6. Role of MtHPI in cytotoxicity of isoniazid**

It is estimated that one third the world's population is infected with *Mycobacterium tuberculosis*, the pathogen responsible for pulmonary tuberculosis (Bloom and Murray, 1992). While effective combination drug mediated treatments including isoniazid, rifampicin, pyrazinamide, and ethambutol have been used to cure patients suffering from the disease (Heym *et al.*, 1994), various factors are now contributing to the development of strains of resistant and multi-drug resistant (MDR) isolates of *M. tuberculosis*. One such factor is non-compliance with drug regimens, as even the modern short-course therapy requires compliance for a period of six months (Blanchard, 1996). Another factor is the association of tuberculosis infection with the spread of high risk activities (such as drug use) or spread of other diseases, such as AIDS, even in hospital environments (Bloom and Murray, 1992; Ritacco *et al.*, 1997). While development of modifications to current practices of chemotherapy of tuberculosis may significantly reduce the rates of drug resistance and relapse (Weis *et al.*, 1994), the fact remains that cure rates drastically drop when drug resistance to even only two antibiotics develop in clinical cases, with up to 40% of "cured" patients

experiencing relapses of the disease during follow-up periods, with mortality rates of up to 24% in cases of tuberculosis resistant to three antibiotics (Sbarbaro, 1997; Kritski *et al.*, 1997). MDR *M. tuberculosis*, like other MDR pathogens developing worldwide, are thus ever increasing threats to populations in the post-antibiotic era.

The use of isoniazid (isonicotinic acid hydrazide or INH) as an effective antitubercular drug began in 1952. Its utility as a drug was discovered by chance, as it occurred as an intermediate in the synthesis of a thiosemicarbazone antibiotic (Smith, 1977). Ever since, it has remained a front-line antitubercular drug of choice in the treatment of tuberculosis. *Mycobacterium tuberculosis* and *M. bovis* are highly susceptible to INH at concentrations in the range 0.02- 0.2 µg/ml. (Blanchard, 1996). Mycobacteria are also sensitive to INH when compared to other bacteria, all of which require at least 600 µg/ml for effective growth inhibition, which in itself has suggested that INH targets a metabolic pathway unique to mycobacteria.

It has long been recognized that resistance of *M. tuberculosis* to INH correlates with the loss of catalase and peroxidase activities in resistant strains (Winder, 1964). The possibility that mutations in only one structural gene for an enzyme possessing both these activities was thus proposed early on, as was the possibility that INH resistance could also affect a locus or operon controlling synthesis of genes encoding distinct catalase and peroxidase enzymes (Winder, 1964). Other clues to the mode of action of INH included evidence that the drug inhibits the synthesis of a lipid component of the cell envelope of mycobacteria, which were subsequently identified to be mycolic acids, extremely long chained, β-branched fatty acids unique to mycobacteria (Winder, 1982). Following initial purifications of catalase and peroxidase activities from *M. tuberculosis* (Diaz and Wayne, 1974; Gayathri Devi *et al.*, 1978), it was discovered that both catalase and peroxidase activity was present in both enzyme preparations, and that both could react with isoniazid, although this was not conclusively shown to be a distinct enzymatic property at the time. This led to

the proposal that catalase-peroxidase may be involved in chemical modification of INH to an active form, or some other catalase-peroxidase mediated mechanism in order to exert cytotoxicity on *M. tuberculosis* cells (Winder, 1982).

The work of Zhang *et al.* (1992) was first to demonstrate the genetic basis for INH resistance connected with loss of catalase-peroxidase in *M. tuberculosis*, upon isolation, cloning, and sequencing of the *katG* gene. This study also established that overexpression of the *M. tuberculosis* KatG in *E. coli* cells could lead to low level susceptibility to INH in a heterologous organism which is normally very resistant to the drug (Zhang *et al.*, 1992). Subsequent work by Schultz and colleagues established that the recombinant, homogeneously purified KatG (or MthPI), was capable of enzymatic oxidation of INH to electrophilic radical species (Johnsson and Schultz, 1994). The authors speculated that INH could be oxidized *in vivo* to yield a number of highly reactive species, including diazenyl, hydrazide, or acyl radicals, which could then go on to oxidize or acylate groups in proteins.

Consistent with the concept that INH is a prodrug that could be converted into an active form and then go on to inactivate another protein or proteins, a potential target protein for INH and ethionamide (an antitubercular structural homolog to INH) was identified in *M. tuberculosis* by complementation genetic studies and the locus named *inhA* (Banerjee *et al.*, 1994). *inhA* was found to encode a structural gene for a protein with homology to the 3-ketoacyl-acyl carrier protein (ACP) reductase from *E. coli*, and corroborating experiments suggested that this protein was involved in mycolic acid synthesis in *M. tuberculosis*, and that inactivation by mutation of *inhA* conferred resistance to INH in strains of *M. smegmatis* and *M. bovis* (Banerjee *et al.*, 1994). Binding of MthPI-activated INH to wild-type and mutant *M. tuberculosis* enoyl-ACP reductases *in vitro* was demonstrated a short time thereafter, and indicated that the activated form of INH forms an adduct on the InhA protein in a region involved in NADH binding (Johnsson *et al.*, 1995; Quemard *et al.*, 1996). The

determination of the InhA crystal structure (Dessen *et al.*, 1995) as well as that of the homolog from *E. coli* (Baldock *et al.*, 1996) provided further clues as to the possible mechanism by which activated INH could interact with the protein to cause irreversible inactivation. Recently, however, the crystal structure of InhA inhibited by the INH derived adduct has shown that the mode of inactivation is via covalent attachment of the activated form of the drug to the nicotinamide ring of NADH bound within the active site of InhA, yielding an isonicotinic acyl-NADH (Rozwarski *et al.*, 1998). Inability of InhA to release the NADH adduct is believed to be the mode in which permanent inhibition of the enzyme occurs leading to prevention of mycolic acid synthesis.

While the evidence that the mode of action of INH involves its activation and subsequent irreversible binding to InhA is compelling, there is evidence that InhA may not be the relevant target in *M. tuberculosis*, as *inhA* expression has only been shown to confer INH resistance on *M. smegmatis* and *M. bovis*. There is a paucity of evidence for polymorphisms in *inhA* from many clinical isolates of *M. tuberculosis*, apart from a few in which expression of *inhA* is up-regulated, leading to resistance by overexpression of the protein target (Mdluli *et al.*, 1996). KasA, a  $\beta$ -ketoacyl acyl carrier protein synthase associated with a homolog of AcpM, an acyl carrier protein of *E. coli*, was found to carry saturated hexacosanoic acid (C26:0) in response to INH treatment in *M. tuberculosis*. KasA is probably part of an as yet uncharacterized type II fatty acid synthase of *M. tuberculosis*, and may be the relevant activated INH target further along in the mycolic acid synthesis pathway in *M. tuberculosis* (Mdluli *et al.*, 1998). Additionally, arguments have been made for the possibility that INH oxidation by MtHPI is actually mediated by a manganese peroxidase activity apparently identified in the homologous enzyme from *M. smegmatis* (Magliozzo and Marcinkeviciene, 1997), or that the oxyferrous form of the catalase-peroxidase is actually responsible for activation of the drug (Magliozzo and Marcinkeviciene, 1996).

While there has long been sufficient evidence for catalytic mediation by INH/O<sub>2</sub>/Mn(II) (Zinner *et al.*, 1976) that can apparently lead to an increase in the rate of InhA inactivation (Zabinski and Blanchard, 1997), it is unclear whether this is a property of catalase-peroxidases, or whether this is due to non-enzymatic catalytic reactions related to complex formation of INH with divalent metal cations (Winder and Denny, 1959; Cymerman-Craig *et al.*, 1955).

The INH mode of action in its cytotoxicity toward *M. tuberculosis* can thus be summarized (Figure 1.1) as follows: 1) the drug is taken up by *M. tuberculosis* cells, probably be a process of passive diffusion (Bardou *et al.*, 1998), 2) the drug interacts with MtHPI (KatG) and binds it (Wengenack *et al.*, 1997; Wengenack *et al.*, 1998), and via several potential mechanisms, generates INH-derived free radical species, 3) the radical species generated can interact with InhA, the enoyl ACP reductase, KasA, the ketoacyl synthase, or go on to oxidize other non-specific cellular components or inhibit MtHPI itself (Brimnes *et al.*, 1999), 4) interaction with InhA or KasA with activated INH leads to their irreversible inactivation by forming an NADH isonicotinic acyl adduct, or an as yet to be characterized protein adduct, respectively; leading to inhibition of mycolic acid synthesis, and eventual cell death.

### **1.7. Object of the thesis**

This study encompasses three interrelated foci, namely: 1) comparison of some physical and biochemical properties of the catalase-peroxidases of *E. coli* and *M. tuberculosis*, 2) determination of the intracellular location of *E. coli* catalase-peroxidase HPI, and 3) construction and characterization of various mutant variants of *E. coli* catalase-peroxidase HPI. The goals of foci 1) and 2) of this research are to determine whether there are specific structural, biochemical, or intracellular environmental differences between the *E. coli* and *M. tuberculosis* HPI enzymes with regard to their interaction with the antitubercular drug, isoniazid, in order to help

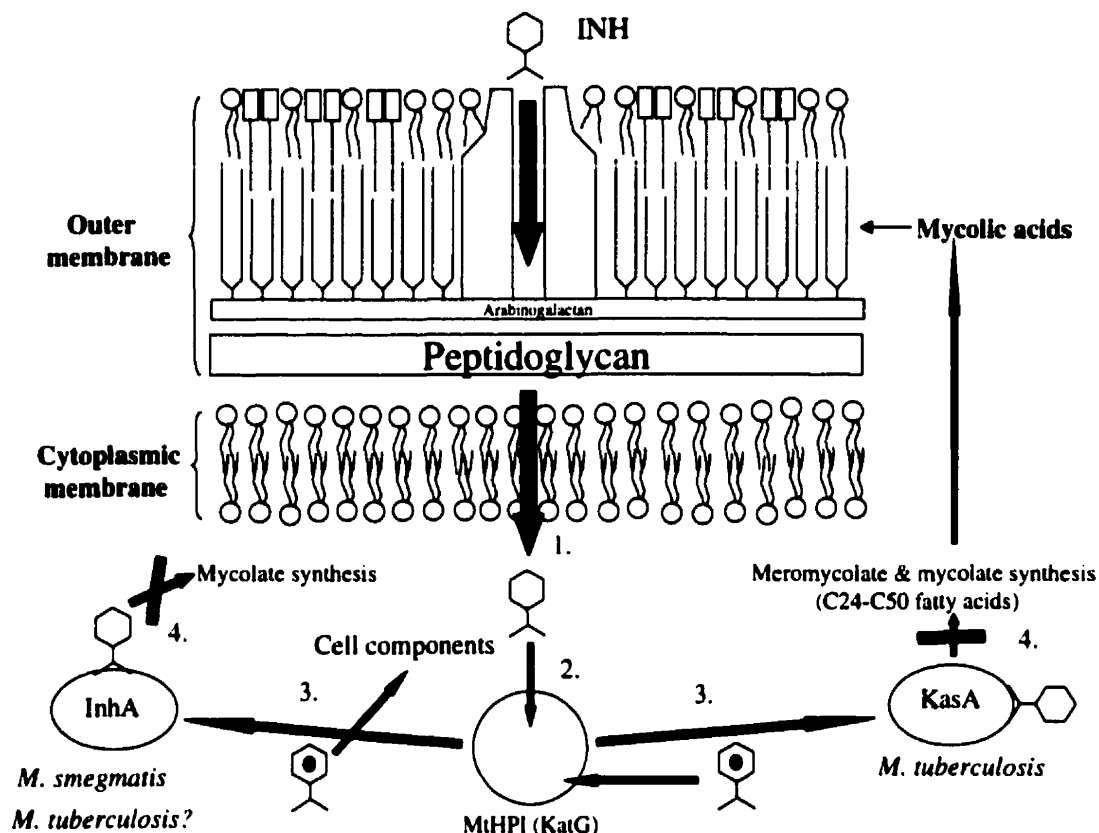


**Figure 1.1** Cartoon representation of the mode of action of isoniazid (INH) in *Mycobacterium tuberculosis* and *M. smegmatis*. 1. Uptake of INH via passive diffusion. 2. Interaction of INH with MthPI (KatG), leading to INH oxidation and formation of radical species. 3. Radical species diffuse away and interact with either InhA (*M. smegmatis*) or KasA (*M. tuberculosis*) enzymes, forming inactivated adducts. 4. Inactivation of either InhA or KasA prevents synthesis of mycolic acids.

explain the basis of *M. tuberculosis*' inherent sensitivity to the drug compared with *E. coli*. The goals of focus 3) of this research are a structure-function study of *E. coli* catalase-peroxidase by modifying certain putative active site (His106, Arg102, Trp105, His267) and other residues (Lys419) in the enzyme via site-directed mutagenesis methodology and fragment excision (putative loop deletion), in order to ascertain their importance in catalysis or structure, as well as to attempt to modulate the catalase and peroxidase activities specifically, such that one activity might be changed at the expense of the other.

## 2. MATERIALS AND METHODS

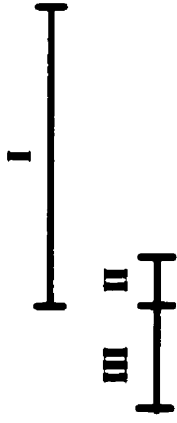
### 2.1. *Escherichia coli* strains, plasmids and bacteriophage

*E. coli* strains, plasmids, and bacteriophage used in this study are listed in Table 2.1. The *E. coli katG* gene encoding HPI catalase-peroxidase was originally cloned into a pBR322 derived plasmid to generate pBT22 (Triggs-Raine and Loewen, 1987), but was cloned into pSK+ or pKS- (Stratagene Cloning Systems) as pAH6 and pAH8, respectively, for site-directed mutagenesis and subsequent mutant protein expression. Strain CJ236, harbouring plasmids pAH2, pAH10, or pAH300 containing subcloned fragments I, II, or III of the *E. coli katG* gene (Fig. 2.1) respectively, was used for generation of single-stranded, uracil-containing, DNA templates employed for site-directed mutagenesis. Strain NM522 was used for cloning, plasmid propagation, and occasional production of single-stranded DNA for sequencing. Helper phage R408 was used for infection of strains CJ236 and NM522 to generate single-stranded DNA. Strain JM109 was used for production of plasmid DNA for double-stranded DNA sequencing. Strain UM262, which is catalase negative, was used for routine expression of catalase proteins from various plasmids. Strains MP180, UM120, and UM202 which are wild type, EchPII negative, and EchPI negative, respectively, were used in studies characterizing the intracellular location of EchPI. The *M. tuberculosis katG* gene, originally in pYZ55 (Zhang *et al.*, 1992), was recloned as an *EcoRV-KpnI* fragment into pSK+ as pAH1 (Fig. 2.1), which was then used to express MtHPI protein in UM262. Plasmids pQE11 (Qiagen) and pBAD24 (Guzman *et al.*, 1995) were used to construct pBAD-KAT and subsequently pAH6-H. Both plasmids contain *E. coli katG* modified to encode a N-terminal polyhistidine-tagged EchPI protein.

**Table 2.1.** Summary of *Escherichia coli* strains, plasmids and bacteriophage used in this study.

Genotype or characteristics	Source	
<b><u>Strains</u></b>		
CJ236	<i>dut1 ung1 thi-1 relA1/pCJ105/·cam<sup>r</sup>F'</i>	Kunkel <i>et al.</i> , 1987
NM522	<i>supE Δ(lac-proAB) hsd-5 [F' proAB lacI<sup>q</sup> lacZΔ15]</i>	Mead <i>et al.</i> , 1985
JM109	<i>recA1 supE44 endA1 hsdA1 hsdR17 gyrA96 relA1 thi Δ(lac-proAB)</i>	Yanisch-Perron <i>et al.</i> , 1985
UM262	<i>recA katG::Tn10 pro leu rpsL hsdM hsdR endI lacY</i>	Loewen <i>et al.</i> , 1990
MP180	<i>thi-1, HfrH</i>	Pearson, 1972
UM120	as MP180, but <i>katE12::Tn10</i>	Loewen and Triggs, 1984
UM202	as MP180, but <i>katG17::Tn10</i>	Loewen <i>et al.</i> , 1985
<b><u>Plasmids</u></b>		
pSK+, pKS-	Amp <sup>R</sup>	Stratagene Cloning Systems
pYZ55 (pUC18, <i>mtkatG</i> clone)	Amp <sup>R</sup>	Zhang <i>et al.</i> , 1992
pBT22 (pBR322, <i>E. coli katG</i> clone)	Amp <sup>R</sup>	Triggs-Raine and Loewen, 1987
pAH8 (pKS-, <i>E. coli katG</i> clone)	Amp <sup>R</sup>	this study
pAH6 (pSK+, <i>E. coli katG</i> clone)	Amp <sup>R</sup>	this study
pAH1 (pSK+, <i>M. tuberculosis katG</i> clone)	Amp <sup>R</sup>	this study
pAH2 (pSK+, subclone I)	Amp <sup>R</sup>	this study
pAH10 (pSK+, subclone II)	Amp <sup>R</sup>	this study
pAH300 (pSK+, subclone III)	Amp <sup>R</sup>	this study
pQE11	Amp <sup>R</sup>	Qiagen Inc.
pBAD24	Amp <sup>R</sup>	Guzman <i>et al.</i> , 1995
pBAD-KAT (pBAD24, H- <i>E. coli katG</i> clone)	Amp <sup>R</sup>	this study
pAH6-H	Amp <sup>R</sup>	this study
<b><u>Bacteriophage</u></b>		
R408 (helper phage)		Stratagene Cloning Systems

### A. *E. coli* *katG*



*EcoRI* (338-343)

*Hind* III (1)

*Cla* I (485-490)

*Bam*H I (1225-1230)

*Hind* III (3964)

*katG*

2178

### B. *M. tuberculosis* *katG*

*EcoRV* (1)

*Kpn* I (2901)

*katG*

2211

**Fig. 2.1.** Simplified restriction maps of the chromosomal inserts containing A. the *E. coli* *katG* gene in plasmids pBT22/ pAH6/ pAH8 and B. the *M. tuberculosis* *katG* gene in plasmid pAH1. The genes  are indicated as part of the chromosomal inserts  as are the three insert fragments (I, II, III) used to construct the subclone vectors employed in site-directed mutagenesis of *E. coli* *katG*.

## 2.2. Biochemicals and common reagents

All common biochemicals and reagents, as well as antibiotics, used in the course of these studies, were usually obtained from either Sigma Chemical Co. (St. Louis, Mo.), or from Fisher Scientific Ltd (Mississauga, Ont.). Media used for growth of cell cultures were usually obtained from GIBCO-BRL Ltd. (Burlington, Ont.). Unless otherwise stated, solutions were normally prepared using reverse osmosis distilled water.

## 2.3. Media, growth conditions and storage of cultures

*E. coli* cultures were usually grown in LB (Luria-Bertani) medium containing 10 g/l tryptone, 5 g/l yeast extract, and 5 g/l NaCl. Solid LB media contained between 14 and 20 g/l agar. Ampicillin was added to between 100 and 250 µg/ml for maintenance of selection pressure on plasmid-harboring strains grown in liquid media, and to 100 µg/ml for growth on solid media. Chloramphenicol was added to 40 µg/ml in order to maintain the presence of the F' episome for the growth of strain CJ236. In addition, tetracycline was occasionally added to 30 µg/ml to maintain selection pressure for growth of strain UM262. Growth of strains harbouring pBAD-KAT was in glucose minimal medium containing 6g Na<sub>2</sub>HPO<sub>4</sub>, 3g KH<sub>2</sub>PO<sub>4</sub>, 0.5g NaCl, 1g NH<sub>4</sub>Cl, 50mg casamino acids per litre, autoclaved, with the following sterile solutions added: MgSO<sub>4</sub> to 1mM, vitamin B1 to 1 nM, glucose to 0.3% w/v, and 1ml of a trace elements solution comprising 2.5 g FeSO<sub>4</sub>·H<sub>2</sub>O, 2.9 g H<sub>3</sub>BO<sub>4</sub>, 1.2 g CoSO<sub>4</sub>·7H<sub>2</sub>O, 0.1 g CuSO<sub>4</sub>·5H<sub>2</sub>O, 0.09 g MnCl<sub>2</sub>·4H<sub>2</sub>O, 2.5 g Na<sub>2</sub>MoO<sub>4</sub>·7H<sub>2</sub>O, 2.1 g ZnSO<sub>4</sub>·7H<sub>2</sub>O, and 5 ml conc. H<sub>2</sub>SO<sub>4</sub> per litre. For expression of protein from the pBAD-KAT plasmid, glucose minimal medium was supplemented to 0.2% (w/v) L-arabinose (Sigma).

*E. coli* strains in both liquid and solid media were usually grown at 37°C, but 28°C was used for cells in liquid media expressing protein mutants. In liquid media, all strains were grown with good aeration in shake flasks. Long term storage of stock cultures was

in 8% dimethylsulfoxide at -60°C. Bacteriophage R408 was maintained at 4°C in LB culture supernatant.

## **2.4. DNA Manipulation**

### **2.4.1. Preparation of synthetic oligonucleotides**

Oligonucleotides used for mutagenesis were synthesized using a PCR-Mate DNA synthesizer (Applied Biosystems Inc.). Extraction of oligonucleotide DNA from the synthesis columns was accomplished by gently and repetitively washing the columns with 1 ml volumes of concentrated NH<sub>4</sub>OH. The NH<sub>4</sub>OH wash was then incubated at 55°C overnight, evaporated to dryness under vacuum, and resuspended in HPLC grade distilled water and stored at -20°C until further use. Concentrations of oligonucleotide DNA were determined spectrophotometrically at 260nm, where 1 unit of absorbance ≈ 20 µg / ml single-stranded oligonucleotide DNA (Sambrook *et al.*, 1989).

Oligonucleotides used for site-directed mutagenesis were phosphorylated at the 5' end using T4 kinase (GIBCO-BRL) according to Ausubel *et al.* (1989). Approximately 100 ng of oligonucleotide DNA in a volume of 25 µl, containing 1mM ATP and 10 units of kinase were incubated in appropriately diluted buffer supplied by the manufacturer at 37°C for 30min. The reaction was terminated by heat inactivation at 65°C for 5min.

### **2.4.2. DNA isolation and purification**

Plasmid DNA was isolated according to Sambrook *et al.* (1989). Procedures were carried out at 4°C. Plasmid containing cells from 5 ml LB cultures grown to stationary phase were pelleted by centrifugation and resuspended in 0.2 ml volumes Tris-glucose-EDTA buffer (25 mM Tris-HCl, pH 8.0, 1% glucose, 10 mM Na-EDTA). Resuspended cells were lysed by addition of 0.4 ml 1% SDS (w/v), 0.2 M NaOH solution and gentle mixing. This was then neutralized by addition of 0.3 ml 6.2 M ammonium acetate, pH

5.9. After 10 min incubation, the mixture was centrifuged twice to remove all precipitates. Plasmid DNA was then precipitated by addition of 0.55 ml isopropanol to the remaining supernatant followed by a 15 min incubation at room temperature. Plasmid DNA was pelleted by centrifugation, washed twice with 70% (v/v) ice-cold ethanol, and then dried under vacuum. The DNA pellet was either stored in this condition at -20°C or was resuspended in HPLC grade distilled water or TE buffer (10 mM Tris, pH 8, 1 mM Na-EDTA) prior to being stored at -20°C until further use.

Preparation of single-stranded template DNA for site-directed mutagenesis or DNA sequencing was carried out according to Vieira and Messing (1987). Plasmid containing cells in a 5 ml LB culture in early exponential phase were infected with 10-50  $\mu$ l of helper phage R408 ( $10^{11}$ - $10^{12}$  PFU per ml) and grown overnight. After centrifuging 1-2 ml of culture in order to remove cells and debris, a solution of 300  $\mu$ l of 1.5 M NaCl, 20% PEG 6000 was added per ml of medium supernatant and mixed. This mixture was incubated for 15 min at room temperature and then centrifuged to pellet the phage particles. The pellet was then resuspended in TE buffer on ice and extracted first with an equal volume of buffer-saturated phenol, followed by extraction with an equal volume of water-saturated chloroform. Single-stranded DNA was precipitated by addition of an equal volume of 7.5 M ammonium acetate, pH 7.5 and 4 volumes of ice-cold 95% ethanol followed by incubation at -20°C for 30min. Single-stranded DNA was recovered by centrifugation and the pellet washed 3 times with 70% (v/v) ethanol. The dried pellet was stored at -20°C until further use.

#### **2.4.3. Restriction nuclease digestion**

Restriction nucleases and buffers used in this study were products of GIBCO-BRL Ltd. Restriction digestions were carried out at 37°C for 2-5hrs in total volumes of 10 $\mu$ l, containing 1  $\mu$ g RNase, 1  $\mu$ l of 10X appropriate buffer provided by the supplier, -1-5  $\mu$ g DNA, and 0.5-1  $\mu$ l (50-2,500 Units) of endonuclease. 5'-Phosphate groups of vector

DNA were removed during the latter 0.5-1 h of restriction digestions by addition of 12.5-25 units calf intestinal alkaline phosphatase (GIBCO-BRL).

#### **2.3.4. Agarose gel electrophoresis**

Electrophoresis of restriction endonuclease digested DNA was performed according to Sambrook *et al.* (1989). Agarose gels consisting of TAE buffer (40 mM Tris-Acetate and 1 mM EDTA, pH 8.0), 1-2% (w/v) agarose, and 0.1 µg/ml ethidium bromide were cast in Bio-Rad Mini Sub Cell plexiglass horizontal electrophoresis trays. Samples of 10 µl volumes were mixed with 3 µL Stop buffer (40% [v/v] glycerol, 10 mM EDTA pH 8.0, 0.25% [w/v] bromophenol blue). 1 kb DNA Ladder or 1kbPlus DNA Ladder (GIBCO-BRL) were used as molecular weight size standards. Electrophoresis was carried out at 40-60 mA constant current in TAE buffer, usually until the bromophenol blue marker dye front had migrated approximately half the length of the gel. Following electrophoresis, DNA bands were visualized with ultraviolet light and recorded using a red filter with Polaroid type 667 black and white film, or in digitized form using a Gel Doc 1000 image capture system (Bio-Rad).

#### **2.4.5. Ligation**

DNA fragments to be ligated were excised from agarose gels and purified using the GeneClean DNA extraction kit (Bio/Can Scientific Inc.) according to the instructions supplied by the manufacturer. In cases where fragments of DNA to be recovered were less than 200 bp in length, the incubation step with Glass Milk™ was carried out 30 min longer than recommended, to allow for better DNA adherence and recovery. Ligation of insert DNA into vector DNA was carried out according to Sambrook *et al.* (1989). Purified DNA was mixed in a ratio of 2-3 of insert to vector in 10 µl volumes, containing 1 unit of T4 DNA ligase (GIBCO-BRL), and the manufacturer's supplied buffer at the

appropriate concentration. Ligation mixtures were incubated overnight at 15°C. A mixture with no insert DNA added was used as the control.

#### **2.4.6. Transformation**

Transformation of *E. coli* cells with the various plasmids was achieved according to Chung *et al.* (1989). 5 ml LB cultures of cells grown to exponential phase (2-4h) were harvested by centrifugation and made competent by resuspension in ice-cold 0.1 M CaCl<sub>2</sub> for at least 1 h. 2-10 µg DNA was usually added to 100 µl of this cell suspension, followed by a further 30-45min incubation on ice, and a 90 s heat shock at 42°C. The cells were then added to 0.9 ml LB medium and incubated at 37°C for 45-60 min without aeration. The mixture was then either spread-plated, or (in the case of ligation mixture transformations) mixed with 2.5-3 ml molten (50°C) R-Top agar (0.125 g yeast extract, 1.25 g tryptone, 1 g NaCl, 1 g agar per 125 ml volume with 0.25 ml 1M CaCl<sub>2</sub> and 0.42 ml 30% glucose sterile solutions added after autoclaving) and poured onto ampicillin-containing LB plates.

#### **2.4.7. DNA sequencing**

Sequencing of DNA was performed using the method of Sanger *et al.* (1977). Sequencing was carried out manually with either single or double stranded DNA templates using primers shown in Table 2.2. To prepare a double stranded DNA template, 5 µg plasmid DNA was resuspended and denatured in a 40 µl volume of 0.4M freshly prepared NaOH. This mixture was then incubated for 10min. at 37°C, and then reprecipitated by addition of 10 µl 3 M sodium acetate, pH 4.8 and 140 µl ice-cold 95% ethanol. Following incubation at -20°C for 30min, the DNA pellet was recovered by centrifugation, washed once with 1ml 95% ice-cold ethanol, and once with 0.1ml 70% ice-cold ethanol, and then evaporated to dryness under vacuum. Annealing and sequencing reactions were carried out using a T7 Sequencing Kit (Pharmacia) according

to the specifications of the supplier and using 5-15  $\mu\text{Ci}$  [ $\alpha$ - $^{32}\text{P}$ ]dATP (NEN-DuPont).

Reaction mixtures were separated and resolved on 8% (w/v) polyacrylamide vertical slab gels containing 7 M urea, 0.13 M Tris, 0.13 M boric acid, and 10 mM EDTA.

Electrophoresis was carried out at 18-24mA constant current in TBE buffer (90 mM Tris, 89 mM borate, 2.2 mM EDTA) for 1.5-5 h as required. Dried gels were exposed to X-ray film (Kodak X-OMAT AR) in order to visualize the DNA bands.

#### **2.4.8. In vitro mutagenesis strategy.**

Mutagenesis was carried out according to the protocol of Kunkel *et al.* (1987) with modification. Subclones constructed from parts of the chromosomal insert containing the *E. coli katG* gene were mutagenized, instead of the entire *E. coli katG* gene, in order to limit the amount of subsequent sequencing required to confirm the mutations in both the subclones and the subclone inserts when re-inserted into the *E. coli katG* gene. A simplified restriction map of *E. coli katG* that indicates the locations of individual subclone fragments is shown in Fig. 2.1. Target codons for mutagenesis were selected from the DNA sequence of *ekatG* shown in Fig. 2.2. DNA sequences for the oligonucleotides used in mutagenesis are listed in Table 2.2. Mutagenesis was performed by annealing the phosphorylated oligonucleotides encoding the desired base modifications to uracil-containing single-stranded DNA templates obtained from the appropriate Bluescript phagemid subclone. The complementary DNA strand was then synthesized *in vitro* by unmodified T7 DNA polymerase (New England Biolabs) using the annealed oligonucleotide as the primer. The 3' and 5' ends of the completed complementary strand were ligated by including T4 DNA ligase (GIBCO-BRL) in the reaction mixture. The DNA was then transformed into NM522 cells where the uracil-containing templates were degraded. Plasmid DNA recovered from transformants was further transformed into JM109, recovered from this strain, and used to screen for the desired mutation in the plasmid subclone by DNA sequencing. Upon identification of a

**Fig. 2.2.** Nucleotide sequence of *E. coli katG* in the chromosomal insert of pBT22, pAH6, and pAH8 plasmids. Sequencing primers and mutagenic oligonucleotides showing base changes are indicated, as are *restriction endonuclease recognition sequences* used for subcloning and excision of an internal gene fragment. 3' ends of sequencing primers are indicated by arrows. The promoter sequences (-35 and -10), the Shine-Dalgarno sequence (SD), and the putative transcription terminator sequences are also indicated in the figure (revised and modified from Triggs-Raine *et al.* 1988, with appended sequence data from Blattner *et al.* 1997, indicating an open reading frame (ORF) in the *katG-gldA* intergenic region).

**HindIII**

```

AAGCTTAATTAAGATCAATTTGATCTACATCTCTTTAACCAACAATATGTAAGATCTCAA    60
CTATCGCATCCGTGGATTAATTCAATTATACTTCTCTCTAACGCTGTGTATCGTAACGG    120
                               -35                               -10

                               -----T G(novo PstI)-----
TAACACTGTAGAGGGGAGCACATTG ATG AGC ACG TCA GAC GAT ATC CAT    169
      SD                               Met Ser Thr Ser Asp Asp Ile His    8

AAC ACC ACA GCC ACT GGC AAA TGC CCG TTC CAT CAG GGC GGT CAC    214
Asn Thr Thr Ala Thr Gly Lys Cys Pro Phe His Gln Gly Gly His    23

GAC CAG AGT GCG GGG GCG GGC ACA ACC ACT CGC GAC TGG TGG CCA    259
Asp Gln Ser Ala Gly Ala Gly Thr Thr Thr Arg Asp Trp Trp Pro    38

                               -----(G1)-----
AAT CAA CTT CGT GTT GAC CTG TTA AAC CAA CAT TCT AAT CGT TCT    304
Asn Gln Leu Arg Val Asp Leu Leu Asn Gln His Ser Asn Arg Ser    53
-->                               EcoR I
AAC CCA CTG GGT GAG GAC TTT GAC TAC CGC AAA GAA TTC AGC AAA    349
Asn Pro Leu Gly Glu Asp Phe Asp Tyr Arg Lys Glu Phe Ser Lys    68

TTA GAT TAC TAC GGC CTG AAA AAA GAT CTG AAA GCC CTG TTG ACA    394
Leu Asp Tyr Tyr Gly Leu Lys Lys Asp Leu Lys Ala Leu Leu Thr    83

GAA TCT CAA CCG TGG TGG CCA GCC GAC TGG GGC AGT TAC GCC GGT    439
Glu Ser Gln Pro Trp Trp Pro Ala Asp Trp Gly Ser Tyr Ala Gly    98

                               -----TAC(H106Y)-----
                               -----TGC(H106C)-----
                               -----CTG(H106L)-----
                               -----TTT(W105F)-----
                               -----TGT(W105C)-----
                               -----CTG(W105L)-----
                               -----AAA(R102K)-----
                               -----TGT(R102C)-----
                               -----CTG(R102L)-----
CTG TTT ATT CGT ATG GCC TGG CAC GGC GCG GGG ACT TAC CGT TCA    484
Leu Phe Ile Arg Met Ala Trp His Gly Ala Gly Thr Tyr Arg Ser    113
Cla I
ATC GAT GGA CGC GGT GGC GCG GGT CGT GGT CAG CAA CGT TTT GCA    529
Ile Asp Gly Arg Gly Gly Ala Gly Arg Gly Gln Gln Arg Phe Ala    128

```

CCG CTG AAC TCC TGG CCG GAT AAC GTA AGC CTC GAT AAA GCG CGT 574  
 Pro Leu Asn Ser Trp Pro Asp Asn Val Ser Leu Asp Lys Ala Arg **143**

----(G2)----->

CGC CTG TTG TGG CCA ATC AAA CAG AAA TAT GGT CAG AAA ATC TCC 619  
 Arg Leu Leu Trp Pro Ile Lys Gln Lys Tyr Gly Gln Lys Ile Ser **158**

TGG GCC GAC CTG TTT ATC CTC GCG GGT AAC GTG GCG CTA GAA AAC 664  
 Trp Ala Asp Leu Phe Ile Leu Ala Gly Asn Val Ala Leu Glu Asn **173**

TCC GGC TTC CGT ACC TTC GGT TTT GGT GCC GGT CGT GAA GAC GTC 709  
 Ser Gly Phe Arg Thr Phe Gly Phe Gly Ala Gly Arg Glu Asp Val **188**

**Hpa I (Hinc II)**xx

TGG GAA CCG GAT CTG GAT GTT AAC TGG GGT GAT GAA AAA GCC TGG 754  
 Trp Glu Pro Asp Leu Asp Val Asn Trp Gly Asp Glu Lys Ala Trp **203**

xxxxxxxxxxxxxxxxxxxxxxxxxxxxxxxx**Hpa I fragment deletion**xxxxxxxxxxxxxxxxxxxxxxxxxxxxxxxx

------(G8)----->

CTG ACT CAC CGT CAT CCG GAA GCG CTG GCG AAA GCA CCG CTG GGT 799  
 Leu Thr His Arg His Pro Glu Ala Leu Ala Lys Ala Pro Leu Gly **218**

xx**Hpa I (Hinc II)**

GCA ACC GAG ATG GGT CTG ATT TAC GTT AAC CCG GAA GGC CCG GAT 844  
 Ala Thr Glu Met Gly Leu Ile Tyr Val Asn Pro Glu Gly Pro Asp **233**

------(G3)----->

CAC AGC GGC GAA CCG CTT TCT GCG GCA GCA GCT ATC CGC GCG ACC 889  
 His Ser Gly Glu Pro Leu Ser Ala Ala Ala Ile Arg Ala Thr **248**

TTC GGC AAC ATG GGC ATG AAC GAC GAA GAA ACC GTG GCG CTG ATT 934  
 Phe Gly Asn Met Gly Met Asn Asp Glu Glu Thr Val Ala Leu Ile **263**

-----TAC (H267Y)-----

GCG GGT GGT CAT ACG CTG GGT AAA ACC CAC GGT GCC GGT CCG ACA 979  
 Ala Gly Gly His Thr Leu Gly Lys Thr His Gly Ala Gly Pro Thr **278**

TCA AAT GTA GGT CCT GAT CCA GAA GCT GCA CCG ATT GAA GAA CAA 1024  
 Ser Asn Val Gly Pro Asp Pro Glu Ala Ala Pro Ile Glu Glu Gln **293**

GGT TTA GGT TGG GCG AGC ACT TAC GGC AGC GGC GTT GGC GCA GAT 1069  
 Gly Leu Gly Trp Ala Ser Thr Tyr Gly Ser Gly Val Gly Ala Asp **308**

GCC ATT ACC TCT GGT CTG GAA GTA GTC TGG ACC CAG ACG CCG ACC 1114  
 Ala Ile Thr Ser Gly Leu Glu Val Val Trp Thr Gln Thr Pro Thr **323**

------(G4)-----

CAG TGG AGC AAC TAT TTC TTC GAG AAC CTG TTC AAG TAT GAG TGG 1159  
 Gln Trp Ser Asn Tyr Phe Phe Glu Asn Leu Phe Lys Tyr Glu Trp **338**

→

GTA CAG ACC CGC AGC CCG GCT GGC GCA ATC CAG TTC GAA GCG GTA 1204  
 Val Gln Thr Arg Ser Pro Ala Gly Ala Ile Gln Phe Glu Ala Val **353**

**BamH I**

GAC GCA CCG GAA ATT ATC CCG GAT CCG TTT GAT CCG TCG AAG AAA 1249  
 Asp Ala Pro Glu Ile Ile Pro Asp Pro Phe Asp Pro Ser Lys Lys **368**

CGT AAA CCG ACA ATG CTG GTG ACC GAC CTG ACG CTG CGT TTT GAT 1294  
 Arg Lys Pro Thr Met Leu Val Thr Asp Leu Thr Leu Arg Phe Asp **383**

CCT GAG TTC GAG AAG ATC TCT CGT CGT TTC CTC AAC GAT CCG CAG 1339  
 Pro Glu Phe Glu Lys Ile Ser Arg Arg Phe Leu Asn Asp Pro Gln **398**

GCG TTC AAC GAA GCC TTT GCC CGT GCC TGG TTC AAA CTG ACG CAC 1384  
 Ala Phe Asn Glu Ala Phe Ala Arg Ala Trp Phe Lys Leu Thr His **413**

-----**TAA (K419END)**-----

AGG GAT ATG GGG CCG AAA TCT CGC TAC ATC GGG CCG GAA GTG CCG 1429  
 Arg Asp Met Gly Pro Lys Ser Arg Tyr Ile Gly Pro Glu Val Pro **428**

AAA GAA GAT CTG ATC TGG CAA GAT CCG CTG CCG CAG CCG ATC TAC 1474  
 Lys Glu Asp Leu Ile Trp Gln Asp Pro Leu Pro Gln Pro Ile Tyr **443**

AAC CCG ACC GAG CAG GAC ATT ATC GAT CTG AAA TTC GCG ATT GCG 1519  
 Asn Pro Thr Glu Gln Asp Ile Ile Asp Leu Lys Phe Ala Ile Ala **458**

GAT TCT GGT CTG TCT GTT AGT GAG CTG GTA TCG GTG GCC TGG GCA 1564  
 Asp Ser Gly Leu Ser Val Ser Glu Leu Val Ser Val Ala Trp Ala **473**

TCT GCT TCT ACC TTC CGT GGT GGC GAC AAA CGC GGT GGT GCC AAC 1609  
 Ser Ala Ser Thr Phe Arg Gly Gly Asp Lys Arg Gly Gly Ala Asn **488**

GGT GCG CGT CTG GCA TTA ATG CCG CAG CGC GAC TGG GAT GTG AAC 1654  
 Gly Ala Arg Leu Ala Leu Met Pro Gln Arg Asp Trp Asp Val Asn **503**

GCC GCA GCC GTT CGT GCT CTG CCT GTT CTG GAG AAA ATC CAG AAA 1699  
 Ala Ala Ala Val Arg Ala Leu Pro Val Leu Glu Lys Ile Gln Lys **518**

GAG TCT GGT AAA GCC TCG CTG GCG GAT ATC ATA GTG CTG GCT GGT 1744  
 Glu Ser Gly Lys Ala Ser Leu Ala Asp Ile Ile Val Leu Ala Gly **533**

GTG GTT GGT GTT GAG AAA GCC GCA AGC GCC GCA GGT TTG AGC ATT 1789  
 Val Val Gly Val Glu Lys Ala Ala Ser Ala Ala Gly Leu Ser Ile **548**

CAT GTA CCG TTT GCG CCG GGT CGC GTT GAT GCG CGT CAG GAT CAG 1834  
 His Val Pro Phe Ala Pro Gly Arg Val Asp Ala Arg Gln Asp Gln **563**

ACT GAC ATT GAG ATG TTT GAG CTG CTG GAG CCA ATT GCT GAC GGT 1879  
 Thr Asp Ile Glu Met Phe Glu Leu Leu Glu Pro Ile Ala Asp Gly **578**

TTC CGT AAC TAT CGC GCT CGT CTG GAC GTT TCC ACC ACC GAG TCA 1924  
 Phe Arg Asn Tyr Arg Ala Arg Leu Asp Val Ser Thr Thr Glu Ser **593**

CTG CTG ATC GAC AAA GCA CAG CAA CTG ACG CTG ACC GCG CCG GAA 1969  
 Leu Leu Ile Asp Lys Ala Gln Gln Leu Thr Leu Thr Ala Pro Glu **608**

ATG ACT GCG CTG GTG GGC GGC ATG CGT GTA CTG GGT GCC AAC TTC 2014  
 Met Thr Ala Leu Val Gly Gly Met Arg Val Leu Gly Ala Asn Phe **623**

GAT GGC AGC AAA AAC GGC GTC TTC ACT GAC CGC GTT GGC GTA TTG 2059  
 Asp Gly Ser Lys Asn Gly Val Phe Thr Asp Arg Val Gly Val Leu **638**

AGC AAT GAC TTC TTC GTG AAC TTG CTG GAT ATG CGT TAC GAG TGG 2104  
 Ser Asn Asp Phe Phe Val Asn Leu Leu Asp Met Arg Tyr Glu Trp **653**

AAA GCG ACC GAC GAA TCG AAA GAG CTG TTC GAA GGC CGT GAC CGT 2149  
 Lys Ala Thr Asp Glu Ser Lys Glu Leu Phe Glu Gly Arg Asp Arg **668**

GAA ACC GGC GAA GTG AAA TTT ACG GCC AGC CGT GCG GAT CTG GTG 2194  
 Glu Thr Gly Glu Val Lys Phe Thr Ala Ser Arg Ala Asp Leu Val **683**

TTT GGT TCT AAC TCC GTC CTG CGT GCG GTG GCG GAA GTT TAC GCC 2239  
 Phe Gly Ser Asn Ser Val Leu Arg Ala Val Ala Glu Val Tyr Ala **698**

AGT AGC GAT GCC CAC GAG AAG TTT GTT AAA GAC TTC GTG GCG GCA 2284  
 Ser Ser Asp Ala His Glu Lys Phe Val Lys Asp Phe Val Ala Ala **713**

TGG GTG AAA GTG ATG AAC CTC GAC CGT TTC GAC CTG CTG **TAATCT** 2329  
 Trp Val Lys Val Met Asn Leu Asp Arg Phe Asp Leu Leu **END** **726**

GACCCCGTTTCAGCGGCTGCTTGCTGGCAGTCGCTGAACGTTCTTTACCAGCGTATAGTGG 2389  
**transcription terminator**

**ORF**→

GCGAACGAAAACACTACACACTGGATCTCTCATGTCTGCCGAGGAAAGAGCAACCCACTGG 2449

CAATCAGTGGCCTGGTTGTGCTCACACTTATCTGGAGTTATAGCTGGATTTTCATGAAGC 2509

AAGTCACCAGTTACATCGGTGCCTTCGACTTTACCGCCTTACGCTGCATTTTCGGCGCTC 2569

TCGTTTTATTTCATCGTCCTTTTATTACGTGGTTCGCGGAATGCGCCCGACACCGTTTAAAT 2629

ACACCTTAGCCATTGCCCTGTTACAAACCTGCGGGATGGTTGGTCTGGCGCAGTGGGCGT 2689

TGGTCAGCGGAGGTGCGGGGAAGGTGGCGATCCTGAGCTATAACCATGCCGTTCTGGGTGG 2749

TGATTTTCGCCGCGTTGTTTCTCGGTGAACGCCTGCGACGTGGGCAATATTTTCGCGATTC 2809

TGATTGCCGCTTTCGGCTTATTTTGGTGTGTCAGCCGTGGCAACTCGATTTCTCTTCGA 2869

TGAAAAGTGCCATGCTGGCAATCCTCTCCGGCGTCAGTTGGGGGGCGAGCGCGATTGTTG 2929

CTAACGTCTGTATGCCCGTCATCCGCGCGTGGATTTATGTGCTTAACATCCTGGCAGA 2989

TGCTGTATGCGGCGCTGGTGATGAGTGTGGTCGCTTTACTGGTGCCGCAACGTGAAATTG 3049

ACTGGCAGCCCACCGTGTCTGGGCGCTGGCCTACAGTGGCATTCTGGCGACGGCACTGG 3109

CGTGGAGCTTATGGTTGTTTGTATTGAAAACTTGCCTGCCAGTATTGCCAGCTTAAGCA 3169

CACTGGCCGTTCCCGTTTTCGGCGTACTCTTTTCTGGTGGCTGCTCGGCGAGAATCCGG 3229

GGGCCGTTGAAGGTAGCGGTATTGTGCTGATTGTGCTGGCACTGGCGCTGGTGGAGCCGTA 3289

**←ORF**

AGAAAAAGAAGCCGTCAGTGTA AAAAGGATCTGAATTTTTTCTTCATGTGGGGCGATCT 3349

CTTATTTAACAAAATAACGATAATGCCCCACCATCCGCCAGTTAAACAGCACATCTTCTT 3409

CCTGCGCGCCTGCGCCAATGTTATGTATCACCAGCGGCGTACCGTCGCGGGCGAAGCCAT 3469  
CTGAAACCACCCCAATATGTGCCAGCCCGTTATCCAGTCGCCAGGAGACAATATCGCCCG 3529  
CTTGATAGTCACTGGGGTTCCTTGCTGGTGGGGCGTGTTTTATCATGGCGGCTAAACCAGG 3589  
TTTCCAGATTAGGCACCCGACGGTGATCGATGTTGCTGTCCGGGCGCTTTAACTTCCATT 3649  
TTTGCGGGTACTCAGCAAAATTCTTCGCCATATCTTCGTGAACCAGTTTCTGCAAATCGA 3709  
CCTTCTGGCTGCGCAATGCGCGGATCACCACATCGGAACATAACCCGCTTCTTGCGGAA 3769  
CATCACCGCCAGGATAAGTAAGCTGCACATACGCCGGATCGTAAAATAGCGTGCTGCCAA 3829  
TTTGCTGTCTGGCACCGTCTGCGATGGCAAGGTTGGTATTGGCCTGGATTTGTACCACGG 3889  
TTGGTGGAACGGCGGGAGATTTTAAGGAGTGGCTGGTAAATGCCGTTAGCAGGCTGAGCA 3949  
*Hind III*  
GCGCCAGTGAAGCTT 3964

**Table 2.2** Sequences of the oligonucleotides used for site-directed mutagenesis of *E. coli katG*.

<b>Primer name</b>	<b>Bases changed</b>	<b>Oligonucleotide sequence</b>
novo <i>Pst</i> I	GT→TG	5' -TGATGAGCACT <b>GC</b> CAGACGATATC
R102K	CGT→AAA	5' -TGTTTATT <b>AAA</b> ATGGCCTGG
R102C	CGT→TGT	5' -TGTTTATT <b>TGT</b> ATGGCCTGG
R102L	CGT→CTG	5' -TGTTTATT <b>CTG</b> ATGGCCTGG
W105F	TGG→TTT	5' -CGTATGGCC <b>TTT</b> CACGGCGCG
W105C	TGG→TGT	5' -CGTATGGCC <b>TGT</b> CACGGCGCG
W105L	TGG→CTG	5' -CGTATGGCC <b>CTG</b> CACGGCGCG
H106Y	CAC→TAC	5' -TGGCCTGG <b>TAC</b> GGCGCGGGGA
H106C	CAC→TGC	5' -TGGCCTGG <b>TGC</b> GGCGCGGGGA
H106L	CAC→CTG	5' -TGGCCTGG <b>CTG</b> GGCGCGGGGA
H267Y	CAT→TAC	5' -GCGGGTGGT <b>TAC</b> ACGCTGGGT
K419End	AAA→TAA	5' -ATGGGGCCG <b>TAA</b> TCTCGCTAC

mutated subclone, the complete subclone sequence was ascertained to ensure no other base changes apart from those desired had been introduced. The mutated subclone was then used to reconstruct the complete *E. coli katG* gene, which was then sequenced over the region containing the mutation for final confirmation. Reconstructed, mutated, *E. coli katG* clones were then transformed into UM262 for determination of enzyme activities and visualization of protein from crude extracts or whole cells by SDS-PAGE. Clones expressing high levels of variant HPI enzyme were then grown in larger scale for purification and characterization.

## **2.5. Purification of HPI catalase-peroxidases**

For small scale crude extracts used in determination of relative levels of protein expression, as well as catalase activity, plasmid containing cells were grown in either 5 ml LB medium in test tubes, or in 125 ml flasks of the same medium at 37°C for 16-20 h. The cells were then pelleted and resuspended in 1-2 ml 50mM potassium phosphate buffer, pH 7.0, sonically disrupted, and centrifuged to remove unbroken cells and debris; followed by assay for catalase activity and/or protein expression profile by SDS-PAGE. If only protein visualization was to be carried out (in the case of mutations that had low or no catalase activity), 10 - 50 µl aliquots of the cell suspensions were pelleted by centrifugation, directly resuspended in SDS protein sample buffer, and analyzed via SDS-PAGE.

For large scale preparations of wild type EchPI, MthPI, and mutant EchPI enzymes, UM262 cells overexpressing the desired protein from the appropriate plasmid borne genes were grown in 4-6 l volumes of LB medium containing 100 µg/ml ampicillin for 16-22 h at either 37 or 28°C with good aeration. Isolation of HPI proteins was performed according to Loewen and Switala (1986) with modifications. All steps were carried out at 4°C. Cells were harvested from the growth medium by centrifugation. The cell pellet (approximately 30 g wet weight from a 6 l culture) was then resuspended in

150-250 ml of 50 mM potassium phosphate buffer, pH 7.0 (A buffer). In most purifications, protease inhibitors PMSF and TPCK (100 mM stock solutions) were each added to a final concentration of 100  $\mu$ M, and EDTA (0.5 M stock solution) was added to a final concentration of 5 mM. The cells were disrupted by a single pass through a French pressure cell at 20,000 psi. Unbroken cells and debris were removed by centrifugation, yielding the crude extract, to which was added streptomycin sulfate to a final concentration of 2.5% (w/v). The resulting precipitates were removed by centrifugation and discarded. Solid  $(\text{NH}_4)_2\text{SO}_4$  was then added with gentle stirring to precipitate the desired protein. EchPI and most mutant EchPI proteins were found to precipitate in  $(\text{NH}_4)_2\text{SO}_4$  at 25-30% saturation, while MthPI was found to precipitate at 35-40% saturation. Pellets from the  $(\text{NH}_4)_2\text{SO}_4$  precipitations were usually resuspended in 20-40 ml of buffer A. In the case of MthPI preparations, the resuspension was heat treated at 42°C for 45min. Resuspensions were centrifuged to remove any remaining precipitates, and dialyzed overnight using a 12,000-14,000 molecular weight cutoff membrane, against approximately 100 volumes buffer A. The dialyzed resuspensions were then centrifuged and loaded onto a 2.5cm x 23cm column of DEAE-cellulose A-500 (cellufine, Amicon) equilibrated with buffer A. The column was washed with buffer A until the  $\text{OD}_{280}$  of the eluting solution was below 0.025. The protein of interest was then eluted with a 0-0.25M NaCl linear gradient in buffer A, usually in a total volume of 1 l. Eighty drop fractions were collected throughout. Selected fractions were pooled and concentrated under nitrogen in a stirred pressure cell (Model 8050, Amicon) using a YM-30 (Amicon) membrane, to volumes of between 5-10 ml. The concentrated protein sample was then dialyzed against approximately 100-500 volumes buffer A overnight. For the EchPI and mutant EchPI enzymes, no further purification was usually necessary after this step. In the case of MthPI samples, however, the dialyzed protein was loaded onto a 3 x 50 cm Sephadex G-200 column equilibrated with buffer A. Protein was eluted from the column using buffer A, collecting 20 drop fractions throughout. Selected

fractions were then pooled and concentrated as before. Purity of column fractions recovered was normally determined based on OD<sub>280</sub> and catalase activity elution profiles, but occasionally on OD<sub>407/280</sub> (heme/protein) ratio and, in the case of the final column step for the MthPI purification as well as for purification of EchPI mutants having little or no activity, on SDS-PAGE analysis of the fractions. Concentrated, dialyzed samples were then aliquoted to Eppendorf tubes in 0.5 - 1 ml volumes and either dried and/or stored frozen at -60°C until further use.

## **2.6. Polyacrylamide gel electrophoresis of proteins and staining**

Denaturing SDS-PAGE was carried out according to Weber *et al.* (1972). Discontinuous 4% stacking and 8 or 10% separating polyacrylamide gels were cast as vertical slabs of dimensions 15 x 15 cm and 2 mm thickness (large gels) or 10 x 10 cm and 0.5 mm thickness (mini gels). Samples loaded on large gels usually contained about 100 µg protein for crude extracts and 5-10 µg protein for purified proteins. Samples loaded on mini gels usually contained between 5-25 µg protein. Protein samples were mixed with equal volumes of reducing denaturing sample buffer (3.4 mg/ml NaH<sub>2</sub>PO<sub>4</sub>, 10.2 mg/ml Na<sub>2</sub>HPO<sub>4</sub>, 10 mg/ml SDS, 0.13 mM 2-mercaptoethanol, 0.36 g/ml urea and 0.15% bromophenol blue) and boiled for 3 min before loading. Samples were run with 30-50 mA constant current in a BIO-RAD Protean II electrophoresis system (large gels), or at 125-175 V constant voltage in a BIO-RAD Mini-Protean II electrophoresis system (mini gels), using a running buffer containing 14 g glycine, 3 g Tris base, and 1 g SDS per 1 l. Gels were stained for protein by incubation in staining solution containing 0.5 g/l Coomassie Brilliant Blue R-250, 30% ethanol and 10% acetic acid. Gels were destained using a solution containing 15% methanol and 7% acetic acid until the background was judged to be clear, followed by a final soak in a solution containing 7% acetic acid and 1% glycerol. Gels were then mounted on 3mm (Whatman) paper, covered with a clear plastic film, and dried at 60-80°C for 1-4 h on a slab gel dryer under vacuum (Savant).

Non-denaturing PAGE was carried out according to Davis (1964). 9% acrylamide continuous gels were cast as vertical slabs as described for SDS-PAGE. When protein was to be visualized on the gels, sample amounts loaded were as described for SDS-PAGE. When enzymatic activity was to be visualized on the gels, samples were loaded in amounts corresponding to 1 unit catalase activity, or 40 units peroxidase activity. Samples were mixed with equal volumes of 2X sample buffer containing 0.125 M Tris, pH 6.8, 10% (w/v) glycerol, and 0.2% bromophenol blue (modified from Bio-Rad Mini-Protean II instruction manual). Electrophoresis was performed as described for SDS-PAGE, but using a running buffer containing 4.8 g Tris base, 20.8 g glycine per 4 l.

Gels were stained for peroxidase activity according to the method of Gregory and Fridovich (1974) using 3, 3'-diaminobenzidine (DAB) as the electron donor species. Gels were soaked in a solution containing 20 mg DAB in 80 ml of 50 mM potassium phosphate buffer, pH 7.0 for 45 min., followed by a brief wash with water and then a second soak in the same buffer containing 20 mM H<sub>2</sub>O<sub>2</sub>. Peroxidase activity was visualized as brown bands on the gels. Colour development was usually complete within 30 min.

Gels were stained for catalase activity according to the method of Clare *et al.* (1984) with minor modifications. Gels were soaked in a solution containing 50 µg/ml horseradish peroxidase (Sigma) in 50 mM potassium phosphate, pH 7.0 for 45 min, then briefly washed with water, incubated in 20 mM H<sub>2</sub>O<sub>2</sub> for 10 min, and lastly, soaked in a solution of 40 mg DAB in 80 ml water containing 1 ml glycerol. Catalase activity was visualized as zones of clearing on a brown background. Colour development was usually complete within 30 - 60 min.

Staining for peroxidase-mediated oxidation of isoniazid (INH) was performed by soaking the gels in 200 ml potassium phosphate, pH 7.0, containing 9mM INH (Sigma), 0.3 mM Nitro Blue tetrazolium (NBT), and 60 mM H<sub>2</sub>O<sub>2</sub>. INH oxidation was visualized as purple bands on the gels. Colour development was usually complete between 30 - 60

min. Incubation of gels for 16 h in the staining solution from which NBT was omitted also resulted in band development, but the bands were much weaker than those seen using the complete staining solution. When staining of gels was judged to be complete, they were rinsed with water, and soaked in 7% acetic acid, 1% glycerol for several hours or overnight, prior to mounting.

## **2.7. Enzymatic assays and protein quantitation**

Catalase activity was determined by the method of Rørth and Jensen (1967) in a Gilson oxygraph equipped with a Clark electrode. One unit of catalase is defined as the amount of enzyme that decomposes 1  $\mu\text{mol}$   $\text{H}_2\text{O}_2$  in 1 min in 60 mM  $\text{H}_2\text{O}_2$  at 37°C, pH 7.0. Appropriately diluted samples of enzyme or cell culture aliquots were incubated in 1.8 ml 50 mM potassium phosphate buffer, pH 7.0 for 0.5-1.0 min at 37°C followed by addition of  $\text{H}_2\text{O}_2$  to a final concentration of 60 mM. Catalase activity as units/ml was determined from the slope of the plot representing oxygen evolution. Specific catalase activity was expressed as  $\text{units}\cdot\text{ml}^{-1}\cdot\text{mg}^{-1}$  purified protein.

Peroxidase activity was determined spectrophotometrically by the o-dianisidine method described in the Worthington Enzyme Catalogue (Worthington Chemical Co., 1969). Assays were carried out at room temperature in 1 ml final assay volumes containing 1 mM  $\text{H}_2\text{O}_2$ , 0.34 mM o-dianisidine in 50 mM potassium phosphate, pH 6.0. Aliquots (5-20  $\mu\text{l}$ ) of the appropriately diluted enzymes were added to initiate the reaction. Peroxidase activity was determined by the  $\Delta A_{460}/\text{min}$  average over periods of 2-5 min and expressed as  $\text{units}\cdot\text{mg}^{-1}\cdot\text{ml}^{-1}$  purified protein calculated as :  $(\Delta A_{460}/\text{min})/ (11.3 \times \text{mg enzyme}/ \text{ml reaction mixture})$ . Peroxidase activity was also determined spectrophotometrically by the 2,2- *azinobis*(3-ethylbenzothiazolinesulfonic acid) (ABTS) method (Smith *et al.*, 1990) with minor modifications. Assays were carried out in 1 ml final assay volumes containing 2.5 mM  $\text{H}_2\text{O}_2$ , 0.5 mM ABTS in 50mM potassium phosphate, pH 6.0. Aliquots (5-20  $\mu\text{l}$ ) of the appropriately diluted enzymes were added to

initiate the reaction. Peroxidase activity was determined by the  $\Delta A_{405}/\text{min}$  average over periods of 0.25- 2.0 min. Activities were expressed as  $\mu\text{moles}\cdot\text{min}^{-1}\cdot\text{ml}^{-1}$  by using a molar absorption coefficient of the ABTS product of  $36.8 \text{ mM}^{-1} \text{ cm}^{-1}$ .

Peroxidase-mediated oxidation of isoniazid (INH) was determined based on the methods developed by Shoeb *et al.* (1985) for horseradish peroxidase. Reduction of nitroblue tetrazolium (NBT) to formazan dye by enzymatically oxidized radical species of isoniazid was monitored spectrophotometrically at 560nm. Assays were carried out in 1 ml final volumes containing 9 mM INH, 0.2 mM NBT in 50mM potassium phosphate, pH 7.0, at room temperature. For single peroxide addition assays,  $\text{H}_2\text{O}_2$  was added to the reaction mixture to give the desired final concentration. Aliquots (5-20  $\mu\text{l}$ ) of the appropriately diluted enzymes were then added to initiate the reaction. For assays under conditions of constant peroxide generation, 5-10  $\mu\text{g}$  glucose oxidase was added to the reaction mixture followed by the enzyme to be assayed. 20  $\mu\text{l}$  of 0.2 mM D-glucose was added to initiate the reaction. A molar extinction coefficient of  $15,000 \text{ M}^{-1} \text{ cm}^{-1}$  for the monoformazan product from the reduction of NBT was used (Auclair and Voisin, 1985)

Protein concentration (mg/ ml) was estimated spectrophotometrically based on  $A_{280}/A_{260}$  ratios (Layne, 1957). Specific activities were always determined as the average of a minimum of two or more individual determinations.

## **2.8. Absorption spectrophotometry**

Absorption spectra, time courses, and peroxidatic assays were performed using a Milton Roy MR3000 Spectrophotometer or a Pharmacia Ultrospec 4000 Spectrophotometer. All experiments were performed at ambient temperature in 1 ml quartz, semimicro cuvettes. Proteins were normally diluted in 50 mM potassium phosphate buffer, pH 7.0 unless otherwise stated, and the same buffer was used as a reference. For preparation of spectral and time course plots, data collected were transferred to IBM Lotus or SigmaPlot computer program file formats .

## **2.9 Spheroplasting procedures and fraction analysis**

### **2.9.1. Spheroplasting procedures**

30 ml *E. coli* LB cultures (supplemented with 100 µg/ml ampicillin as needed) were grown at 37°C with good aeration for 5 h to late logarithmic phase. Cells were harvested by centrifugation and the pellets washed twice with 5% NaCl. Spheroplasting and fractionation was then carried out according to the method of Merchante *et al.* (1995) with modifications. Cells were resuspended in 1-2 ml of an isotonic buffer solution containing 50mM Tris-HCl, pH 8.0, 16 mM MgCl<sub>2</sub>, and 50% (w/v) sucrose. Lysozyme was added to a final concentration of 200 µg/ml, followed by addition of PMSF to 0.1 mM final concentration. The resuspensions were then incubated for 30-60 min at 37°C. Spheroplasts were obtained by centrifugation at 21,000x g for 15min. In cases where lysis was evident from the inability to obtain a compact pellet, the sample was discarded. The spheroplast supernatant fractions containing periplasmic material were carefully collected. The spheroplast pellets were immediately resuspended in 1 ml of a lysis buffer containing 50 mM Tris-HCl, pH 8.0 and 5 mM MgSO<sub>4</sub> and sonically disrupted to obtain the the cytoplasmic and inner membrane containing fractions. Control experiments were carried out following essentially the same procedure, but omitting the the sucrose from the buffer used during lysozyme digestion

### **2.9.2. Enzymatic assays of the spheroplasting fractions**

The catalase assays employed have been described in section 2.7. Glucose-6-phosphate dehydrogenase was used as the cytoplasmic marker and was determined by the method of Merchante *et al* (1995). NADP<sup>+</sup> reduction was monitored spectrophotometrically at 340 nm in the presence of 1 mM glucose 6- phosphate. One unit of glucose-6-phosphate dehydrogenase activity corresponds to an increase in A<sub>340</sub> by

0.001 min<sup>-1</sup>•ml<sup>-1</sup>. Alkaline phosphatase was used as the periplasmic marker, and was determined according to the method of Torriani (1968). The production of free *p*-nitrophenol due to phosphate group cleavage of the Sigma 104 assay substrate was monitored spectrophotometrically at 410 nm. One unit of alkaline phosphatase activity corresponds to an increase of the A<sub>410</sub> by 1.0 min<sup>-1</sup>•ml<sup>-1</sup> at pH 8.2.

### **2.10. In situ immunogold staining**

Cell suspensions were fixed in 4% formaldehyde prepared from paraformaldehyde in phosphate-buffered saline (PBS) pH 7.2 for 2 h at room temperature. The suspension was centrifuged and the pellet resuspended in 3% agarose, cooled, cut into cubes of approximately 1 mm<sup>3</sup> and washed in PBS pH 7.2. The cubes were dehydrated through a graded ethanol series to 100% ethanol and infiltrated with LR White using LR White plus 100% ethanol solutions of 1:1 for 16 h, 3:1 for 6.5 h, and 100% LR White for 16 h, and then 6.5 h. The last suspension was polymerized at 50°C for 24 h in the absence of oxygen. Sections were cut on a Reichert Ultracut ultratome and collected on formvar-coated nickel grids. Sections were floated on 1% bovine serum albumin in PBS for 30 min and washed for 10 min in PBS. The grids were then floated on a solution of primary rabbit antibody raised against *E. coli* HPI diluted 1:25 in PBS containing 0.05% Tween 20 and 0.1% BSA for 3.5 h. After washing in PBS containing 1% BSA, the grids were floated for 1 h on a drop of goat anti-rabbit IgG conjugated to 10 nm gold spheres diluted 1:15 with PBS containing 0.1% BSA and 0.05% Tween 20. After washing, sections were stained in 2% aqueous uranylacetate for 10 s and Reynolds lead citrate (Reynolds, 1963) for 10 s, washed with water and examined with a Hitachi 7000 transmission electron microscope. A series of control grids were prepared identically, except that the primary antibody was replaced with normal rabbit serum.

### **2.11. Effects of inhibitors**

The effects of KCN,  $\text{NaN}_3$ , and INH on catalase and peroxidase activities, as well as spectral changes, of wild type and mutant HPI proteins were studied. In the case of activity assays in the presence of various concentrations of KCN,  $\text{NaN}_3$ , or INH, the enzyme studied was usually incubated for 1 min in the reaction mixture containing one of the above compounds prior to initiation of the reaction. For spectral analysis, the wild type and mutant EcHPI enzymes were all subjected to individual equilibrium KCN titrations, in which spectral shifts due to cyanide binding were followed as a function of increasing KCN concentrations. Wild type HPI was similarly titrated using INH. In all cases, absorption spectra from 250nm to 750nm were usually obtained.

### **2.12. Determination of sulfhydryl groups**

The number of sulfhydryl groups in HPI proteins was determined spectrophotometrically using 5,5'-dithiobis-(2-nitrobenzoic acid) [DTNB] (Ellman, 1959). Sulfhydryl groups were quantitated on non-denatured protein using  $\approx 1$  mg/ml samples (3-10  $\mu\text{M}$  protein) in 1 ml 50 mM potassium phosphate, pH 8.0 to which was added 20  $\mu\text{l}$  of 10 mM DTNB solution.  $A_{412}$  values were determined at five minute intervals until the absorbance readings were stable and the concentration of sulfhydryl was calculated using an extinction coefficient for DTNB product of  $13,600 \text{ M}^{-1} \text{ cm}^{-1}$ . The ratio of sulfhydryl groups to subunits was then determined assuming a MW of 80,000 per EcHPI subunit. *E. coli* HPII monofunctional catalase was used as a positive control.

### **2.13. Electrospray ionization- time-of-flight (ESI-TOF) mass spectrometry**

Protein samples were prepared for ESI-TOF mass spectrometry as follows: 5 mg protein samples in approximately 1 ml of 50 mM potassium phosphate buffer, pH 7.0, were dialysed overnight against 3.5 l of Milli-Q system (Millipore-Waters Corp.) filter purified water in a 4 l plastic beaker. Recovered dialysates were centrifuged briefly to

remove any remaining precipitates and then loaded into Microcon spin filter microcentrifuge tubes (Amicon). Samples were centrifuged for several successive 15 min periods, during which a solution of 5 mM (99.999%) ammonium acetate was added to the samples in order to achieve complete replacement of the original buffer. 0.5-1 ml samples prepared in this way were removed to microcentrifuge tubes and stored frozen (-20°C). All studies were performed using an ESI-TOF mass spectrometer constructed at the University of Manitoba (Verentchikov *et al.*, 1994) as previously described (Chernushevich *et al.*, 1997; Poitier *et al.*, 1998). Thawed samples were continuously infused into the ion source at a flow rate of 0.4  $\mu\text{l min}^{-1}$  using a syringe pump. Declustering voltages which control the kinetic energy of the ions in the interface, ranged from 100 -320 V. Data were acquired in the positive ion mode using ubiquitin (8565 Da) for calibration.

### **3. RESULTS**

#### **3.1. Purification of MtHPI and comparison with EcHPI**

##### **3.1.1. Introduction**

Isolation of the coding sequence for the *katG* gene from *M. tuberculosis* (Zhang *et al.*, 1992) prior to the initiation of this study, made it possible to clone and express the MtHPI protein in *E. coli* cells. This catalase-peroxidase is 50% identical to EcHPI, and both MtHPI and EcHPI have been shown to be related to the superfamily of peroxidase enzymes (Welinder, 1992). As EcHPI had already been plasmid-expressed and purified from *E. coli* (Loewen and Switala, 1986), a study was undertaken to purify, characterize and compare MtHPI and EcHPI directly via biochemical and physical methods.

##### **3.1.2. Purification of MtHPI**

In order to characterize the MtHPI and EcHPI proteins, the *M. tuberculosis katG* gene was first cloned into a high expression plasmid vector, pAH1, and subsequently expressed in order to purify MtHPI from large scale batch cultures of *E. coli* cells. Including iron in the form FeCl<sub>3</sub> and  $\delta$ -aminolevulinic acid (ALA) in the culture medium was found to yield higher catalase specific activities in small scale cell extracts of *E. coli* expressing MtHPI, as shown in Table 3.1.1. Addition of 50  $\mu$ M FeCl<sub>3</sub> alone led to a marginal increase in catalase specific activities in cultures of *E. coli* overexpressing EcHPI. As both iron and  $\delta$ -aminolevulinate are precursors in the biosynthesis of hemes, their presence in the growth medium probably allows greater levels of heme to be produced within the cells, ensuring more efficient incorporation into the overexpressed HPI apoproteins.

**Table 3.1.1.** Comparison of the effect of supplementing growth medium with  $\text{FeCl}_3$  and  $\delta$ -aminolevulinic acid (ALA) on the expression of catalase activity of EcHPI and MtHPI. Cultures (25 ml) of *E. coli* strain UM262 containing plasmids pBT22 (EcHPI) or pAH1 (MtHPI) were grown for 16-18 h at 37°C in LB medium supplemented with ampicillin. Activity assays were performed on sonicated cell free extracts.

Supplement		Catalase Activity (units/ mg protein)	
[ALA] mM	[ $\text{FeCl}_3$ ] $\mu\text{M}$	EcHPI	MtHPI
unsupplemented		191	7
0	50	229	47
0	100	174	26
0.1	0	152	53
1	0	78	89
0.1	50	155	91
1	50	116	146
0.1	100	124	99
1	100	141	141

The course of a typical purification of MtHPI enzyme from *E. coli* strain UM262, expressed from plasmid pAH1, is summarized in Table 3.1.2. A typical purification of EchPI enzyme expressed from plasmid pBT22 is also shown for comparison. The purification procedure is essentially the same as the one used for purification of EchPI enzyme, with minor modifications. A brief heating of the resuspended ammonium sulfate pellets at 42°C for 45 min was introduced prior to the anion exchange chromatography step, as it was found to precipitate contaminating protein without loss of catalase activity, since the midpoint for thermal inactivation of EchPI is 56°C (Switala *et al.*, 1999). Addition of the ultimate gel filtration chromatography step was found to reduce the levels of contaminating low molecular weight proteins still present in samples eluted from the anion exchange column.

### **3.1.3. Physical characterization of EchPI and MtHPI**

#### **3.1.3a. Optical absorption spectroscopy of the HPI enzymes**

Absorbance spectra of the purified EchPI and MtHPI enzymes in the Soret and visible regions of the spectrum are shown in Fig. 3.1.1. Very similar spectra were obtained for EchPI and MtHPI, with clear maxima at 408 (Sorêt) and 500 nm, although the Sorêt band of MtHPI was slightly narrower and the 639 nm charge transfer band of EchPI was positioned at 628 nm in MtHPI. The 500 nm band for both proteins also showed a distinct shoulder at about 550 nm. The ratio of heme/protein determined by the  $Abs_{407/280}$  ratio was 0.51 for EchPI and 0.37 for MtHPI.

#### **3.1.3b. Polyacrylamide gel electrophoresis of the the HPI enzymes**

Purified EchPI and MtHPI were analyzed by electrophoresis on polyacrylamide gels (Fig. 3.1.2). Under denaturing conditions (Fig. 3.1.2A), both proteins exhibited a predominant single band, with apparent molecular mass of  $\approx 80$  kDA for EchPI, while

**Table 3.1.2.** Purification of MtHPI or EcHPI from *E. coli* strain UM262 harbouring either plasmid pAH1 (*M. tuberculosis katG*) or pBT22 (*E. coli katG*).

<b>Step</b>	<b>Total protein (mg)</b>	<b>Total catalase activity (units x 10<sup>3</sup>)</b>	<b>Specific catalase activity (units/mg)</b>	<b>Recovery (%)</b>	<b>Purification (fold)</b>
<b>MtHPI</b>					
Crude extract	6,148	170	28	100	1
(NH <sub>4</sub> ) <sub>2</sub> SO <sub>4</sub> precipitation	795	121	152	71	5.4
Anion exchange (DEAE- cellulose)	95	71	750	42	26.8
Gel filtration (Sephadex G-200)	59	58	983	34	35
<b>EcHPI</b>					
Crude extract	8,306	3,293	396	100	1
(NH <sub>4</sub> ) <sub>2</sub> SO <sub>4</sub> precipitation	812	1,167	1435	35	3.6
Anion exchange (DEAE- cellulose)	310	741	2,100	23	5.3

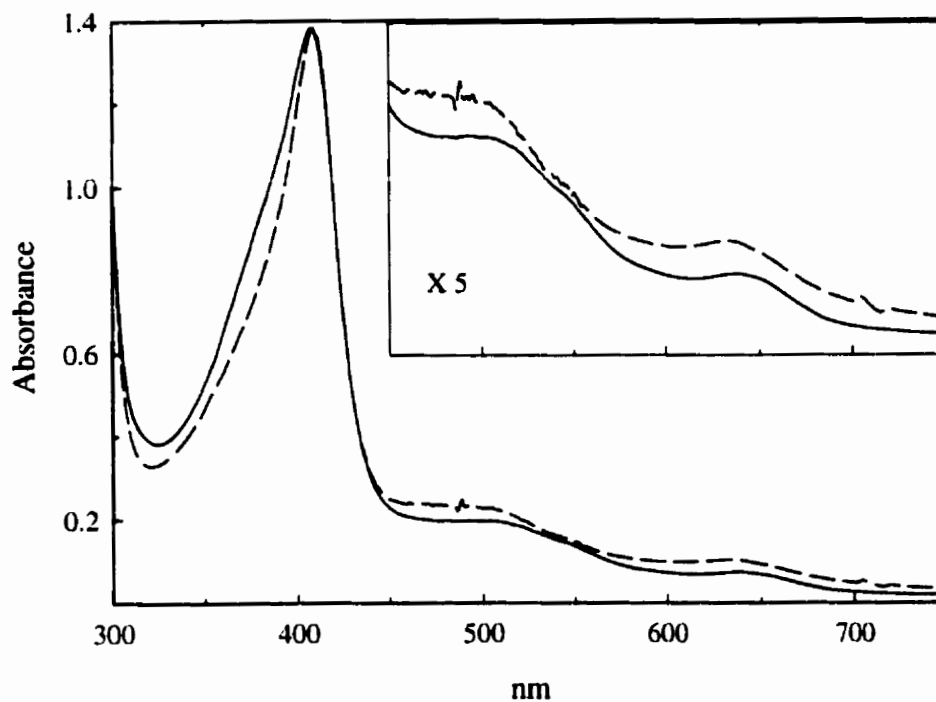


**Figure 3.1.1** Optical absorbance spectra of purified EcHPI (solid line) and MtHPI (broken line). The spectra between 450-750nm are shown in the inset, expanded by the factor shown. Spectra were factor adjusted to absorbance equality at the Sorêt maxima for comparison purposes.

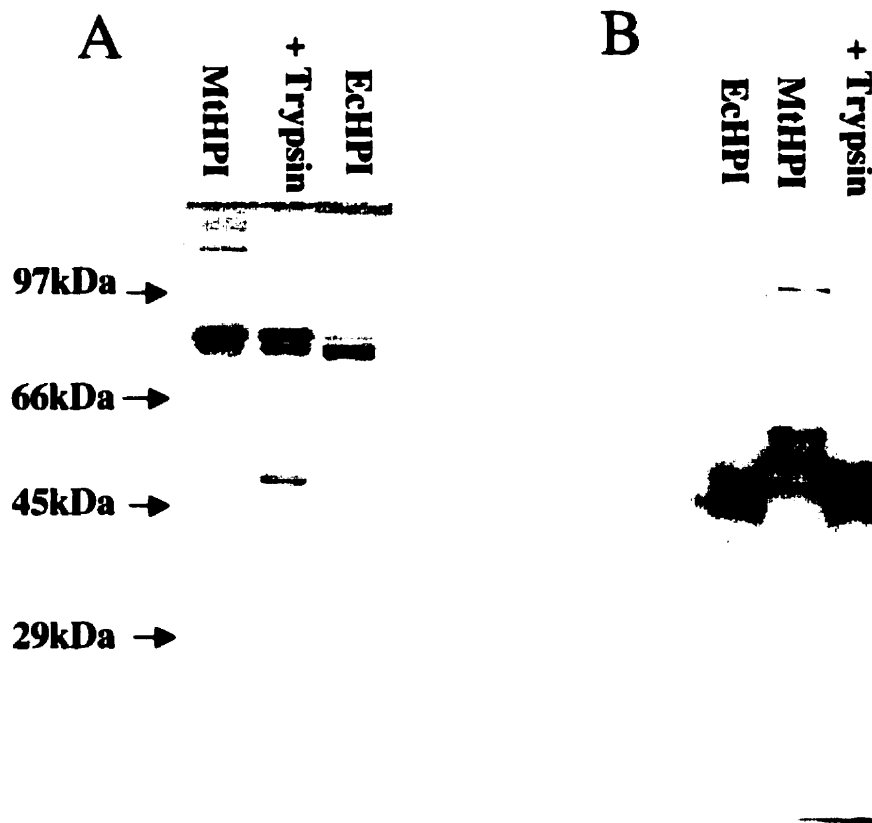


**Figure 3.1.2** A. SDS-polyacrylamide gel electrophoresis analysis of purified EcHPI, MtHPI, and MtHPI partially digested with trypsin. (+ **trypsin**). B. Non-denaturing polyacrylamide gel electrophoresis analysis of purified EcHPI, MtHPI, and MtHPI partially digested with trypsin (+ **trypsin**). Samples of approximately 10  $\mu\text{g}$  were electrophoresed on 8% gels and stained with Coomassie Brilliant Blue.

that of MtHPI had a slightly lower electrophoretic mobility, with an apparent molecular mass 2-3 kDa higher than that of EcHPI. As the MtHPI subunit is predicted to be 11 amino acid residues longer than EcHPI, with a higher proportion of basic to acidic residues as well as a slightly lower predicted pI compared to EcHPI, a difference in electrophoretic mobilities of the proteins may be expected. Limited trypsin digestion of the MtHPI was found to produce a band with the same electrophoretic mobility as EcHPI. The predicted sequence of MtHPI contains several arginine and lysine residues in the carboxyl terminal region that may be the target residues for trypsin cleavage resulting in a coincidentally positioned protein band in SDS-PAGE.

Under nondenaturing conditions (Fig. 3.1.2B) EcHPI exhibited two predominant bands of presumed charge isoforms, while MtHPI exhibited three bands also presumed to be charge isoforms. MtHPI digested with trypsin also exhibited three bands under these conditions, two of which closely corresponded to the position of the bands for the EcHPI protein.

### **3.1.3c. Mass spectrometry of the HPI enzymes**

Purified EcHPI and MtHPI were analyzed by electrospray-ionization time-of-flight (ESI-TOF) mass spectrometry. Mass spectra for EcHPI are shown in Fig. 3.1.3. At lower declustering voltages applied to the sample, the EcHPI spectrum exhibited one predominant broad peak corresponding to an estimated molecular mass of 322,267 Da and a small accessory peak corresponding to an estimated molecular mass of 321,711 Da. At a higher declustering voltage, the spectrum exhibited the same predominant broad peak seen in the initial spectrum (but at 322,225 Da), with a second broad, but less intense peak, corresponding to the position of the accessory peak in the initial spectrum (at 321,631 Da). A third peak of very low intensity at a molecular mass of  $\approx$ 321,100 Da is also apparent in this spectrum. Mass spectra for MtHPI are shown in Fig. 3.1.4. At the

**Figure 3.1.3** Electrospray ionization time-of-flight mass spectroscopic analysis of EchPI. (A) Spectrum of EchPI sample after being subjected to initial declustering potential of 100V. (B) Spectrum of EchPI sample after being subjected to initial declustering potential of 200V. Numbers indicate the average masses of the indicated peaks.

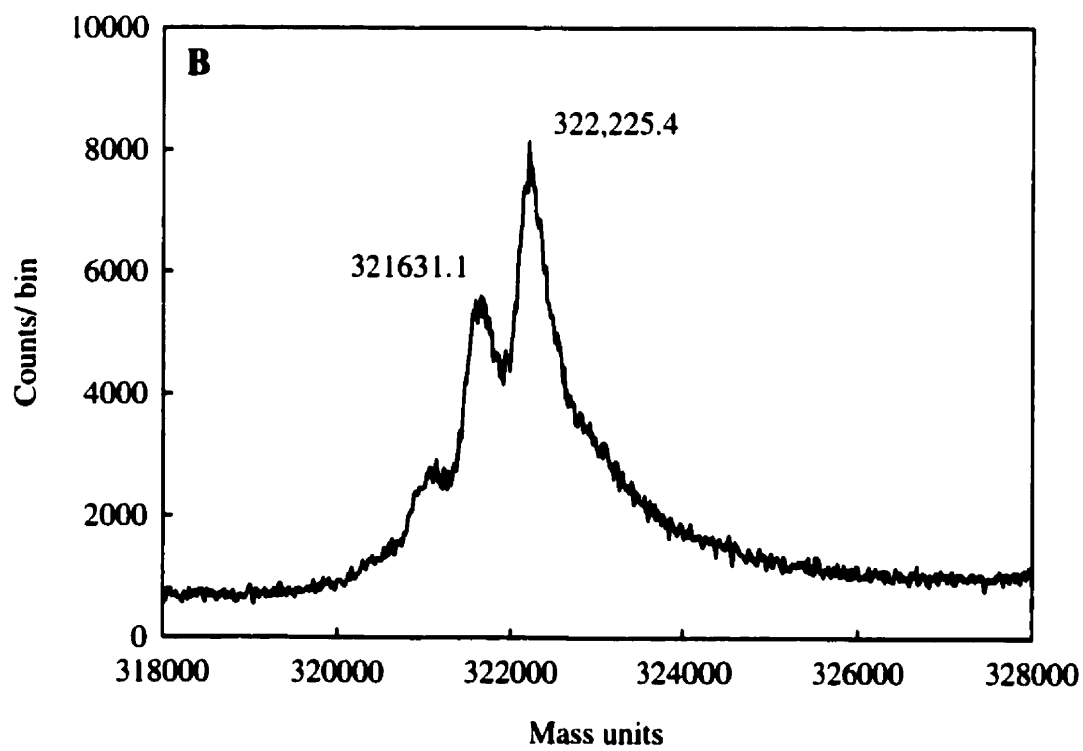
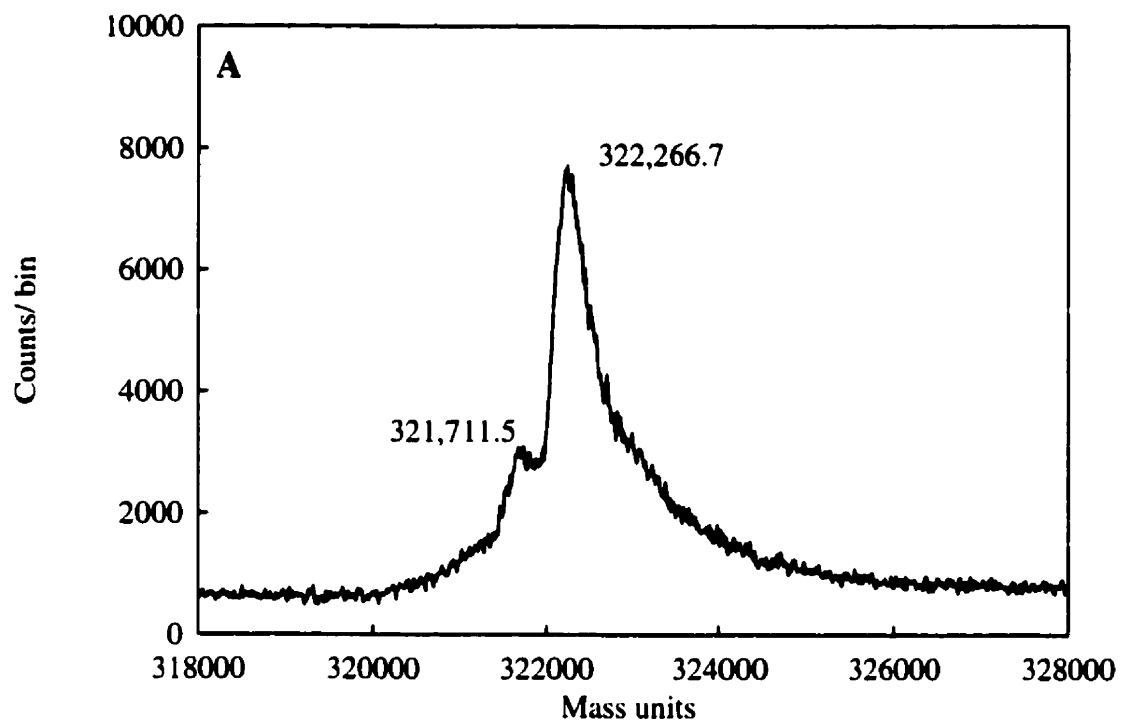
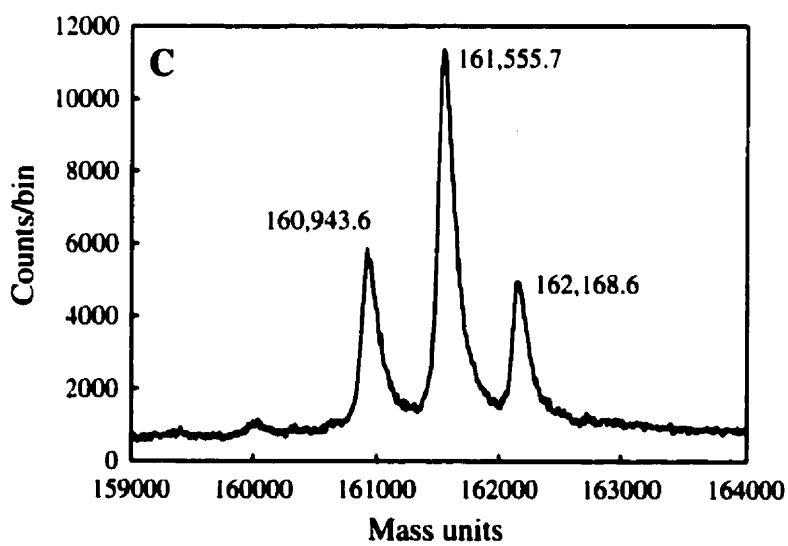
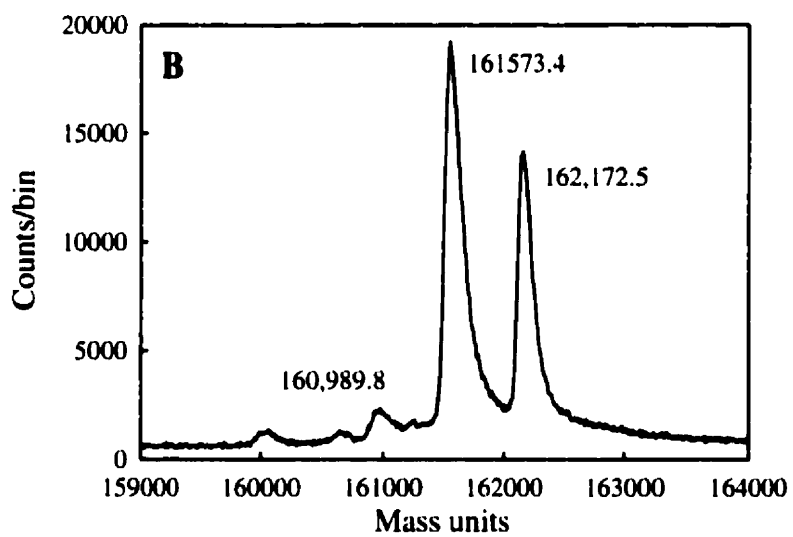
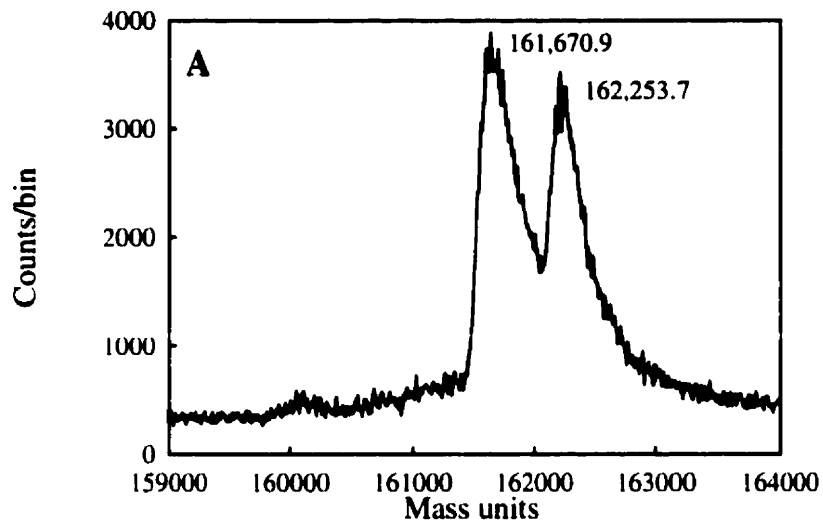


**Figure 3.1.4.** Electrospray ionization time-of-flight mass spectroscopic analysis of MtHPI. (A) Spectrum of MtHPI sample after being subjected to initial declustering potential of 100V. (B) Spectrum of MtHPI sample after being subjected to initial declustering potential of 200V. (C) Spectrum of MtHPI sample after being subjected to initial declustering potential of 320V. Numbers indicate the average masses of the indicated peaks.



lowest declustering voltage applied (100V), the spectrum obtained exhibited two predominant broad peaks of similar intensity corresponding to molecular masses of 161,671 Da and 162,254 Da. Spectra for higher declustering voltages applied also showed the two peaks obtained in the original spectrum as better defined and more intense features of the spectrum, however, a third peak corresponding to a molecular mass of 160,944 Da appeared at 200V. At a declustering voltage of 320V, this peak became a distinct spectral feature, having about the same intensity as the peak at 162.1 kDa, while the intensity of the 162.1 kDa peak had declined greatly with respect to the other two peaks.

Mass unit differences between the peaks in the EcHPI mass spectra were between 555 and 595 mass units for spectra obtained at low and high declustering voltages, while mass unit differences between the peaks in the MtHPI mass spectra ranged between 582 and 612 mass units for differences determined between the lowest and the highest declustering voltage applied. The presence of up to three peaks of differing intensities separated by between 555 and 612 mass units for both EcHPI and MtHPI samples, indicates the presence of up to three populations of molecular species in the samples analyzed. Differences of 555 to 612 mass units would be consistent with the loss of a proportion of either a hematoporphyrin without iron or a heme residue, which would have predicted masses of 560.8 and 616.6 mass units, respectively. As the EcHPI spectra shows molecular masses consistent with a tetrameric protein having 80 kDa subunits, and the MtHPI spectra shows molecular masses consistent with a dimeric protein having 80 kDa subunits, it is possible the mass differences between the peaks is a composite of varying proportions of porphyrins lacking iron as well as intact hemes. The cause of these mass differences may be loss of noncovalently bound hemes, as well as loss of the iron from the hemes during ionization. Therefore, EcHPI and MtHPI are probably inhomogeneous mixtures of species: EcHPI being mainly a tetramer containing four, three, two, one, or no hemes, and MtHPI being a dimer containing two, one, or no hemes

in varying proportions. MthPI is also apparently less stable to ionization than EchPI, perhaps having a much weaker set of quaternary structural ionic interactions between dimers.

### **3.1.4. Biochemical characterization of EchPI and MthPI**

#### **3.1.4a. Specific activities and kinetics of the HPI enzymes**

Fig. 3.1.5. shows the effect of substrate concentrations on the rates of catalase and peroxidase reaction for EchPI and MthPI enzymes, both as primary and Lineweaver-Burk type secondary plots. Table 3.1.3 summarizes the specific activities of the enzymes as catalases and as peroxidases in the presence of two commonly used peroxidatic substrates, as well as calculated kinetic parameters for the catalase and peroxidase reactions. EchPI has higher catalase specific activity, while conversely, MthPI shows higher peroxidase specific activities. Both enzymes have very similar  $K_m$  values for the catalase reaction, but EchPI has a much higher turnover number than MthPI for this reaction. MthPI has a higher  $K_m$  but lower turnover number compared to EchPI for the peroxidase reaction.

#### **3.1.4b. Effects of KCN and NaN<sub>3</sub> as enzyme inhibitors**

Both cyanide and azide are well known as classical inhibitors of hemoprotein enzymes such as catalases and peroxidases. Both species bind the active site heme iron reversibly to form stable complexes. Fig. 3.1.6 shows the inhibition of catalase and peroxidase activities by cyanide and azide for EchPI and MthPI. The inhibition patterns for both the catalase and peroxidase reactions for KCN and azide are very similar, however, MthPI shows a slightly higher end point sensitivity in all cases except for KCN inhibition of catalase activity of the enzyme.

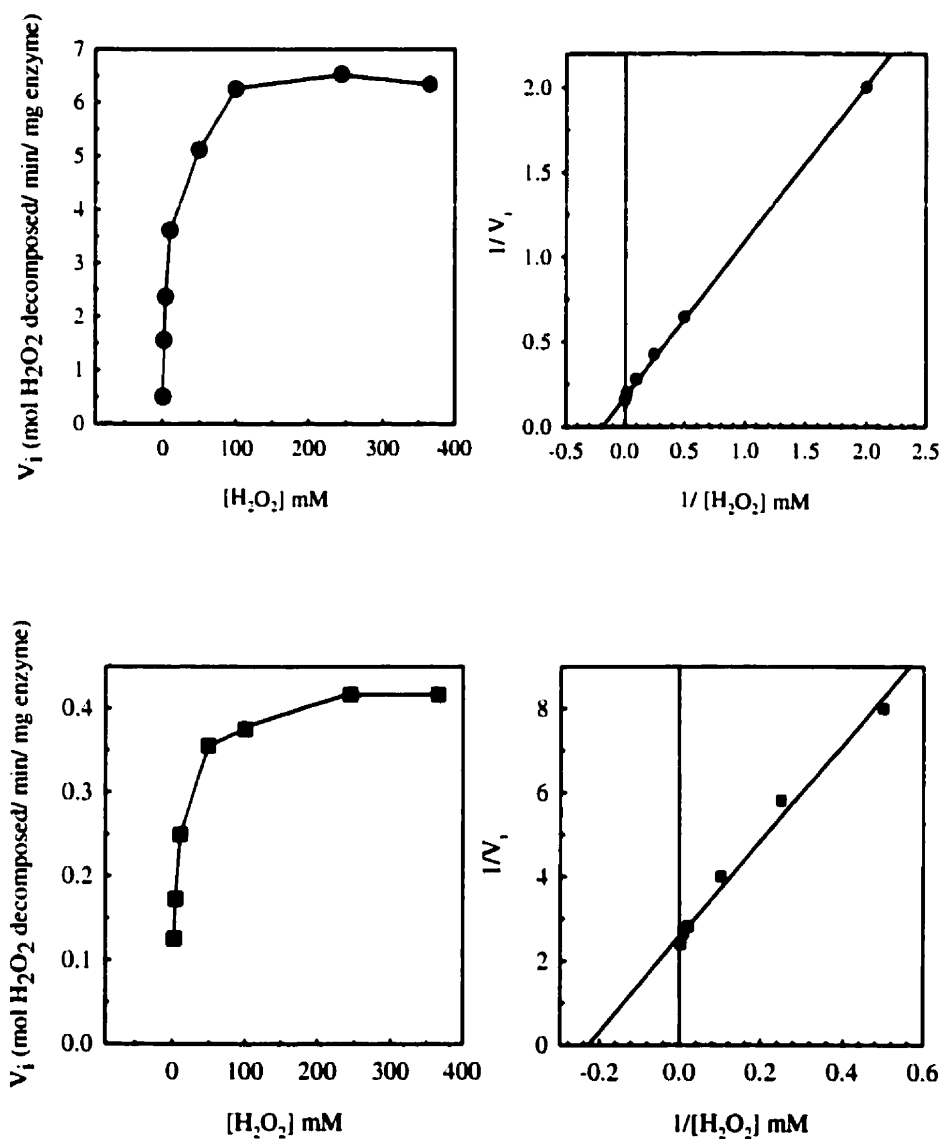


Figure 3.1.5A

**Figure 3.1.5 A** Effect of hydrogen peroxide concentrations on the initial catalytic velocities ( $V_i$ ) of purified EcHPI (circles) and MthPI (squares). **B** Effect of 2,2 -azinobis (3-ethylbenzothiazolinesulfonic acid) {ABTS} on the initial peroxidatic velocities ( $V_i$ ) of purified EcHPI (circles) and MthPI (squares). Leftmost panels: Michaelis-Menten (primary) plots, rightmost panels: Lineweaver-Burk (double reciprocal) plots.

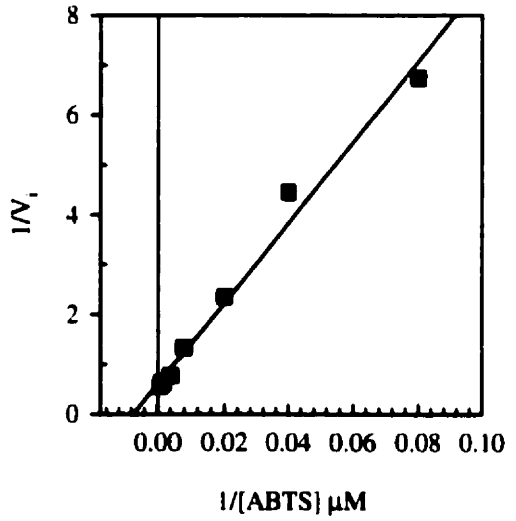
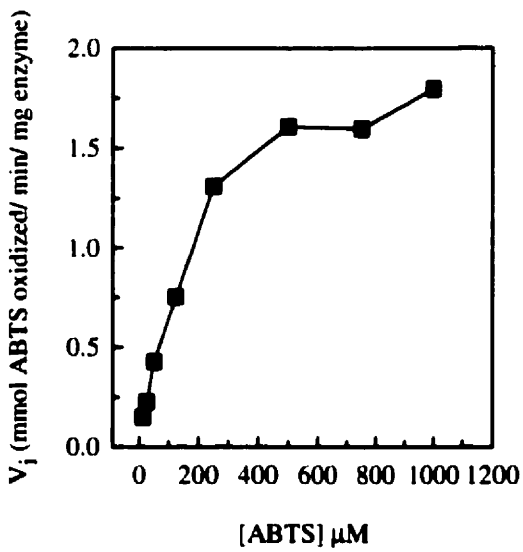
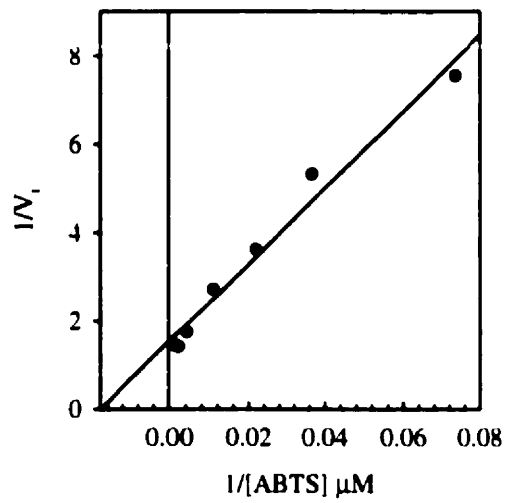
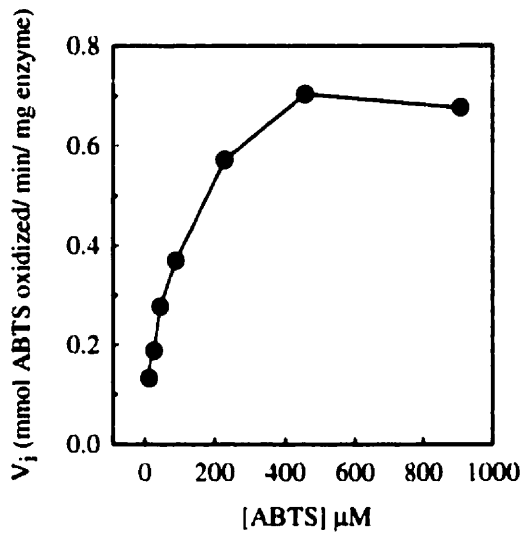
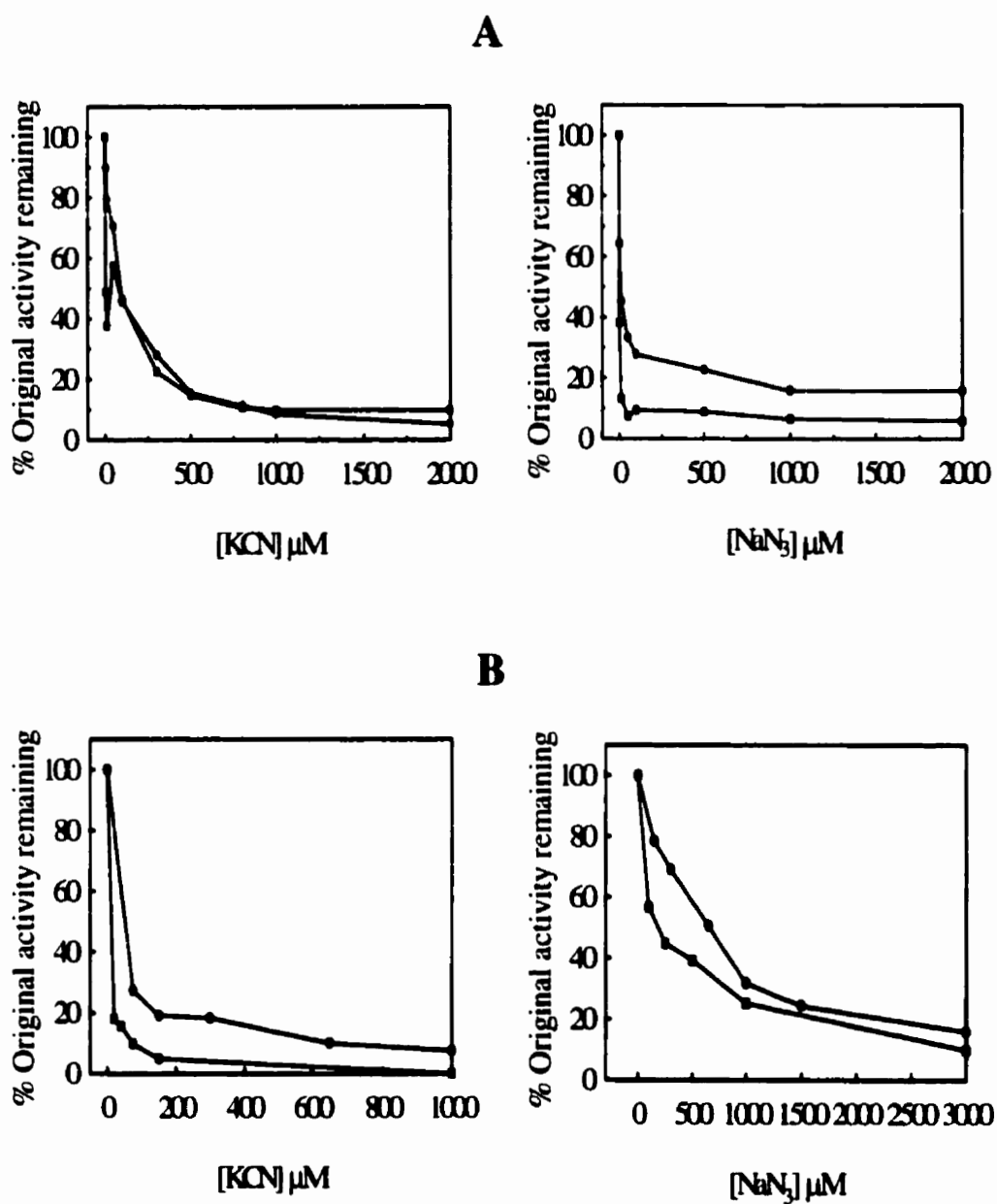


Figure 3.1.5B

**Table 3.1.3.** Comparison of the specific activities and kinetic parameters of purified EcHPI and MthPI enzymes

Enzyme	Specific Activity			Apparent $K_m$ ( $\mu\text{M}$ )	Apparent $V_{max}$ (mol/ min)	$k_{cat}$ ( $\text{s}^{-1}$ )*	
	Catalase (U/mg)	Peroxidase (ABTS, U/mg)	Peroxidase (o-dianisidine, U/mg)				
<b>EcHPI</b>	1900 $\pm$ 400	660 $\pm$ 40	3.2 $\pm$ 0.1	<b>Catalase</b>	5,900	5.9	$1.6 \times 10^7$
				<b>Peroxidase (ABTS)</b>	55	$6.5 \times 10^{-3}$	$1.7 \times 10^4$
<b>MthPI</b>	970 $\pm$ 70	2,500 $\pm$ 300	5.2 $\pm$ 0.2	<b>Catalase</b>	4,500	0.39	$1.0 \times 10^6$
				<b>Peroxidase (ABTS)</b>	142	$1.7 \times 10^{-2}$	$4.5 \times 10^3$

\*calculated based on two active sites per holotetrameric enzyme for EcHPI and one active site per dimeric enzyme for MthPI



### 3.1.4c. Effect of KCN on HPI enzymes as a heme ligand

Spectral titration of EcHPI and MtHPI with increasing concentrations of KCN was performed as shown in Fig. 3.1.7. Both enzymes show spectral shifts in which the Sorêt band is red shifted and reduced in intensity, while the charge transfer band at 640 nm is replaced by double bands at between 550 nm and 600 nm. This type of spectral shift is consistent with the formation of a low spin (diamagnetic) heme-ligand complex. When the difference spectra of the fully titrated (cyanide-ligated) enzymes minus the free and partially titrated enzymes are calculated and superimposed, as shown in the insets to Fig. 3.1.7., the relative maxima and minima for the titration of either enzyme can be determined, and a clear isosbestic point at  $\approx 430$  nm is apparent, indicating only two absorbing species are present during the course of the titration. These data can also be used to plot the total absorbance change of the difference spectra maxima minus minima in the Sorêt region as a function of increasing KCN concentration, as shown in Fig. 3.1.8 (upper panels), and then recalculated as double reciprocal plots to provide an estimate of the equilibrium dissociation constant of cyanide binding to either enzyme, as shown in Fig. 3.1.8 (lower panels,  $1/x$ -intercepts). EcHPI has a higher apparent  $K_d$  than that for MtHPI. The difference in  $K_d$  may be due to slightly higher steric constraints in the active site of EcHPI.

### 3.1.4d. Determination of free sulfhydryl groups in EcHPI and MtHPI

Free sulfhydryl groups were quantitated in purified EcHPI, MtHPI, and the *E. coli* catalase hydroperoxidase II (HPH) as a positive control. Results for the various enzymes are shown in Table 3.1.4. HPH is known to have only one reactive cysteine residue per protein subunit located at the surface of the protein. This was confirmed within error by the data obtained. Interestingly, MtHPI has three cysteine residues predicted by its coding

**Figure 3.1.7.** Spectral titrations of EcHPI and MtHPI with KCN. Arrows indicate the direction of the spectral changes. (A) Representative absorption spectra of purified EcHPI in the presence of increasing [KCN]. Spectra shown are for EcHPI in the presence of 0, 3.7, 7.4, 50, 87, 180, 365, 2,600, and 6,300  $\mu\text{M}$  KCN. Difference spectra for the cyanide-EcHPI complex (fully titrated) minus EcHPI in the presence of 0-2.6 mM KCN, are shown in the inset. (B) Representative absorption spectra of purified MtHPI in the presence of increasing [KCN]. Spectra shown are for MtHPI in the presence of 0, 4, 10, 25, 45, 155, 355, 3,600, and 7,600  $\mu\text{M}$  KCN. Difference spectra for the cyanide-MtHPI (fully titrated) minus MtHPI in the presence of 0-3.6 mM KCN, are shown in the inset.

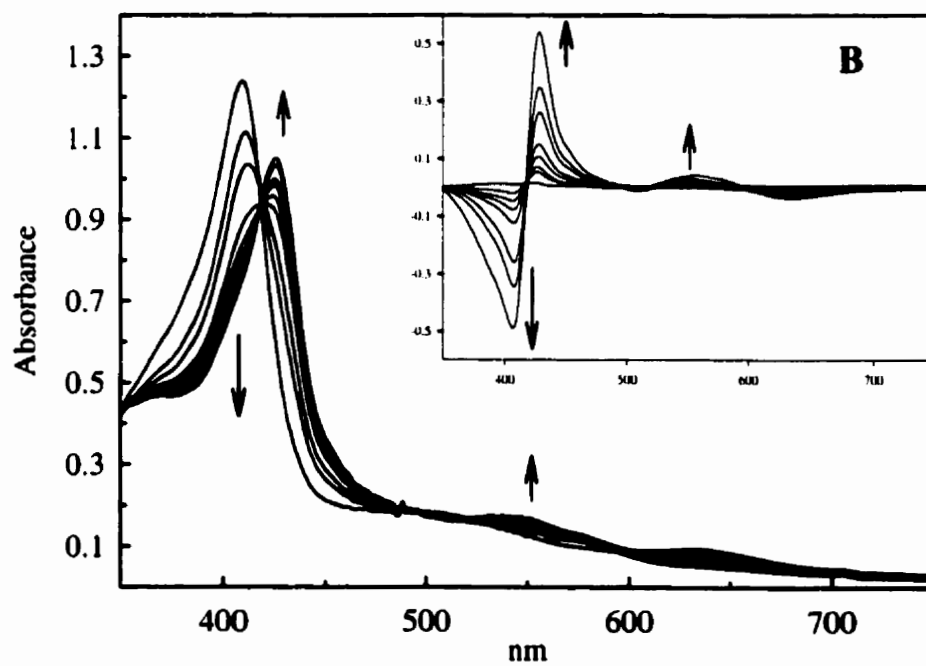
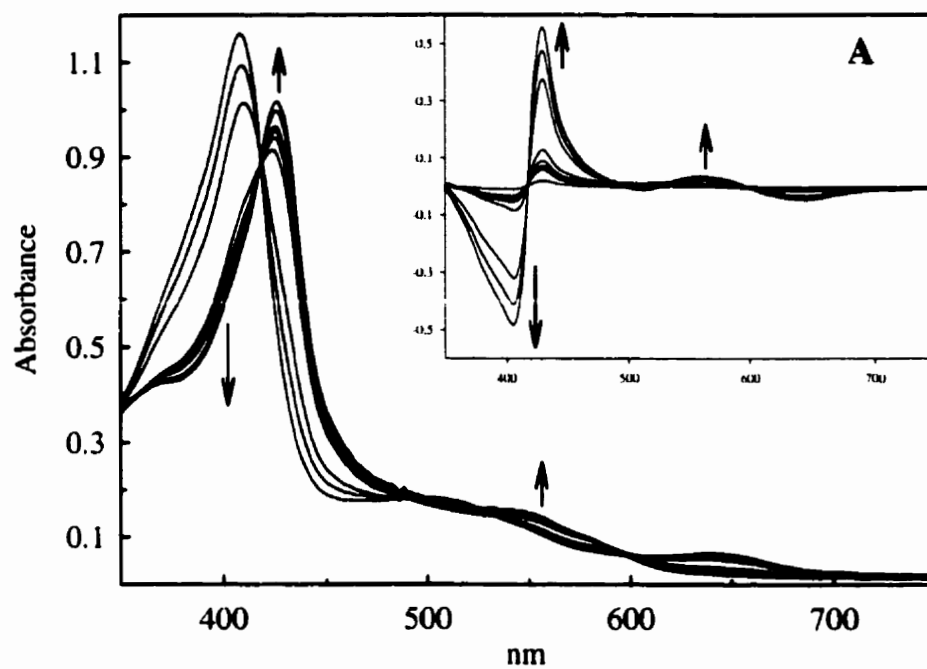


**Figure 3.1.8** Equilibrium spectrophotometric cyanide binding titrations of EcHPI and MtHPI: primary and secondary plots. (A) Primary plot (upper panel) and double reciprocal plot (lower panel) based on spectral absorbance data (Fig. 3.1.7A), for EcHPI titration with cyanide. (B) Primary plot (upper panel) and double reciprocal plot (lower panel) based on spectral absorbance data (Fig. 3.1.7B), for MtHPI titration with cyanide.

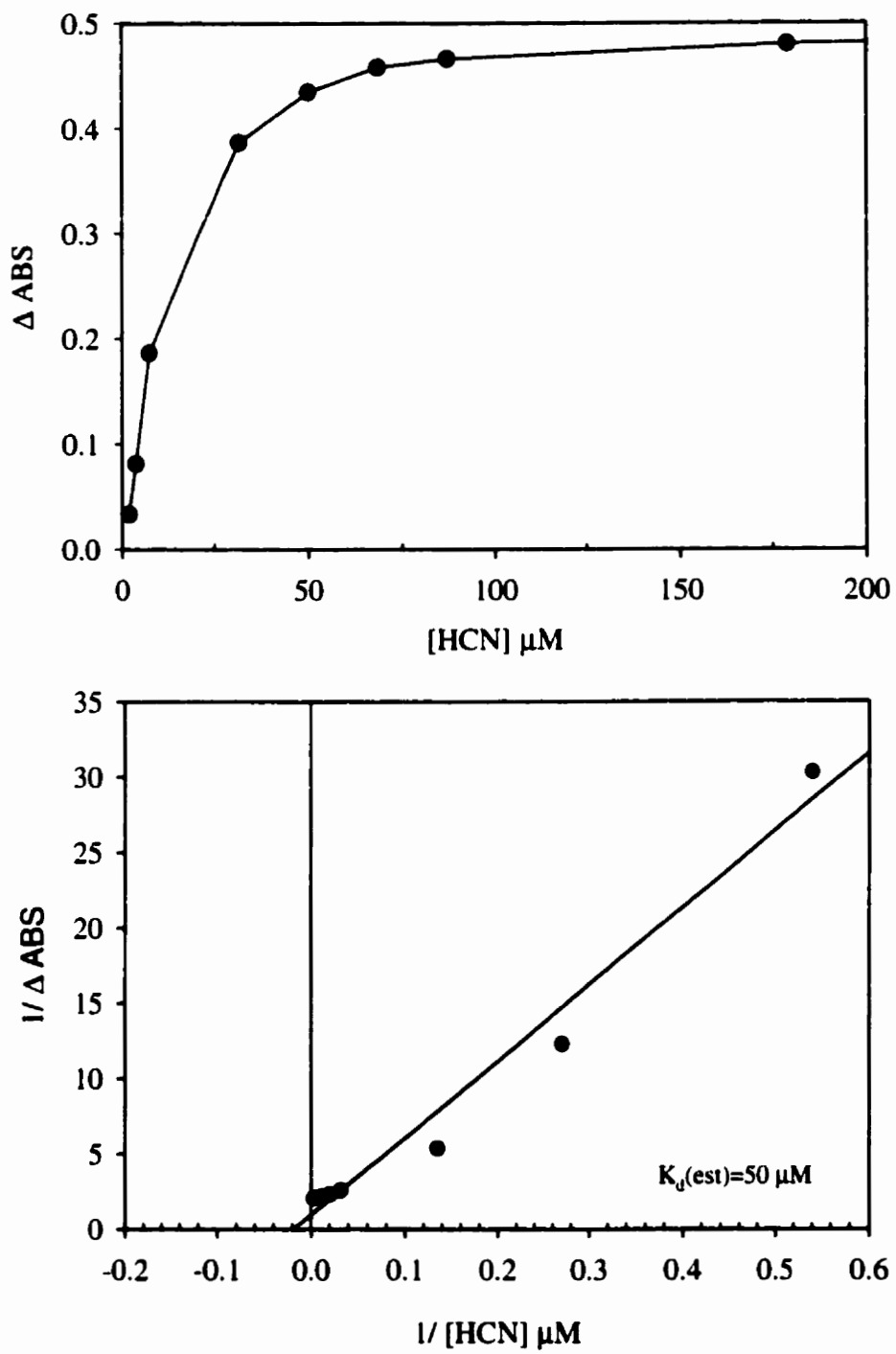


Figure 3.1.8A

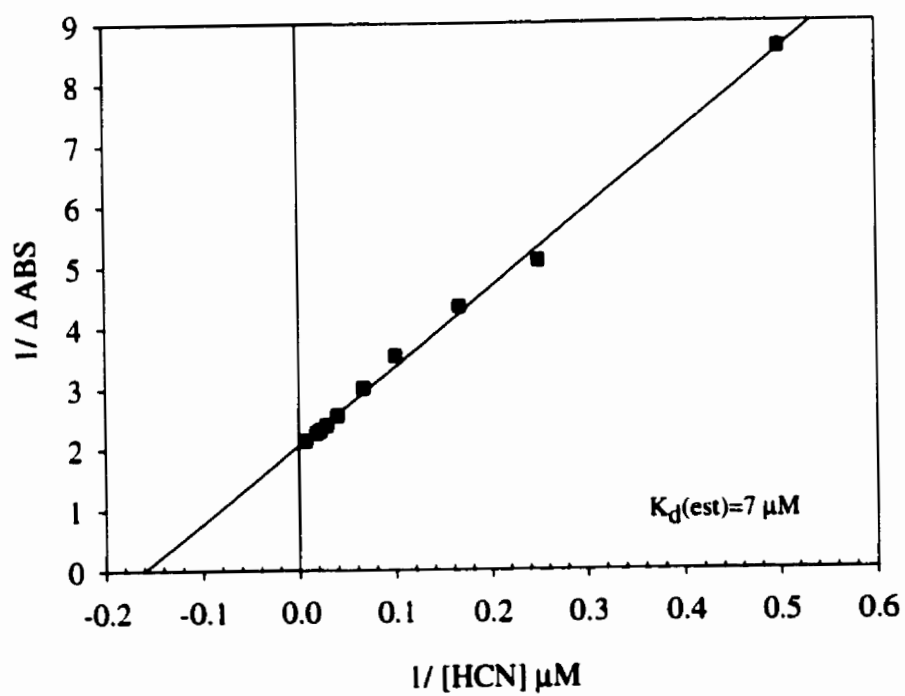
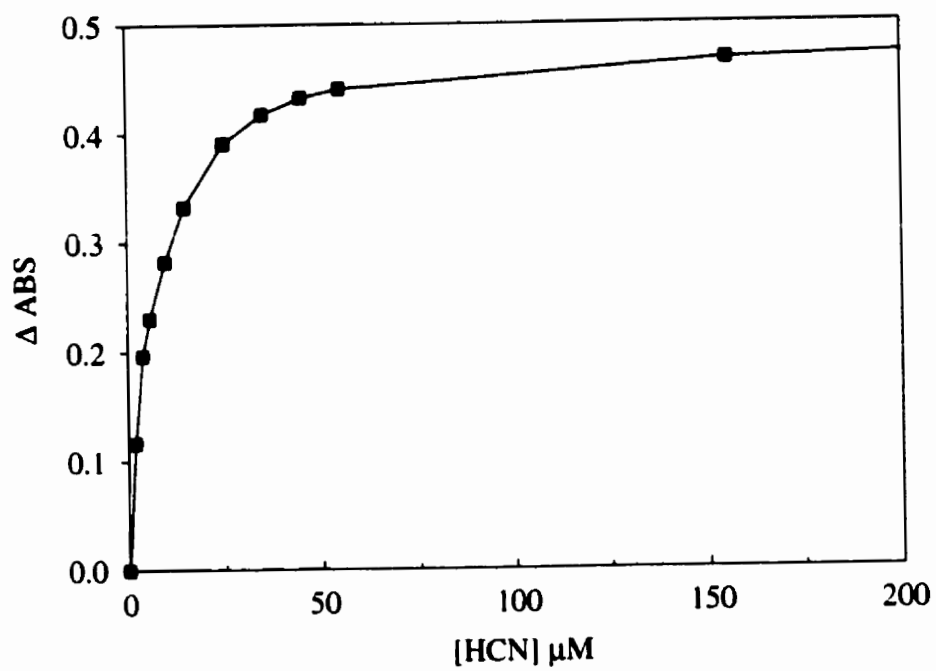


Figure 3.1.8B

**Table 3.1.4** Quantitation of free sulfhydryl groups of purified EcHPI and MtHPI with 5,5' -dithiobis-(2-nitrobenzoic acid).

Enzyme	-SH/ subunit
HPII (positive control)	$0.88 \pm 0.12$
MtHPI	$0.74 \pm 0.06$
EcHPI	$0.12 \pm 0.13$

sequence, but only partial reaction of one cysteine residue was observed based on the data. The possibility that the remaining two residues per subunit could be either inaccessible or involved in either intra- or inter-subunit disulphide bonds cannot be immediately excluded, however these possibilities were not investigated further. EchPI has only one cysteine residue predicted by its coding sequence, but apparently this residue was not reactive. Whether the residue is simply inaccessible to the sulfhydryl reagent or involved in an intersubunit disulphide bond was not investigated further.

## **3.2. Isoniazid oxidation catalyzed by EchPI and MthPI**

### **3.2.1. Introduction**

Isonicotinic acid hydrazide (isoniazid, INH) is a front line drug used in the treatment of *Mycobacterium tuberculosis* infections. The drug is ineffective against strains of *E. coli*, even at high concentrations. While it has long been recognized that catalase-deficient strains of *M. tuberculosis* are resistant to INH (Winder, 1982), only more recently has it been shown that either deletion (Zhang *et al.*, 1992) or point mutation (Altamirano *et al.*, 1994) of the *katG* gene in *M. tuberculosis* may give rise to this phenotype. The biochemical basis for *M. tuberculosis* resistance to INH has been the subject of intensive investigations in the past few years. Considerable evidence now indicates that MthPI oxidizes INH *in vivo* to an electrophilic species which binds to, and inactivates, InhA, an acyl carrier protein reductase (Banerjee *et al.*, 1994; Rozwarski *et al.*, 1998), or other potential targets (Mdluli *et al.*, 1996; Mdluli *et al.*, 1998) causing inhibition of the synthesis of mycolic acids, which are long-chain fatty acids that make up part of the *M. tuberculosis* cell envelope.

MthPI, when overexpressed in *E. coli*, results in the increased susceptibility of the cells to INH (Zhang *et al.*, 1992). This result suggests that MthPI is at least partially responsible for the cytotoxicity of the drug, even in a heterologous host, but also implies

that there must be some physico-chemical differences between EcHPI and MtHPI enzymes with respect to their interactions with INH. In order to clarify the role that the HPI enzymes may play in oxidation of INH, a simple colorimetric assay for peroxidase mediated oxidation of INH was adopted and used qualitatively in peroxidase activity staining of non-denaturing polyacrylamide gels, and to quantitate the rate of reaction with horseradish peroxidase and both EcHPI and MtHPI enzymes. As well, the absorption spectra of both enzymes during direct titration with INH were monitored and the absorption changes used to determine the apparent equilibrium dissociation constants for INH of both enzymes.

### **3.2.2. Peroxidase staining of non-denaturing polyacrylamide gels**

Staining for peroxidase activity in polyacrylamide gels may be accomplished by several procedures (Gregory and Fridovich, 1974; Clare *et al.*, 1984). An alternative peroxidase stain was suggested by the observation of Shoeb *et al.* (1985) that horseradish peroxidase (HRP) reacts with INH and  $H_2O_2$  to produce radical products that can reduce nitroblue tetrazolium (NBT) to its purple formazan product. NBT has been used for other activity stains on polyacrylamide gels including the superoxide dismutase stain. (Gregory and Fridovich, 1974). As HRP, EcHPI, and MtHPI are all able to oxidize organic electron donors such as o-dianisidine and diaminobenzidine, it was reasonable to assume that EcHPI and MtHPI would catalyze oxidation of INH to form radical species which could be detected by reduction of NBT. Fig. 3.2.1 shows an electrophoretogram of EcHPI, MtHPI, and HRP on non-denaturing polyacrylamide gels, followed by staining for catalase, peroxidase-mediated oxidation of DAB, or peroxidase-mediated oxidation of INH as detected by NBT. Both EcHPI and MtHPI stain as two bands for catalase and for peroxidase using both substrate, although the upper band for the EcHPI stains

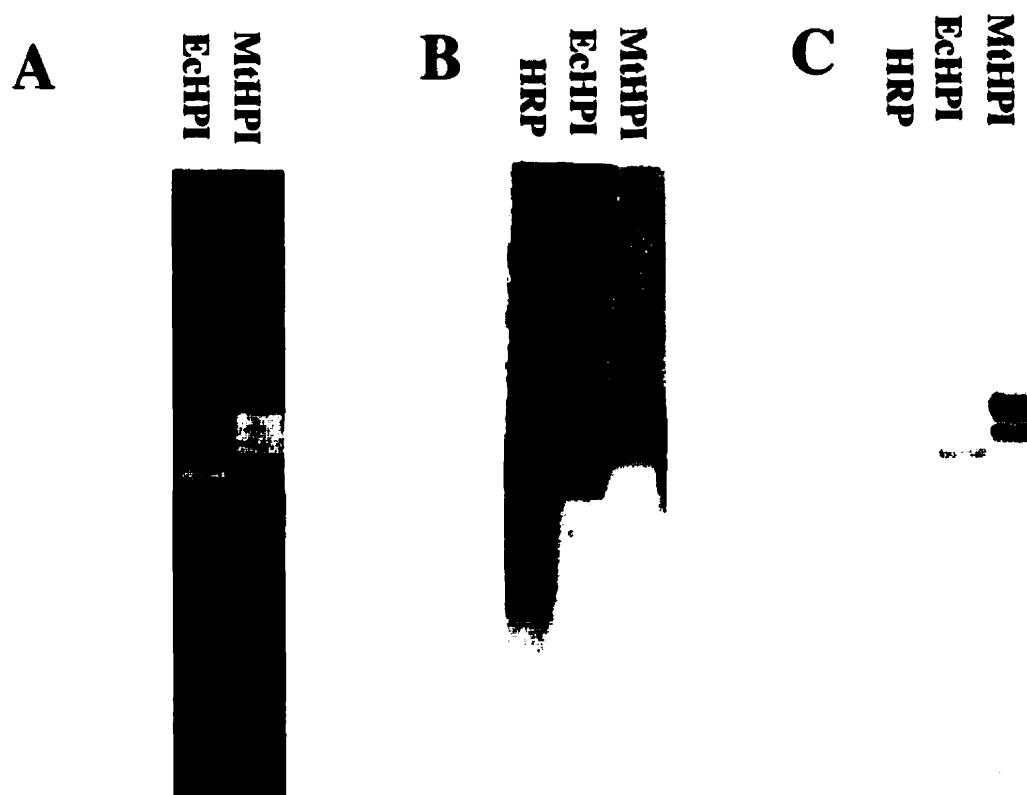


**Figure 3.2.1** *In situ* enzymatic activity staining following non-denaturing polyacrylamide gel electrophoresis of EChPI, MhPI, and horseradish peroxidase (HRP).

**A.** Electrophoretogram stained for catalase. **B.** Electrophoretogram stained for peroxidase using diaminobenzidine. **C.** Electrophoretogram stained for peroxidatic oxidation of INH with nitroblue tetrazolium. Samples were all run on 9% polyacrylamide gels. An estimated 1U catalase activity was loaded per lane in **A**, with an estimated 25  $\mu$ g protein loaded for all lanes in **B** and **C**.

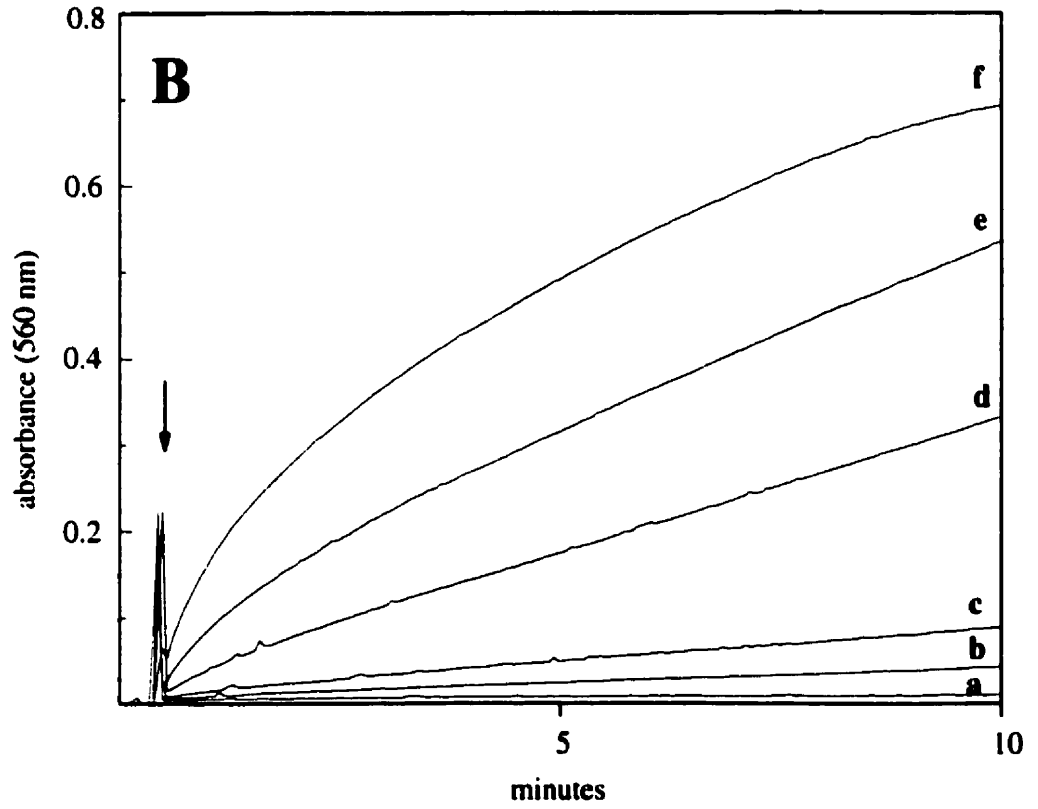
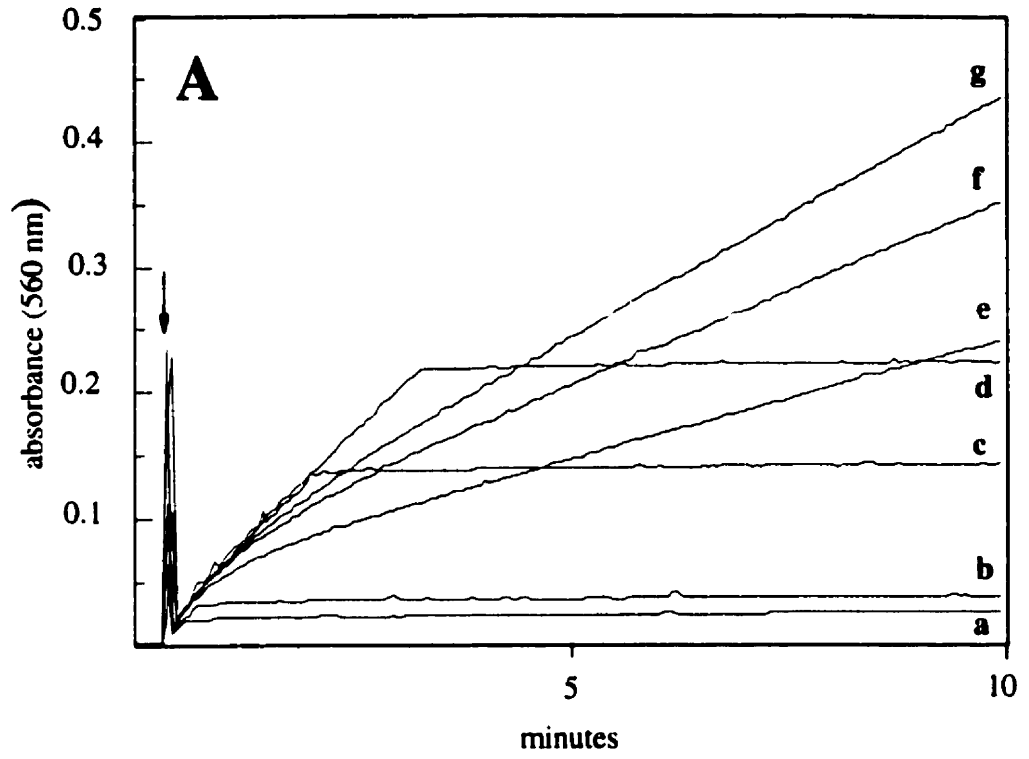
more weakly in all cases. Fig. 3.2.1C indicates that peroxidase mediated oxidation of INH can be effectively visualized using NBT, and that both ECHPI and HRP stain much more weakly than MtHPI. The results also confirm that in all cases the HPI bands showing activity migrate to the same relative locations on the gel.

### **3.2.3. Isoniazid/ H<sub>2</sub>O<sub>2</sub> dependent generation of free radicals by HRP**

Previous studies on both HRP (Shoeb *et al.*, 1985) and myeloperoxidase (van der Walt *et al.*, 1994) confirmed that both enzymes catalyze a reaction dependent on the presence of INH and H<sub>2</sub>O<sub>2</sub> that may be followed by reduction of NBT to its formazan product. Experiments with HRP also indicated that the presence of exogenous catalase caused an increase in the rate of NBT reduction by HRP and a faster termination of the reaction rather than the expected cessation of reaction as catalase removed the substrate H<sub>2</sub>O<sub>2</sub>, and that the presence of superoxide dismutase did not inhibit NBT reduction.

To determine if the catalase effect on HRP was solely the result of the lower [H<sub>2</sub>O<sub>2</sub>], the initial [H<sub>2</sub>O<sub>2</sub>] was varied and the INH/H<sub>2</sub>O<sub>2</sub>-dependent NBT reduction by HRP was followed spectrophotometrically at 560nm, as shown in Fig. 3.2.2A. Two distinct patterns of NBT reduction were observed depending on the initial [H<sub>2</sub>O<sub>2</sub>]. At [H<sub>2</sub>O<sub>2</sub>] up to 100 μM, there was a rapid reaction rate which ceased after a time proportional to the initial [H<sub>2</sub>O<sub>2</sub>]. At higher [H<sub>2</sub>O<sub>2</sub>], the initial fast phase became progressively shorter and, eventually, indistinguishable from the second, slower phase. The maximal initial reaction rate of NBT reduction with 100 μM H<sub>2</sub>O<sub>2</sub>, added was estimated to be 9 nmol/ min/ ml. [NBT] was varied from 20 to 600 μM to determine whether efficiency of the reaction could be improved by reducing the probability of any side reactions of the radicals generated. Apart from a marginal increase in the rate of the initial phase of the reaction at lower [NBT] (20 μM), varying the [NBT] had no effect over the concentration range tested. The reaction was also monitored in the presence of

**Figure 3.2.2.** Time courses for horseradish peroxidase (HRP) mediated oxidation of isoniazid (INH) followed by NBT reduction. Experiments done at room temperature in semi-micro quartz cuvettes containing 1 ml final volumes of NBT (0.2 mM), HRP (30  $\mu\text{g}$ ), and 50 mM potassium phosphate buffer, pH 7.0. (A) In the presence of 9 mM INH,  $\text{H}_2\text{O}_2$  addition initiated the reaction at the time indicated by the arrow at the following initial concentrations: (a) 5  $\mu\text{M}$ , (b) 10  $\mu\text{M}$ , (c) 50  $\mu\text{M}$ , (d) 100  $\mu\text{M}$ , (e) 1 mM, (f) 500  $\mu\text{M}$ , (g) 250  $\mu\text{M}$ . (B)  $\text{H}_2\text{O}_2$  addition (250  $\mu\text{M}$ ) initiated the reaction (arrow) in the presence of the following initial concentrations of INH: (a) 87.5  $\mu\text{M}$ , (b) 440  $\mu\text{M}$ , (c) 875  $\mu\text{M}$ , (d) 4.4 mM, (e) 17.5 mM, and (f) 52.5 mM.



superoxide dismutase (1.5U), added both prior to and following the initiation of NBT reduction, to ensure that superoxide radical anion was not a significant proportion of the radicals produced. No decline in reaction rate occurred for these experimental controls.

The effect of INH concentration on NBT reduction at an initial  $[H_2O_2]$  of 250  $\mu M$  is shown in Fig 3.2.2B. The initial rate of reduction was proportional to INH concentration and there was no evidence of termination of the reduction at higher INH concentrations. This suggests that the termination of radical production seen for HRP observed in Fig. 3.2.2B is dependent upon  $[H_2O_2]$ , not the ratio of  $[H_2O_2]$  to [donor].

#### **3.2.4. Comparison of isoniazid/ $H_2O_2$ dependent generation of free radicals by HRP, EcHPI and MthPI**

Initial attempts at evaluating the capacity of MthPI and EcHPI to mediate the oxidation of INH via the NBT reduction assay used for HRP were problematic due to the high catalase activities of the HPI enzymes, which obscured their peroxidatic activities under conditions of single peroxide additions. Under conditions of single peroxide additions to the reaction mixtures, the catalase activities of the enzymes would rapidly remove  $H_2O_2$  from the medium. To overcome this problem, the assay procedure was modified to generate a constant source of  $H_2O_2$  derived from glucose oxidase and glucose in the reaction mixture. The additions of glucose oxidase and glucose to the assay system allowed generation of  $H_2O_2$  at a rate of approximately 10 nmol/ ml/ min. Fig. 3.2.3 shows the rate of NBT reduction of EcHPI, MthPI, and HRP in the presence of INH and a constant flux of  $H_2O_2$  generated by glucose oxidase and glucose. MthPI supports a higher level of NBT reduction per mg enzyme from INH oxidation than EcHPI, and at a rate comparable to that of HRP, even though the molar concentration of HRP is almost ten times higher for this experiment.

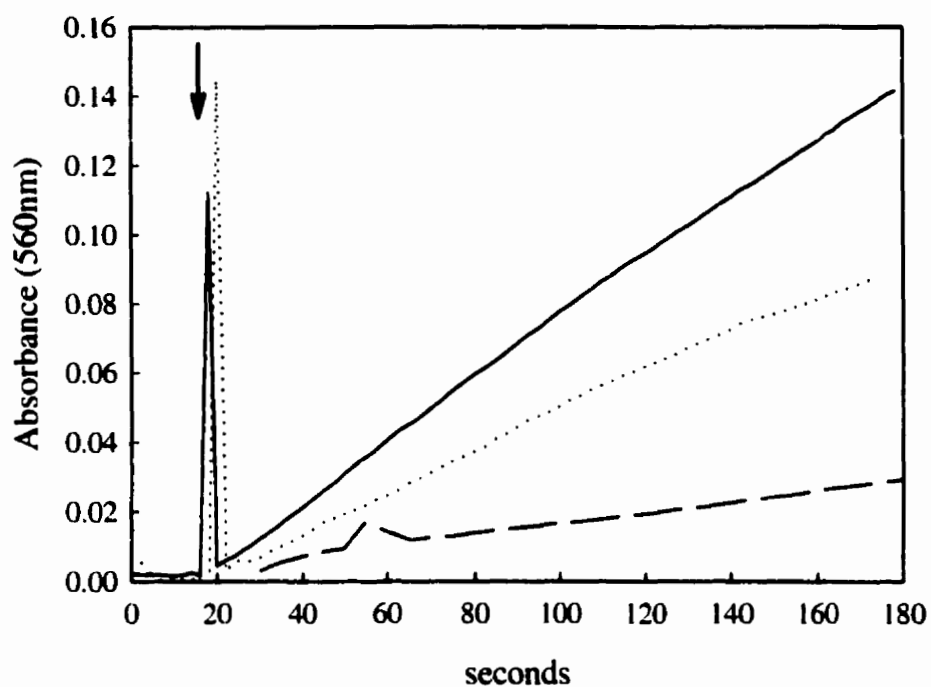
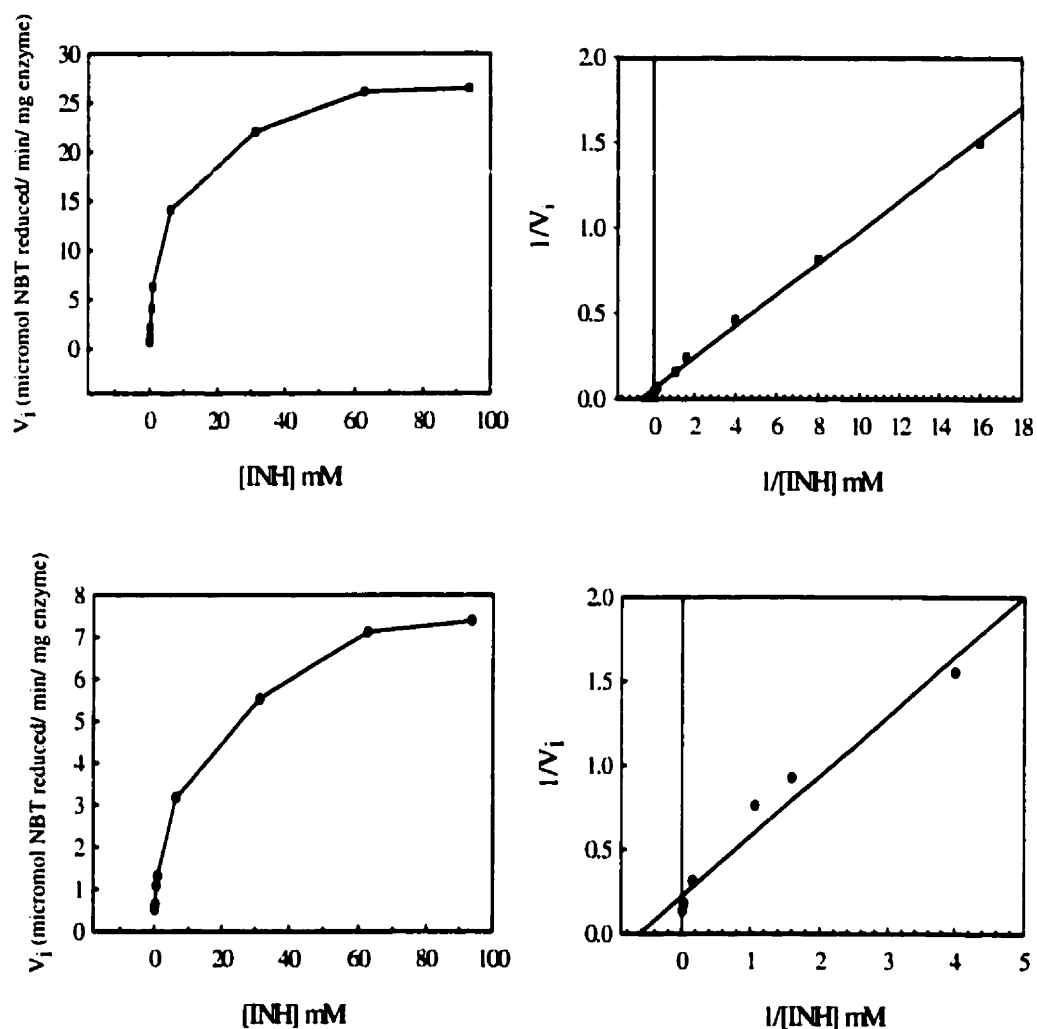


**Figure 3.2.3** Comparison of INH oxidation rates of catalase-peroxidases and horseradish peroxidase. Experiments done at room temperature in semimicro quartz cuvettes containing 1 ml final volumes of NBT (0.2 mM), INH(9 mM), glucose oxidase (5  $\mu$ g), and 0.2 mg of either HRP (4.8  $\mu$ M: solid line), MhPI (0.6  $\mu$ M: dotted line), or EcHPI (0.6  $\mu$ M: broken line). Addition of glucose (4mM) initiated the reaction at the time indicated by the arrow.

Fig. 3.2.4 shows how the rate of NBT reduction by the glucose oxidase/glucose/INH system varies as a function of substrate [INH], and also shows Lineweaver-Burk type double reciprocal replots of the data for determination of kinetic parameters. Under conditions of constant peroxide flux, the estimated  $K_m$  for MtHPI was 1.3 mM with a  $k_{cat}$  of  $8.7 \times 10^4 \text{ s}^{-1}$ . For EchPI under the same conditions, the  $K_m$  was 1.7 mM with a  $k_{cat}$  of  $2.4 \times 10^4 \text{ s}^{-1}$ . Thus MtHPI has slightly higher enzymatic affinity for, as well as higher turnover of, INH as a substrate under conditions of constant peroxide flux.

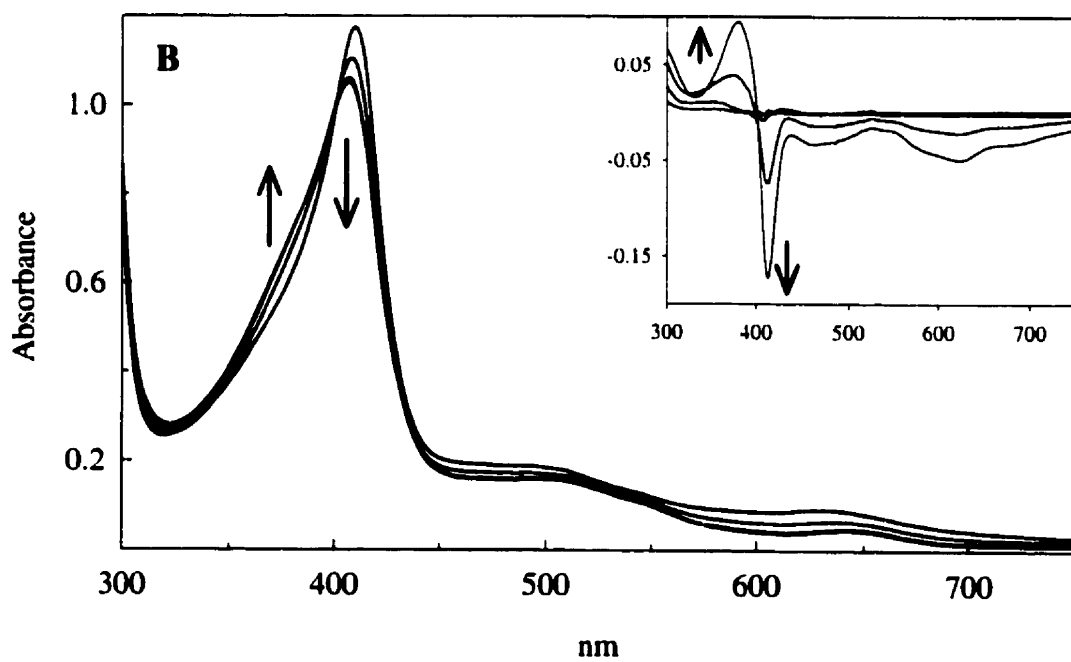
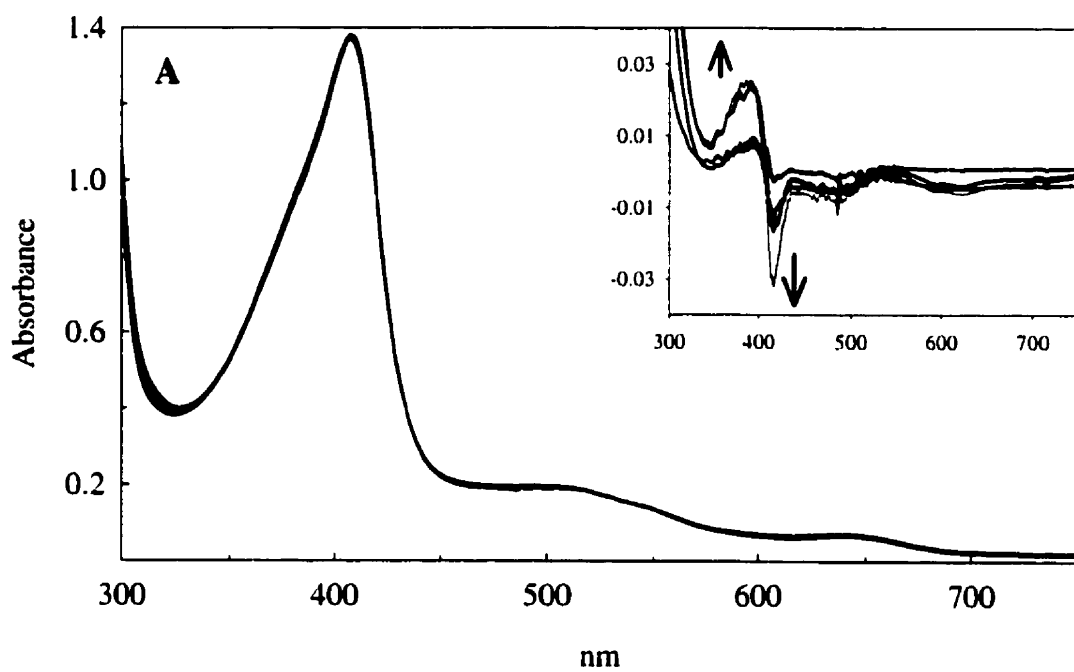
### 3.2.5. Spectral evaluation of EchPI and MtHPI interaction with isoniazid

Fig. 3.2.5 shows the spectral titration of EchPI and MtHPI with increasing concentrations of INH. The spectral shift for MtHPI is characterized by a decrease and slight blue shifting of the Sorêt maximum, with a small increase in absorbance intensity over all bands in the visible region of the spectrum. The spectral shift observed for EchPI is much less pronounced, but also consists of a slight decline in absorbance and blue shifting of the Sorêt maximum. Subtraction of the INH-complexed spectrum from the original spectrum obtained results in very similar difference spectra (Fig. 3.2.5 insets) for both enzymes, with an isosbestic point apparent for MtHPI at approximately 400 nm. The total  $\Delta$ absorbance for the difference spectra maxima minus minima may be plotted as a function of INH concentration, and the data replotted as double reciprocals, as shown in Fig. 3.2.6, to estimate the equilibrium dissociation constants for the INH-enzyme complexes. Based on this analysis, the estimated equilibrium  $K_d$  for MtHPI was 17  $\mu\text{M}$ , while that for EchPI was 130  $\mu\text{M}$ , confirming that MtHPI has a much higher binding affinity for INH than EchPI.



**Figure 3.2.4** Effect of isoniazid (INH) concentrations on the initial rate of peroxidatic oxidation as detected by nitroblue tetrazolium reduction ( $V_i$ ) of purified MthPI (squares) and EChPI (circles). Leftmost panels: Michaelis-Menten (primary) plots, rightmost panels: Lineweaver-Burk (double reciprocal) plots.

**Figure 3.2.5.** Spectral titrations of EcHPI and MtHPI with INH. Arrows indicate the direction of the spectral changes. **(A)** Representative absorption spectra of purified EcHPI in the presence of increasing [INH]. Spectra shown are for EcHPI in the presence of 0, 20, 60, 150, and 200  $\mu\text{M}$  INH. Difference spectra for the INH-EcHPI complex (fully titrated) minus EcHPI in the presence of 0-150  $\mu\text{M}$  INH, are shown in the inset. **(B)** Representative absorption spectra of purified MtHPI in the presence of increasing [INH]. Spectra shown are for MtHPI in the presence of 0, 20, 40, 60, and 80  $\mu\text{M}$  INH. Difference spectra for the INH-MtHPI (fully titrated) complex minus MtHPI in the presence of 0-60  $\mu\text{M}$  INH, are shown in the inset.



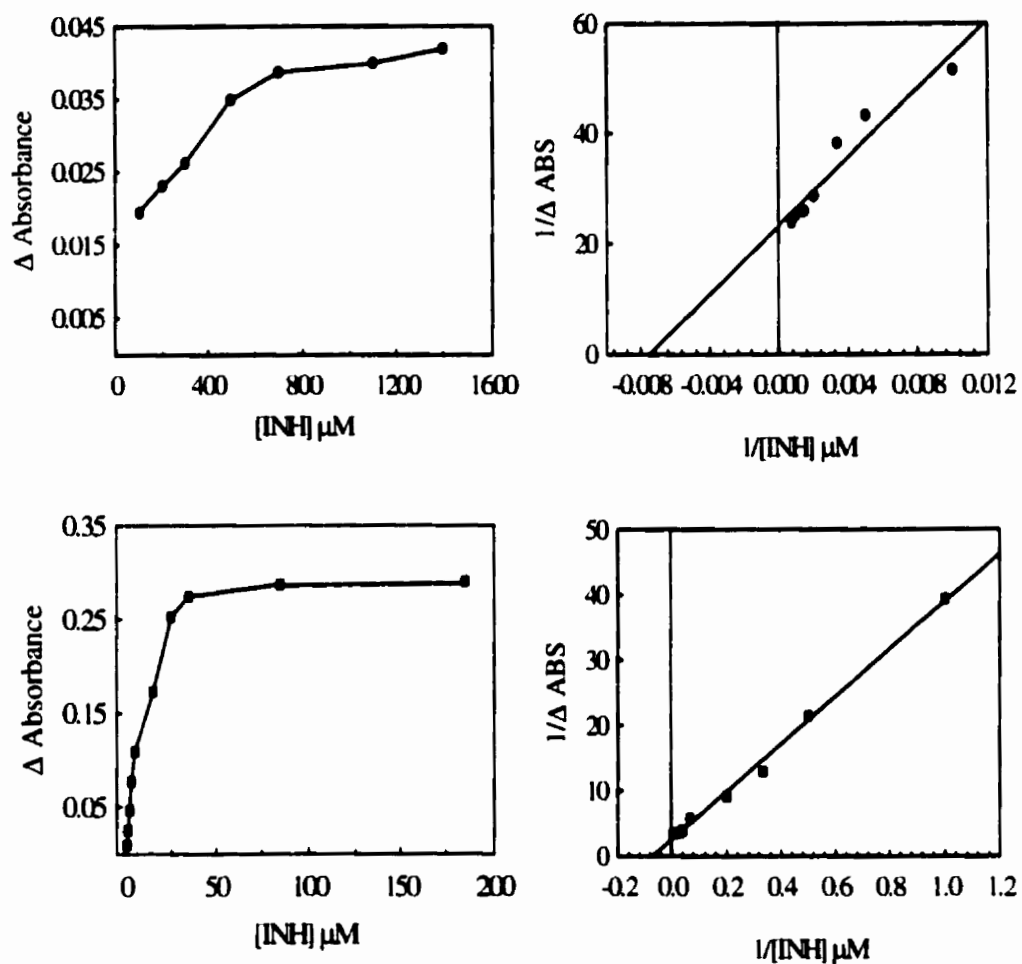


**Figure 3.2.6.** Equilibrium spectrophotometric isoniazid (INH) binding titrations of EchPI and MthPI: primary and secondary plots. Data for EchPI is represented by circles; data for MthPI is represented by squares. Primary plots (leftmost panels) and double reciprocal plots (rightmost panels) are based on the titrimetric spectral absorbance data (Fig. 3.2.5).

### **3.3 Intracellular location of EchPI**

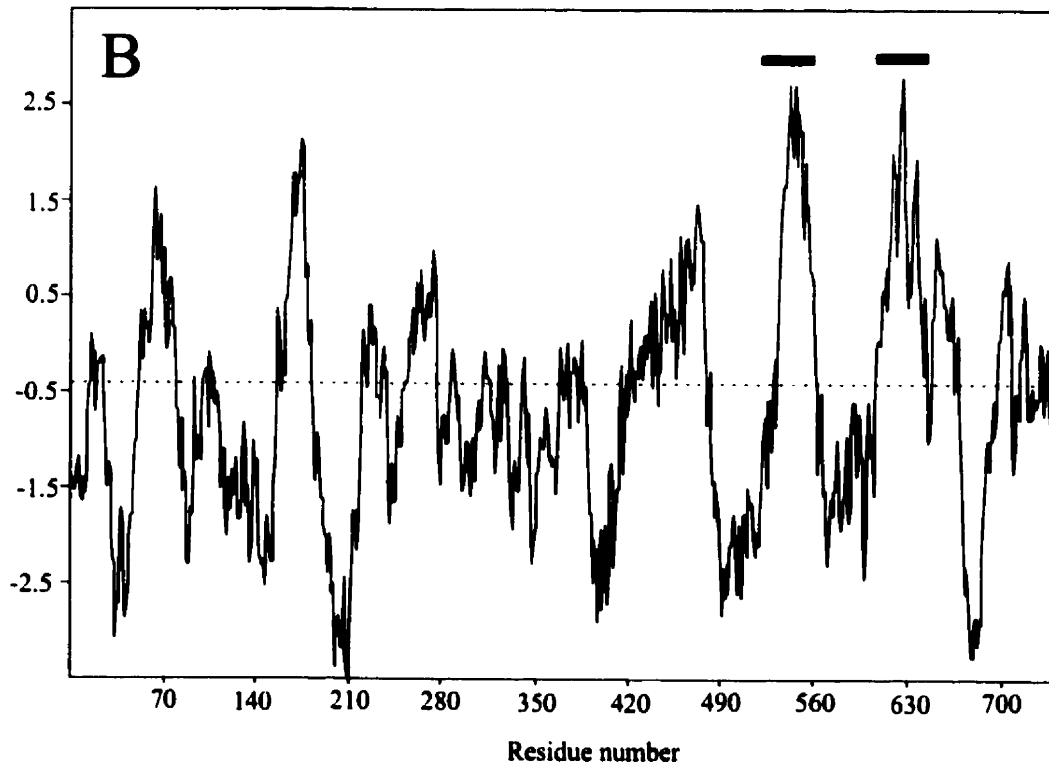
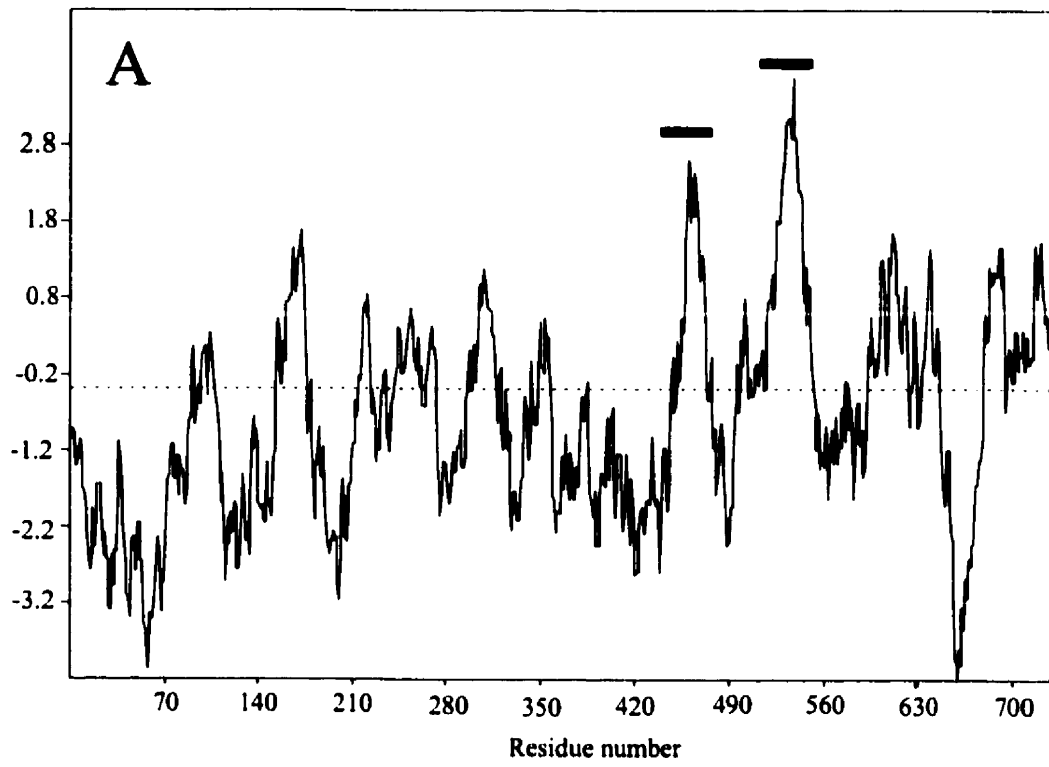
#### **3.3.1. Introduction**

*E. coli* cells have much higher natural resistance to INH than *M. tuberculosis* cells. The relative efficiencies of INH activation by *E. coli* as compared to *M. tuberculosis* HPI could be influenced by the intracellular localization or concentration of the enzyme, which could partially explain such a difference in INH susceptibility. While recent evidence has discounted the possibility of a role for catalase-peroxidase in INH transport (Bardou *et al.*, 1998), earlier work with strains of *Mycobacterium bovis* and *M. smegmatis*, have suggested that a portion of their catalase activities may be noncytoplasmic (Winder, 1960). Examination of hydrophobicity plots of both EchPI and MtHPI, as shown in Fig. 3.3.1, indicates that both enzymes have at least two hydrophobic regions that could potentially be membrane spanning, or at least allow association of the proteins with the inner membrane. More recent studies on EchPI have given rise to conflicting reports in which EchPI was localized to the periplasm of *E. coli* cells (Heimberger and Eisenstark, 1988), or alternatively, shown to be largely cytoplasmic (Brunner *et al.*, 1996). To address this unresolved question, the cellular location of EchPI in *E. coli* was ascertained using both enzymatic assays of spheroplast fractions and immunogold labelling *in situ*.

#### **3.3.2 Catalase levels in spheroplast fractions**

Spheroplasts are generated by lysozyme solubilization of the cell wall and membrane under isotonic conditions. Periplasmic material is released into the medium and cytoplasmic material is retained within the spheroplast creating a simple procedure for determining whether an enzyme is periplasmic or cytoplasmic. Care must be taken

**Figure 3.3.1** Hydrophobicity plots for EchPI (A) and MthPI (B). Plots were determined using the method of Kyte and Doolittle (1982), with a window size of 20 amino acid residues per calculation, by the physico-chemical profiles algorithm forming part of the OWL database program (Boguski *et al.*, 1992). Regions of significant hydrophobicity (index value > 2.5) are indicated by solid bars in the figure.



to prevent spheroplast lysis which will lead to contamination of the periplasmic fraction with cytoplasmic components. Glucose-6-phosphate dehydrogenase (GDH) has been characterized as an exclusively cytoplasmic enzyme, and was chosen as a cytoplasmic marker enzyme and control, in order to monitor the amount of spheroplast lysis under experimental conditions. Under the conditions of the spheroplasting procedures employed here, GDH was found predominantly (>95%) in the spheroplast fraction (cytoplasmic plus inner membrane) in all strains assayed, as is shown in Fig. 3.3.2A-C. This confirmed that the isotonic protocol used caused only minor lysis. In order to confirm that most of cells subjected to lysozyme digestion had been converted to protoplasts, the periplasmic marker enzyme, alkaline phosphatase, was also assayed. An average of at least 67% of the total alkaline phosphatase activity was released during the protoplasting procedure, confirming that at least that percentage of cells had been converted to protoplasts by the method used.

Catalase activity in *E. coli* was found to have a distribution pattern between the periplasm and cytoplasm similar to that of GDH. The wild-type *E. coli* strain MP180 expressing both catalases, HPI and HPII, contained most of the catalase activity (>95%) in the cytoplasmic fraction (Fig. 3.3.2A). This suggested that both catalases were located predominantly in the cytoplasm and this was confirmed using strains lacking one or the other of the enzymes. When assayed individually, HPI in the *katE*-containing strain UM120 (lacking HPII) and HPII in the *katG*-containing strain UM202 (lacking EcHPI) were found predominantly (85%-95%) in the cytoplasm (Fig 3.3.2B,C). Even the overexpression of HPI in a strain transformed with a *katG*-encoding plasmid, shown in Fig. 3.3.3, did not result in a significant increase in the periplasmic content of catalase activity.

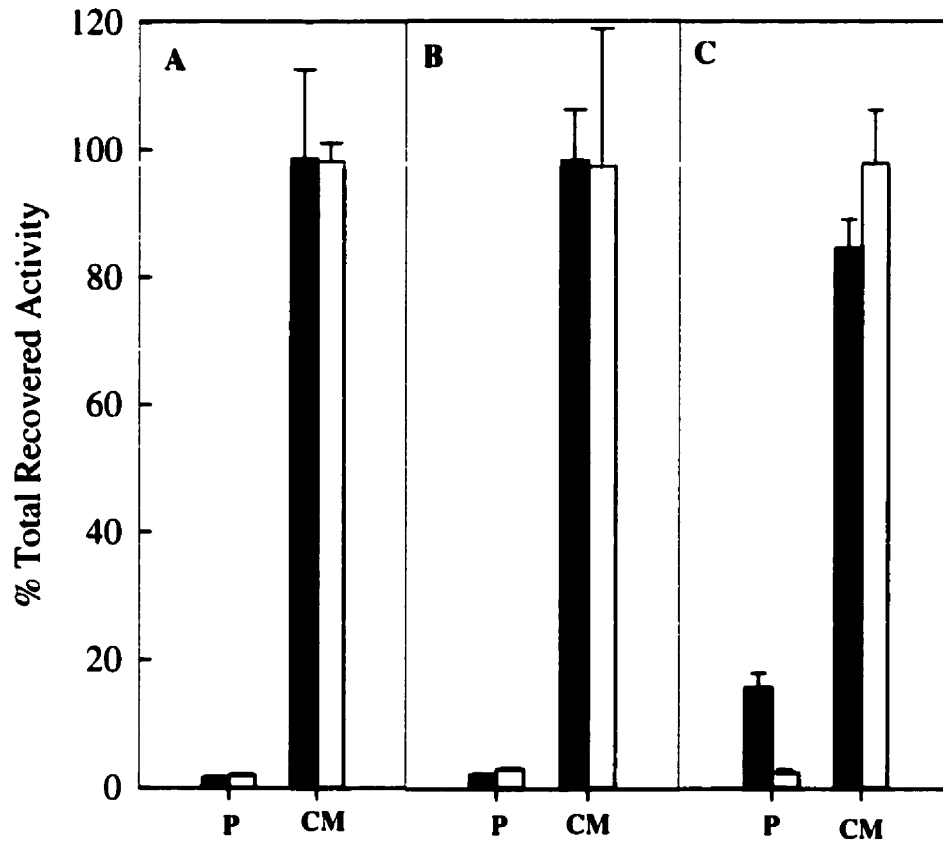


**Figure 3.3.2** Recovery of catalase and glucose-6-phosphate dehydrogenase activities from spheroplast fractions. Solid bars represent catalase activity, open bars represent glucose-6-phosphate dehydrogenase activity. **P** indicates periplasmic and **CM** indicates cytoplasmic and inner membrane fractions. Error bars indicate standard error of the mean of three individual assays. (A) Results for *E. coli* strain MP180 (wild-type). (B) Results for *E. coli* strain UM120 (*katE* or *HPII* deficient). (C) Results for *E. coli* strain UM202 (*katG* or *HPI* deficient).

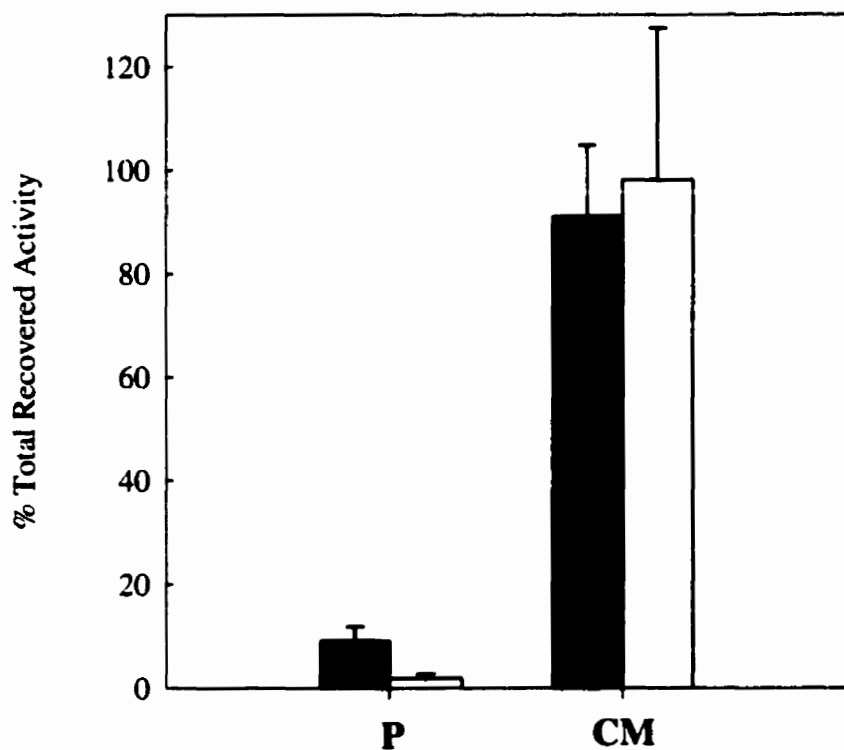


**Figure 3.3.3** Recovery of catalase and glucose-6-phosphate dehydrogenase activities from spheroplast fractions of *E. coli* strain UM262, harboring plasmid pBT22. Solid bars represent catalase activity, open bars represent glucose-6-phosphate dehydrogenase activity. P indicates periplasmic and CM indicates cytoplasmic and inner membrane fractions. Error bars indicate standard error of the mean of three individual assays.

### **3.3.3. In situ localization of EchPI by immunogold staining.**

In order to provide an independent confirmation of the localization of EchPI, *in situ* immunogold labeling of the enzyme was carried out, as is shown in Fig. 3.3.4. Wild type strain MP180 showed a sparse, but even, distribution of the gold label across the cell section (Fig. 3.3.4A). For comparison, the *katG*-containing mutant strain UM202 (not expressing EchPI) exhibited no gold staining (Fig. 3.3.4B). Strain UM262 harbouring plasmid pBT22, encoding *katG*, and producing high levels of EchPI, exhibited a pattern of very dense gold label that was evenly distributed across the cell (Fig. 3.3.4C). In both Fig. 3.3.4A and C, there were significantly more gold particles within the cell than in an equivalent background area. The gold labeling pattern is indicative of EchPI being distributed throughout the cytoplasm with no bias towards the periplasm.

## **3.4. Construction and characterization of EchPI mutants**

### **3.4.1. Introduction**

Amino acid residues have been shown to be highly conserved between EchPI and the superfamily of peroxidase enzymes (Welinder, 1992). Evidence also indicates that the *E. coli katG* gene is the culmination of gene duplication of a peroxidase, based on homology of the first half of the sequence to the second half (Welinder, 1991). Using alignment of the EchPI protein sequence to that of the cytochrome *c* peroxidase (CCP) sequence, for which the detailed 3-D crystallographic structure is already known, allowed identification of residues in EchPI that correspond to catalytic residues identified in CCP. Not surprisingly, many of these residues are highly conserved among the peroxidases and catalase-peroxidases (Loewen, 1997). In the current absence of a crystal structure for any catalase-peroxidase, several putative active site residues in EchPI were selected to be



**Figure 3.3.4** Immunogold staining to visualize the intracellular location of EchPI in *E. coli* strains: (A) MP180, a wild-type strain; (B) UM202, a *katG*-containing mutant strain; (C) UM262 [pBT22] which over-produces HPI. The bar in A represents 0.25  $\mu\text{m}$ . The ratio of particles in the cell to particles in the background (averaged from 6 areas equivalent in size to the cell) was 10:2.7 in A, 0:1.8 in B and 150:8.2 in C.

changed via site-directed mutagenesis. The goal in changing the putative active site residues was twofold: 1) it would provide confirmation of the catalytic role of the residues, and provide a basis for comparison of the modifications with the same or similar modifications carried out in previous site-directed mutagenesis studies of CCP and HRP and, 2) it would allow the opportunity to modify other amino acids in the active site which could allow modulation of the two enzymatic activities (i.e. increase or decrease either catalase or peroxidase activity with respect to the other).

Residues in the putative EchPI active site identified for mutagenesis were histidine 106, arginine 102, tryptophan 105, and histidine 267, as shown in Figure 3.4.1, based upon the active site structure from CCP. His106 corresponds to His52 of CCP, which is located immediately above the heme iron in the distal (above the heme plane) part of the active site, and acts to base-catalyze the initiation of the enzymatic reaction cycle leading to formation of compound I. Arg102 corresponds to Arg48 of CCP, which is also in the distal heme pocket, and is believed to stabilize the formation of compound I through hydrogen bonding. Trp105, corresponding to Trp51 of CCP, is often substituted for a Phe residue in other peroxidases, and may therefore have a role in modulating relative catalase and peroxidase activities. His267 corresponds to His175 of CCP, which is located immediately below the heme iron in the proximal (below the heme plane) part of the active site, and coordinates via its imidazole nitrogen to form the fifth ligand to the heme iron. In catalases, this residue is usually substituted by a tyrosine.

In order to study the roles of the putative active site residues identified, all were changed by site-directed mutagenesis. A summary of the amino acid changes specified by the modifications in the DNA sequence for the mutant *katGs* constructed is shown in Table 3.4.1. This table also summarizes whether overexpression of the mutant proteins was achieved in *E. coli*, and whether or not the mutant was successfully purified. Included in the table is mutant Lys419Stop, which was constructed to evaluate whether

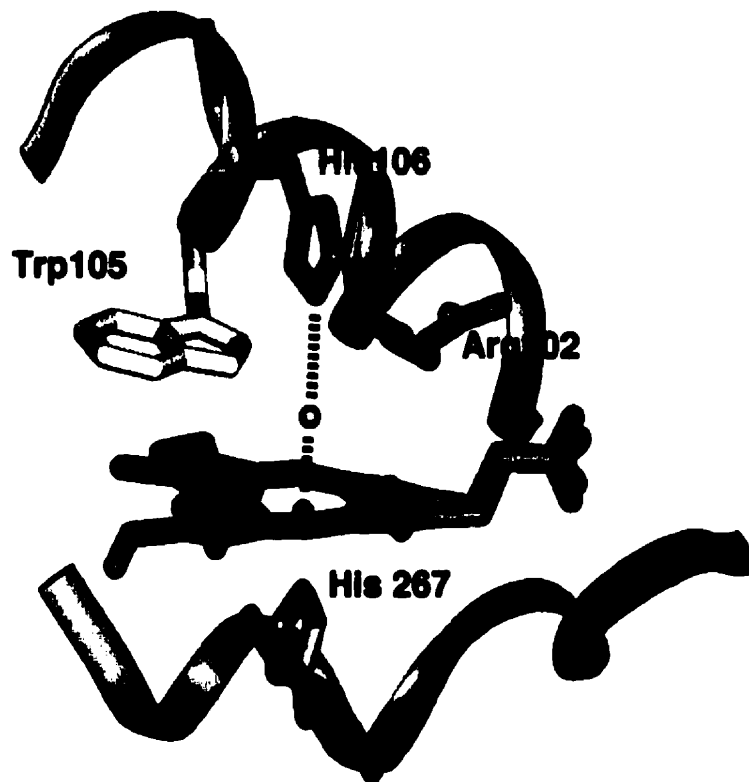


**Figure 3.4.1** Representation of the relative positions of key residues in EcHPI based on the structure of cytochrome c peroxidase. The heme is shown in red.

**Table 3.4.1** Summary of EchPI mutants constructed

<b>Mutant/ Modification</b>	<b>Expressed in <i>E. coli</i></b>	<b>Purified</b>
<b>Active Site Mutants</b>		
His106Leu	Yes	No (unstable)
His106Cys	Yes	Yes
His106Tyr	Yes	Yes
Arg102Leu	Yes	Yes
Arg102Cys	Yes	Yes
Arg102Lys	Yes	Yes
Trp105Leu	Yes	Yes
Trp105Cys	No	-
Trp105Phe	Yes	Yes
His267Tyr (proximal)	Yes	Yes
<b>Other Mutants</b>		
Arg419Stop	No	No

only the first half of the protein sequence could be successfully expressed in *Escherichia coli*, based on the assumption that the *E. coli katG* is gene duplicated. The Trp105Cys mutant construct failed to express enzyme as judged by SDS-PAGE of crude extracts, while the His106Leu mutant construct did express the expected protein band in SDS-PAGE, but was not successfully purified, perhaps due to inherent instability of the enzyme making it susceptible to degradation.

### 3.4.2 Structural characterization of EchPI mutants

Purified EchPI mutants were analyzed by SDS-PAGE, as shown in Figure 3.4.2. Compared to the EchPI band on the same electrophoretogram, the predominant bands for all the mutant proteins migrated to the same position at 80 kDa. The presence of larger bands at  $\approx 160$  kDa and at  $>160$  kDa (presumed to be 320 kDa) probably represent either the dimeric or tetrameric forms of the enzymes, which are presumably the result of some intersubunit covalent cross-links which are not labile to reduction by either  $\beta$ -mercaptoethanol or dithiothreitol added to the sample buffer.

Purified EchPI mutants were also analyzed by non-denaturing PAGE, as shown in Figure 3.4.3. All the mutant enzymes except for the H106 variants show only one major band or isoform, compared to at least two bands which are observed in the case of wild type EchPI. The mobilities of these bands also differ slightly from that observed for EchPI wild type protein.

Figure 3.4.4 shows the optical absorbance spectra of all the mutants compared to the spectrum for wild type EchPI. Table 3.4.2 summarizes the position of the absorption maxima observed for all the mutants and wild type EchPI, and also shows the heme/protein ratio for each species as the  $Abs_{407/280}$  value. In the majority of mutants, the Sorêt band is at or within one nm of the position of the same maximum for EchPI. The exceptions are the R102C and H267Y mutants, for which this maximum is red shifted by four and three nm, respectively. Similarly, the charge transfer bands of the

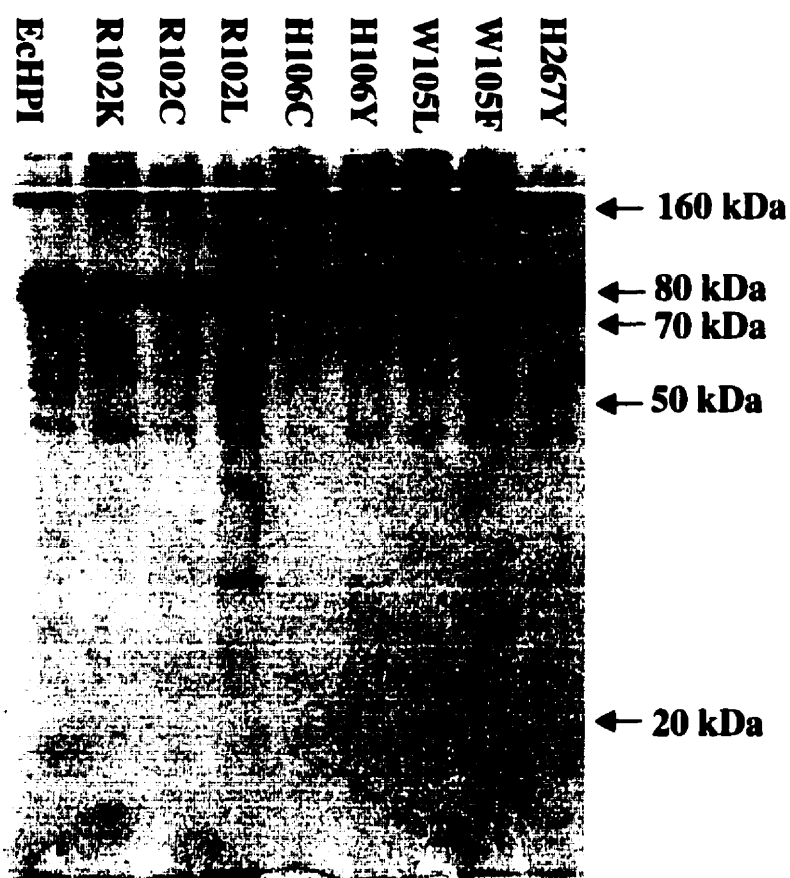


**Figure 3.4.2** SDS-polyacrylamide gel electrophoresis analysis of EchPI and the putative active site mutants of EchPI following purification. Samples of approximately 7.5  $\mu\text{g}$  were electrophoresed in an 8% gel and stained for protein with Coomassie Brilliant Blue.

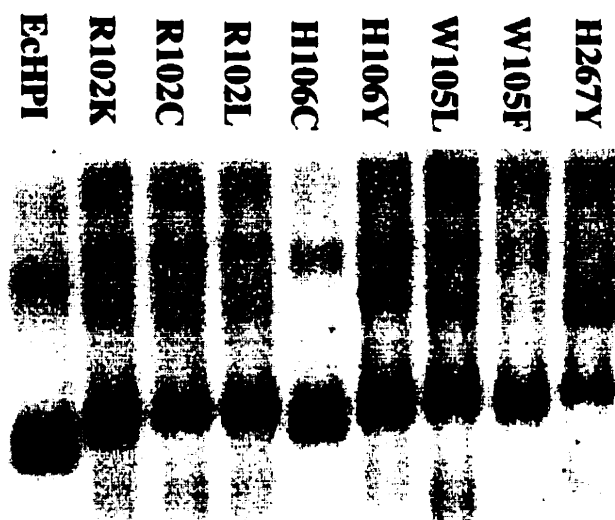


**Fig. 3.4.3.** Non-denaturing polyacrylamide gel electrophoresis analysis of EcHPI and the putative active site mutants of EcHPI following purification. Samples of approximately 7.5  $\mu$ g were electrophoresed in an 9% gel and stained for protein with Coomassie Brilliant Blue.

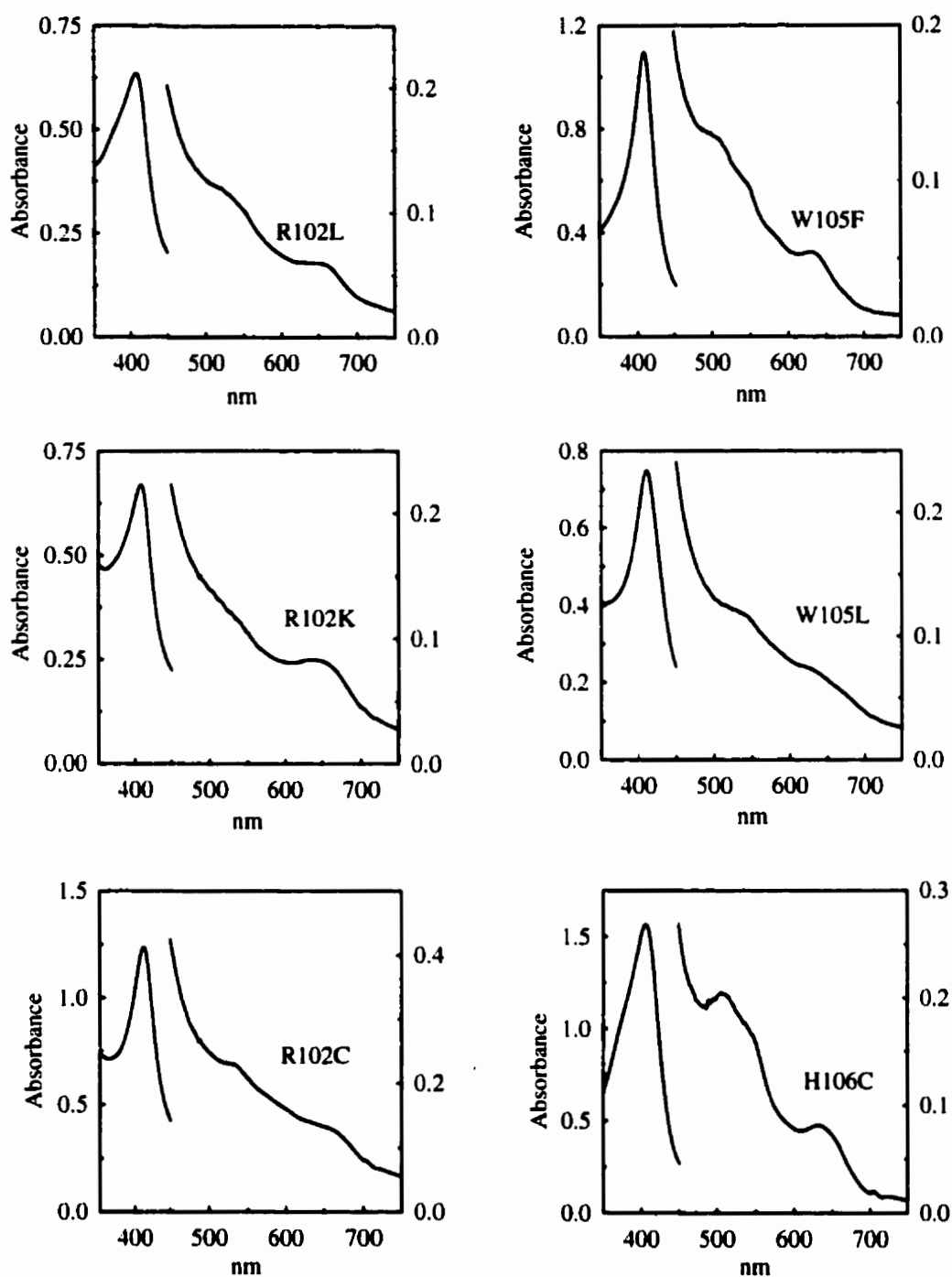


**Figure 3.4.4** Absorption spectra of EchPI mutant enzymes compared to EchPI wild type. Left axis scales apply to the 350-450 nm wavelength range. Right axis scales (Absorbance) apply to the 450-750 nm wavelength range.

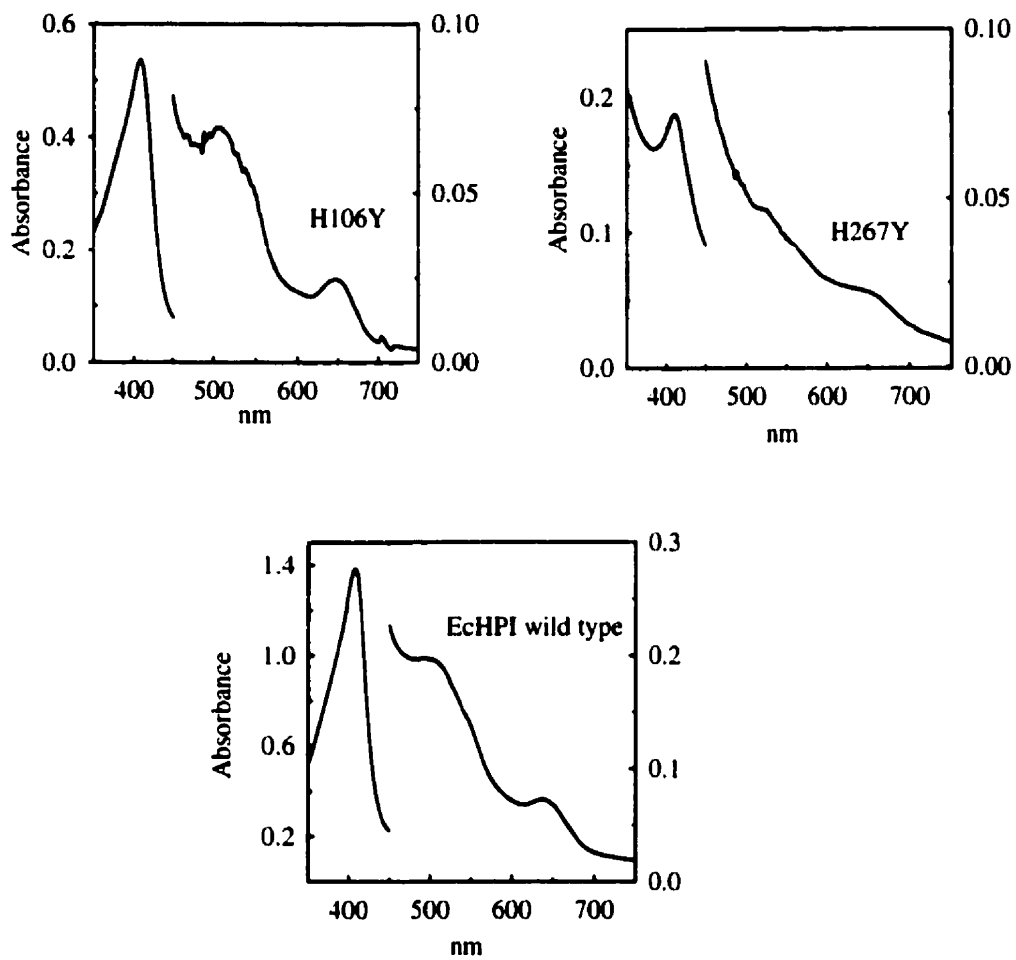


**Figure 3.4.4.** (continued)

**Table 3.4.2** Summary of observed optical absorbance maxima and heme/protein ratios for purified EchPI and mutants.

Mutant	Sorêt maximum (nm)	$\alpha$ -charge transfer band (nm)	$\beta$ -charge transfer bands (nm)	$A_{407/280}$
Wild type	408	640	510, $\approx$ 540	0.51
R102L	408	650	-, $\approx$ 540	0.07
R102K	408	640	-	0.11
R102C	412	$\approx$ 660	$\approx$ 530, -	0.10
H106Y	408	645	510, 540	0.16
H106C	407	635	510, 540	0.37
W105F	409	630	$\approx$ 510, $\approx$ 540	0.36
W105L	409	630	-, $\approx$ 540	0.19
H267Y	411	$\approx$ 655	$\approx$ 510, $\approx$ 560	0.022

His106 mutants are at positions identical with those of the wild type EcHPI, but the remaining mutants all show some shifting of these bands with respect to their position in the wild type enzyme. Such shifts are general indicators of changes in the hydrogen bonding network in the vicinity of the heme. All the mutants also show lower heme/protein ratios than the wild type enzyme, with H267Y having as little as 5% of the heme present in the wild type enzyme.

### **3.4.3. Biochemical characterization of EcHPI mutants**

#### **3.4.3a. Specific activities and kinetics of EcHPI mutants**

Table 3.4.3 summarizes the specific enzymatic activities of all the EcHPI mutants and compares these data with those for the wild type enzyme. Catalase activities of all the mutants are reduced compared to that of wild type EcHPI. The H106 mutants show only about 0.01% the activity of wild type EcHPI, while the R102 mutants show 1- 2% the wild type enzymatic activity. The W105 mutants and the H267Y mutant had catalase specific activities intermediate between the values obtained for the R102 and H106 mutants, with the W105 mutants showing up to 0.3% wild type catalase activity, while the H267Y mutant showed only 0.05% wild type activity.

Peroxidase specific activities for the H106, R102, and H267Y mutants also were below that of wild type EcHPI, for all peroxidase substrates tested. The ratios of mutant to wild type peroxidase activities in all cases were higher, but not necessarily consistent with the ratios observed for the catalase activities. Of greatest interest was the observation that the W105 mutants not only retained, but exceeded, the wild type EcHPI peroxidase activity for each of the peroxidatic substrates tested. W105F, for example, had up to 50-150% higher specific activity than wild type enzyme in reaction with substrate donors ABTS, o-dianisidine, and INH (INH-NBT reduction assay). W105L showed lower absolute activity than W105F with o-dianisidine and INH, but still

**Table 3.4.3.** Specific enzymatic activities of EchPI mutants

<b>Mutant</b>	<b>Catalase (U/mg)</b>	<b>Peroxidase (ABTS, U/mg)</b>	<b>Peroxidase (o- dianisidine, U/mg)</b>	<b>INH oxidation (U<sup>◇</sup> /mg)</b>
<b>Wild type</b>	<b>1,900 ± 400</b>	<b>660 ± 40</b>	<b>3.2 ± 0.1</b>	<b>3.2 ± 0.1</b>
R102L	19 ± 10	90 ± 40	0.14 ± 0.07	0.18 ± 0.01
R102C	10 ± 7	60 ± 10	0.84 ± 0.02	0.24 ± 0.01
R102K	35 ± 7	90 ± 10	0.19 ± 0.01	0.49 ± 0.09
H106C	0.25 ± 0.04	11 ± 1	0.028 ± 0.001	0.30 ± 0.02
H106Y	0.16 ± 0.03	20 ± 10	0.011 ± 0.002	0.09 ± 0.01
W105F	1.9 ± 0.1	1,860 ± 80	4.7 ± 0.4	4.8 ± 0.4
W105L	5.9 ± 0.1	1,300 ± 100	2.0 ± 0.1	1.7 ± 0.2
H267Y	0.95 ± 0.09	11.7	0.0013 ± 0.0002	0.11

<sup>◇</sup> INH oxidation as measured by the NBT reduction assay (in presence of glucose oxidase/glucose), where 1 unit represents 1 μmol monoformazan dye produced per ml per min.

had double the activity of the wild type enzyme with ABTS as donor substrate.

The effect of  $[H_2O_2]$  on the rate of the catalase reaction of several of the EcHPI mutants is shown in Figure 3.4.5. The effect of  $[ABTS]$  on the rate of peroxidase reaction of several of the EcHPI mutants is shown in Figure 3.4.6. These data are replotted as Lineweaver-Burk type plots in Figures 3.4.7 and 3.4.8, for catalase and peroxidase, respectively. Above 300 mM  $H_2O_2$ , mutants R102C and W105L showed a decline in initial catalase reaction rates, suggesting that some of the EcHPI mutants are susceptible to substrate inactivation at  $[H_2O_2]$  similar to that for the wild type enzyme. In several instances, reaction rates did not reach saturation for either catalase or peroxidase activity at high substrate concentrations. A compilation of selected kinetic parameters derived from the above figures is presented in Table 3.4.4. Turnover numbers for the mutants were deliberately omitted, as the variability in heme/protein ratios for these species would require individual corrections for an estimated reduction in number of active sites per holoenzyme. In the majority of mutants, apparent  $K_m$  values for both the catalase and peroxidase activities increase. The increase in apparent  $K_m$  was most dramatic in the H106Y and the W105 mutants, in which catalase  $K_m$ s were increased at least ten times and peroxidase  $K_m$ s were higher by at least 4-5 times. In all except the W105 mutants, however, maximum reaction rates were greatly reduced for both catalase and peroxidase activities. Greatest reduction in maximal catalase reaction rates was observed for the H106, W105, and H267Y mutants, while the H106 and the R102L mutants had the greatest reduction in maximal peroxidase reaction rates.

### **3.4.3b. Effect of inhibitors on catalytic activities of EcHPI mutants**

Figure 3.4.9 shows the inhibition of catalase activity of EcHPI mutants in the presence of either KCN or  $NaN_3$ . Similarly, figure 3.4.10 shows the inhibition of peroxidase activity of EcHPI mutants in the presence of either KCN or  $NaN_3$ . H267Y

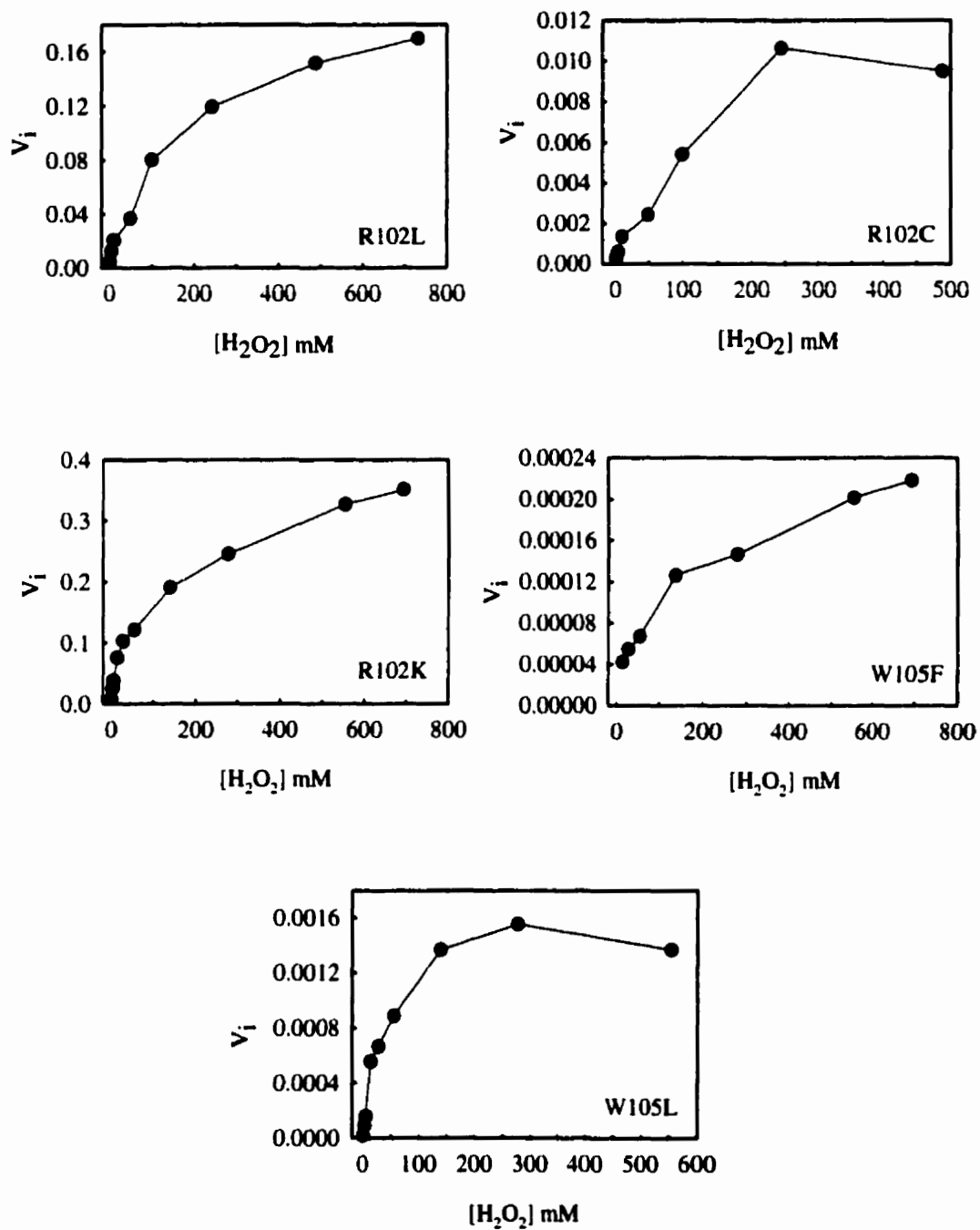


**Figure 3.4.5** Effect of  $\text{H}_2\text{O}_2$  on the initial catalytic velocities ( $V_i$ : mol  $\text{H}_2\text{O}_2$  decomposed/ min/ mg enzyme) of EcHPI mutants: Michaelis-Menten plots.

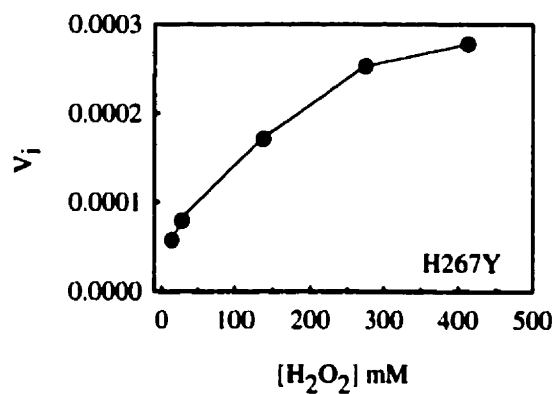
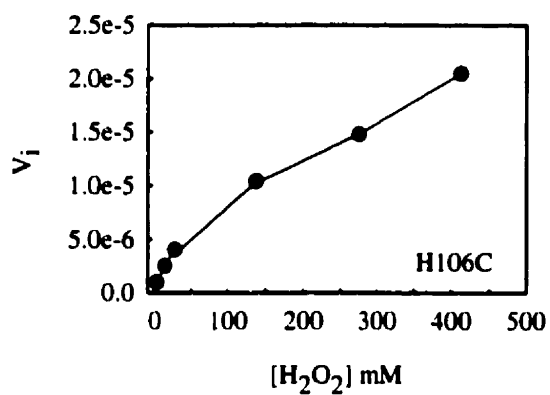
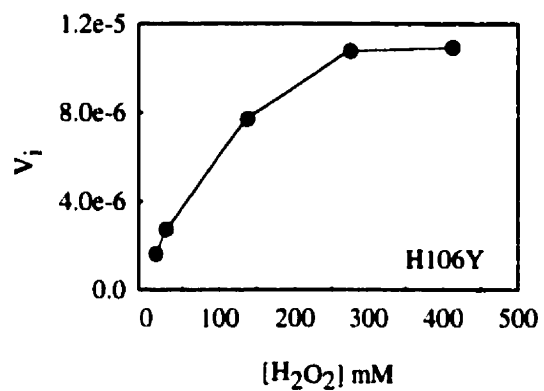


**Figure 3.4.5.** (continued)

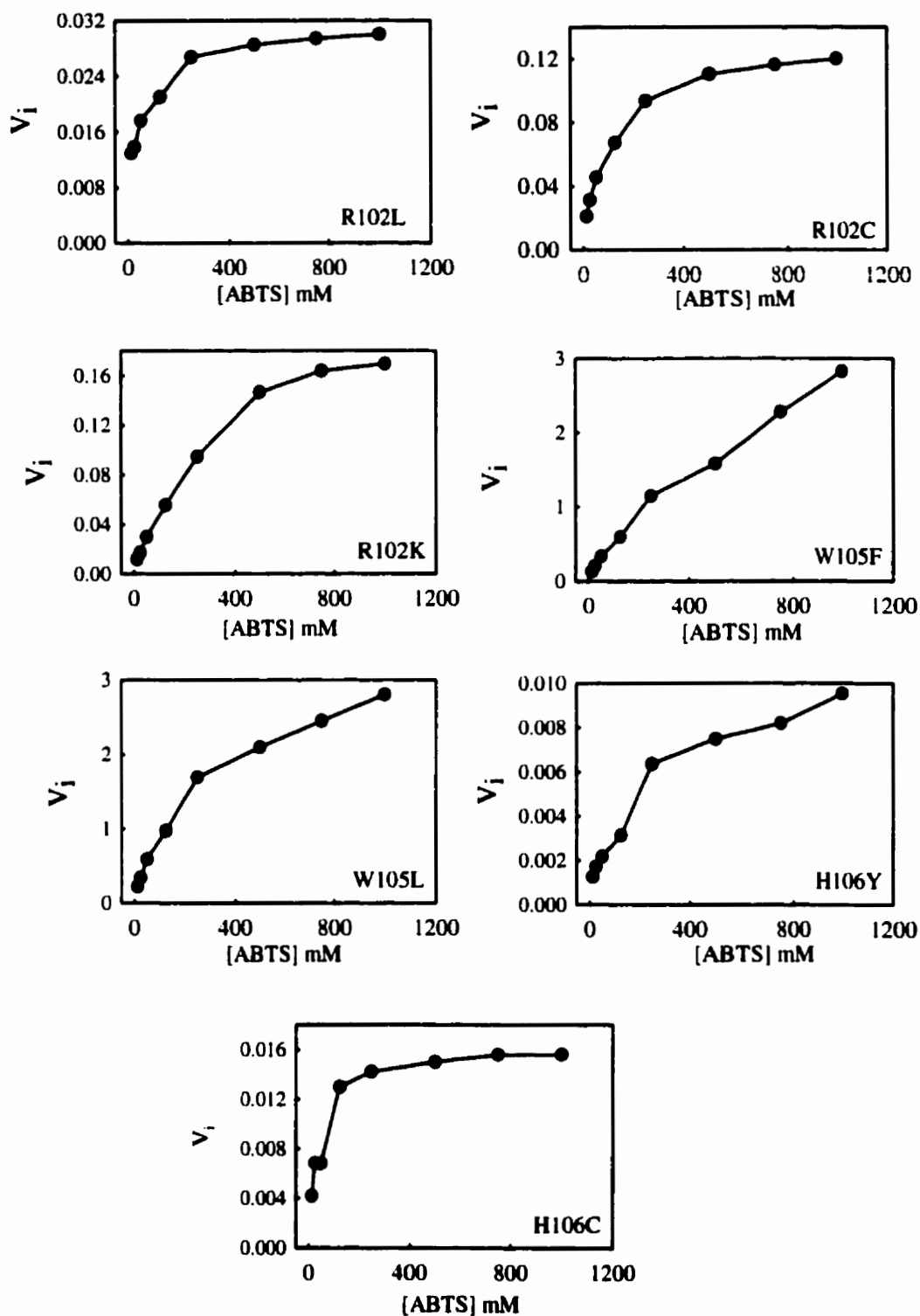


**Figure 3.4.6** Effect of 2,2 -azinobis(3-ethylbenzothiazolinesulfonic acid)( ABTS ) on the initial peroxidatic velocities ( $V_i$ ; mmol ABTS oxidized/ min/ mg enzyme) of EchPI mutants: Michaelis-Menten plots.

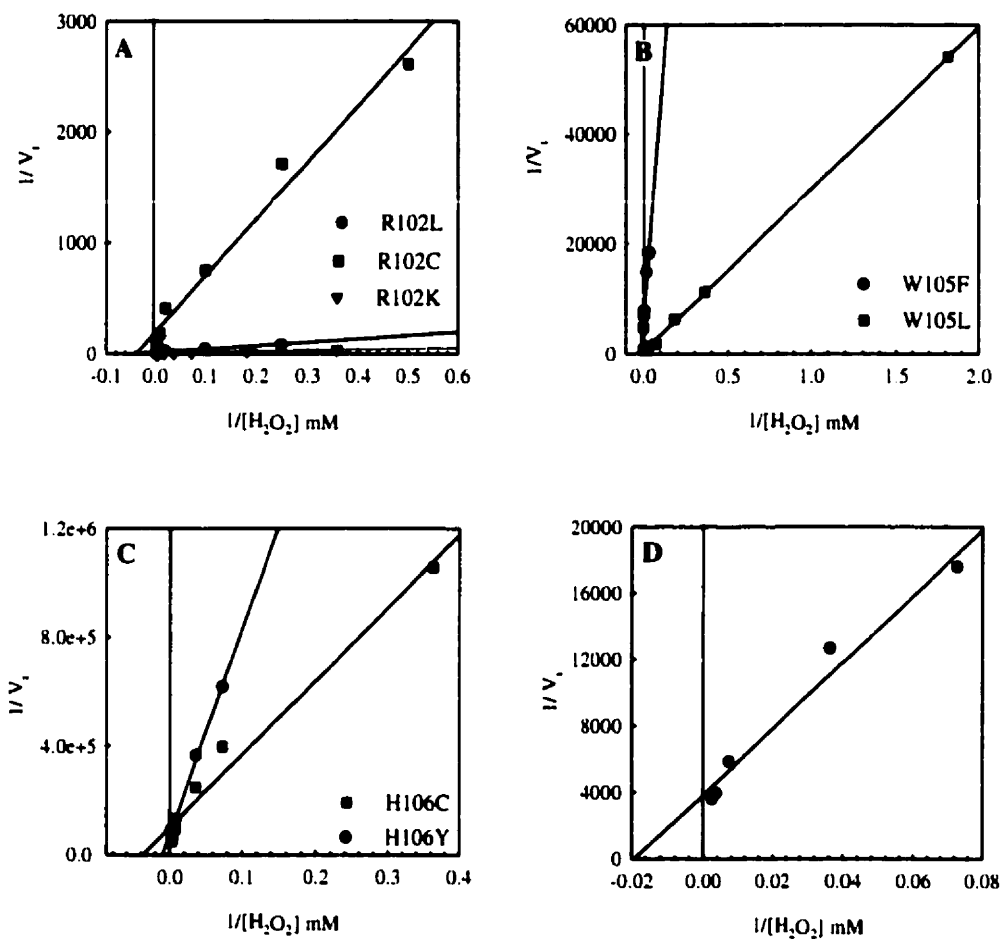


**Figure 3.4.7** Effect of  $\text{H}_2\text{O}_2$  concentrations on the rate of catalase reaction of the EcHPI mutants: Lineweaver-Burk plots. **A)** Results for R102 mutants. **B)** Results for W105 mutants. **C)** Results for H106 mutants. **D)** Results for H267Y mutant

**Figure 3.4.8** Effect of 2,2-azinobis(3-ethylbenzothiazolinesulfonic acid) on the initial peroxidatic velocities ( $V_i$ ; mmol ABTS oxidized/ min/ mg enzyme) of EcHPI mutants: Lineweaver-Burk plots.

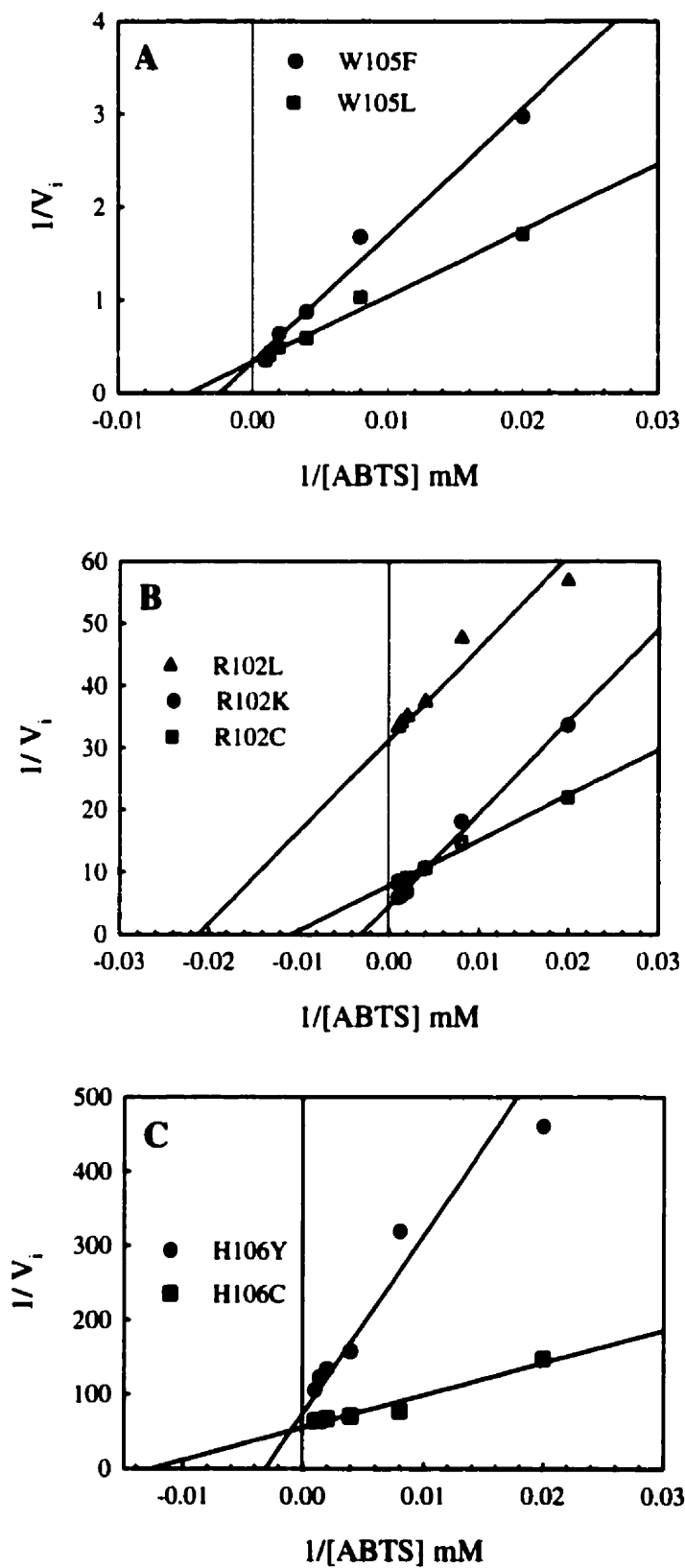


**Table 3.4.4.** Kinetic parameters of EcHPI mutants

Mutant	Catalase		Peroxidase (ABTS)	
	Apparent $V_{max}$ (mol/ min)	Apparent $K_m$ (mM)	Apparent $V_{max}$ (mol/ min)	Apparent $K_m$ ( $\mu$ M)
Wild type	5.9	5.9	$6.5 \times 10^{-3}$	55
R102L	0.094	33	$3.2 \times 10^{-5}$	48
R102K	0.15	12	$2.2 \times 10^{-4}$	400
R102C	0.052	31	$1.3 \times 10^{-4}$	100
H106Y	$1.4 \times 10^{-5}$	100	$1.3 \times 10^{-5}$	330
H106C	$9.9 \times 10^{-5}$	28	$1.9 \times 10^{-5}$	80
W105F	$2.0 \times 10^{-4}$	91	$3.0 \times 10^{-3}$	480
W105L	$2.0 \times 10^{-3}$	77	$3.0 \times 10^{-3}$	240
H267Y	$2.6 \times 10^{-4}$	53	ND	ND

ND: Not determined

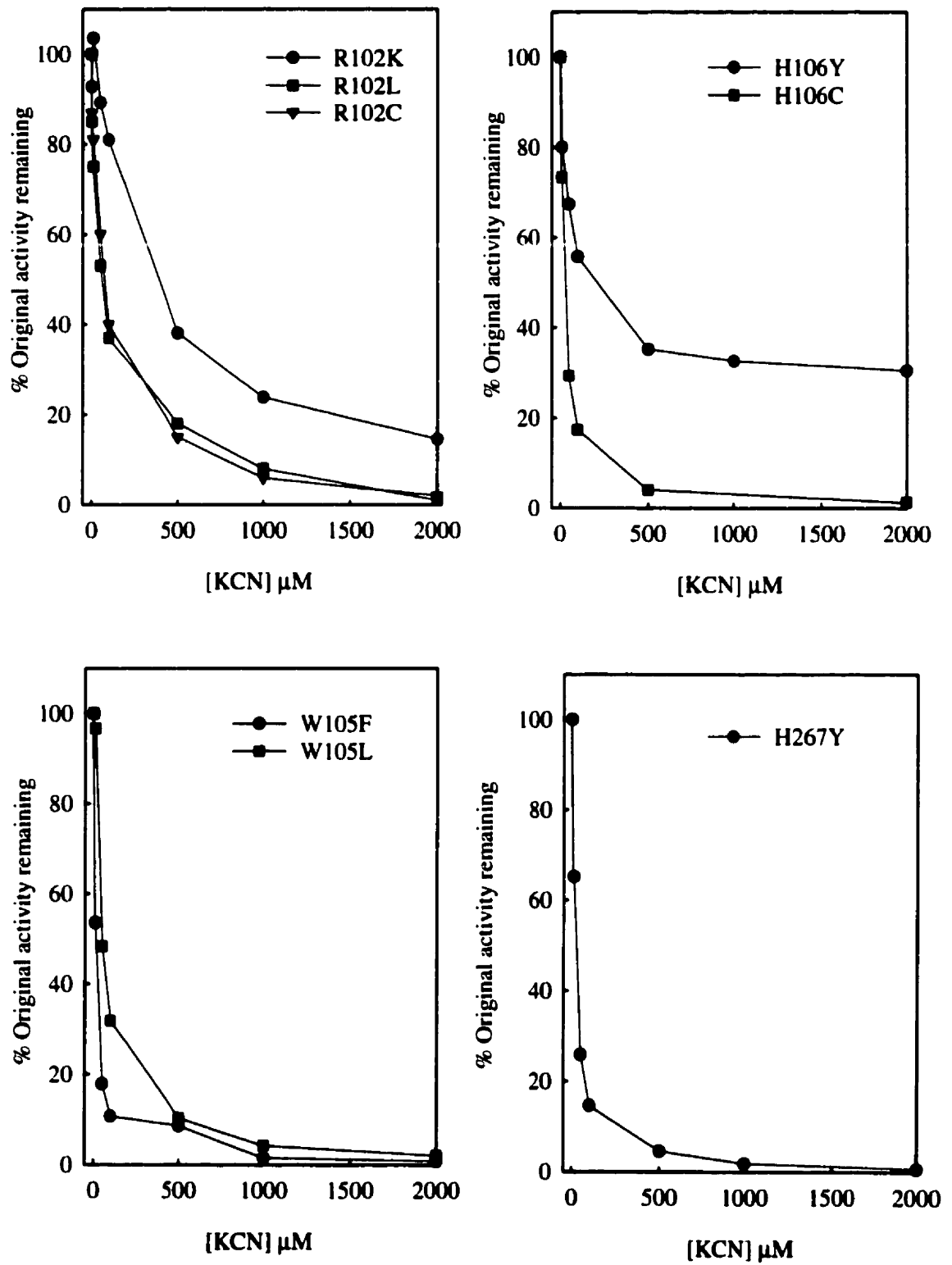


Figure 3.4.9A

**Figure 3.4.9.** Inhibition of catalase activity of EchPI mutants by A) KCN, or B)  $\text{NaN}_3$ .

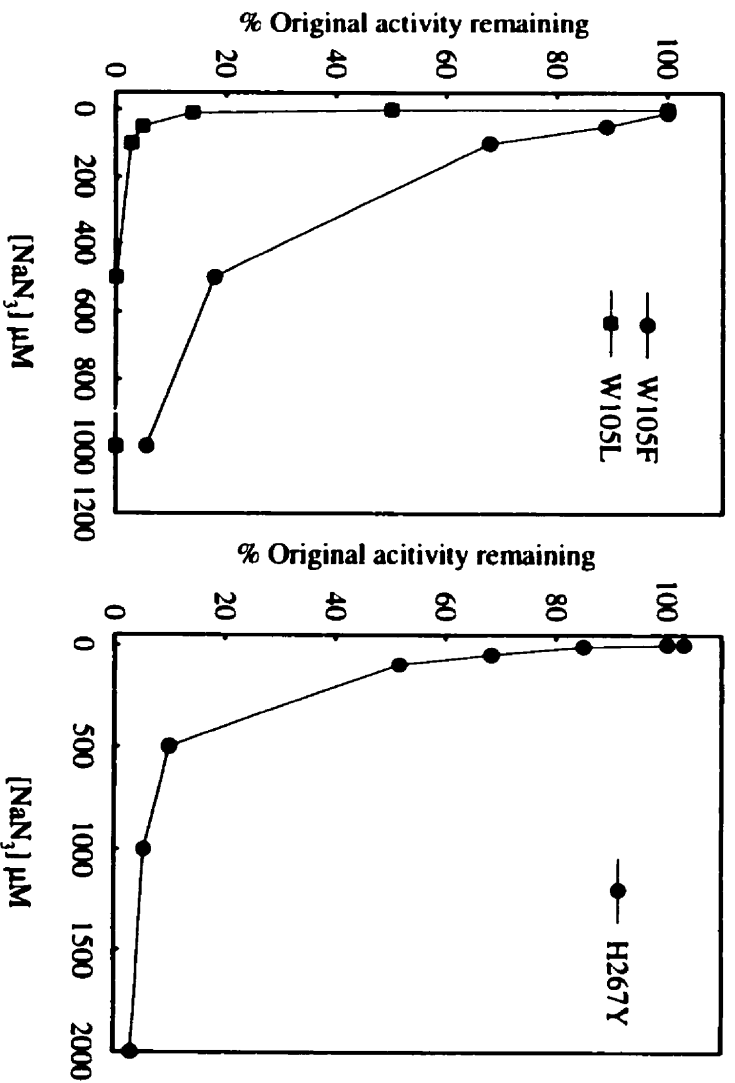
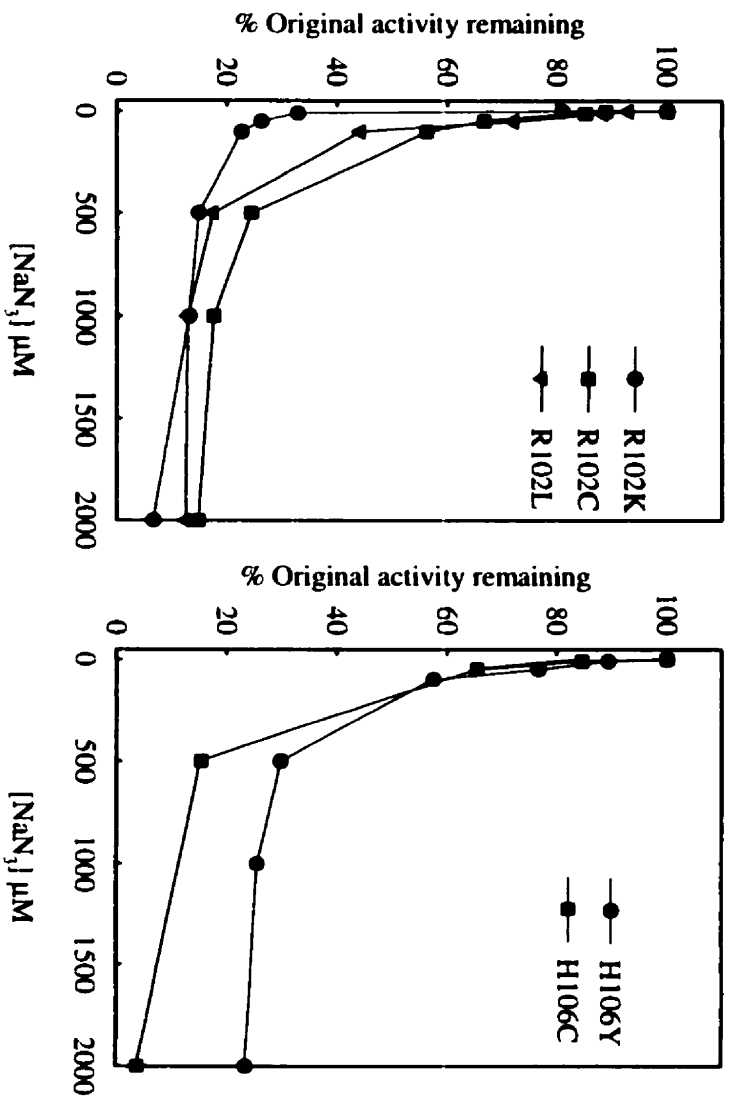


Figure 3.4.9B

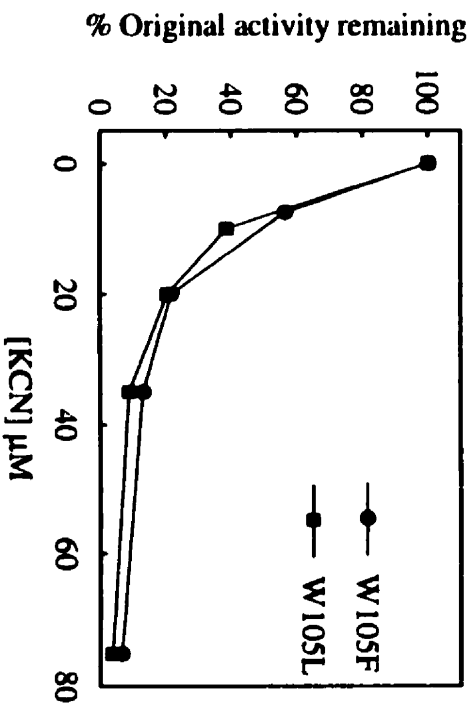
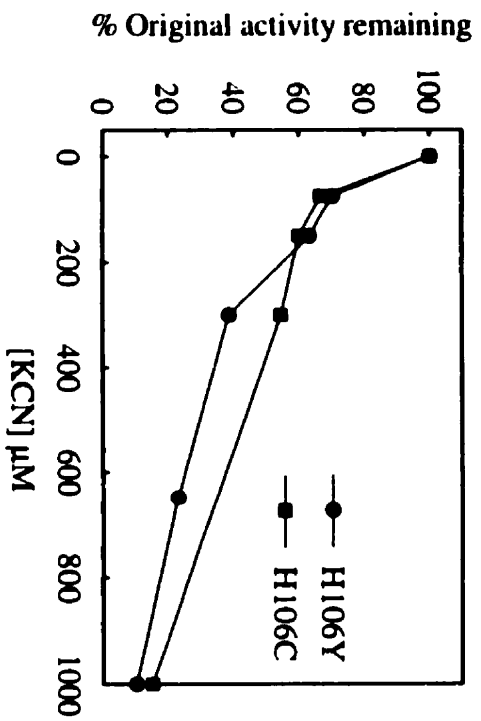
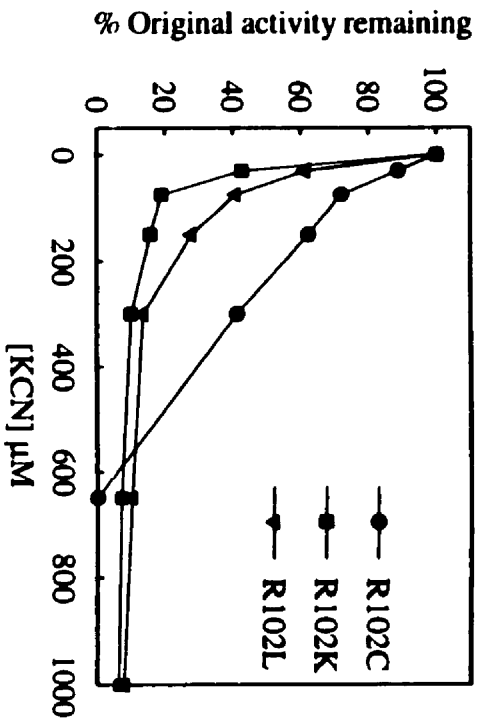


Figure 3.4.10A

**Figure 3.4.10.** Inhibition of ABTS peroxidase activity of ECHPI mutants by A) KCN, or B)  $\text{NaN}_3$ .

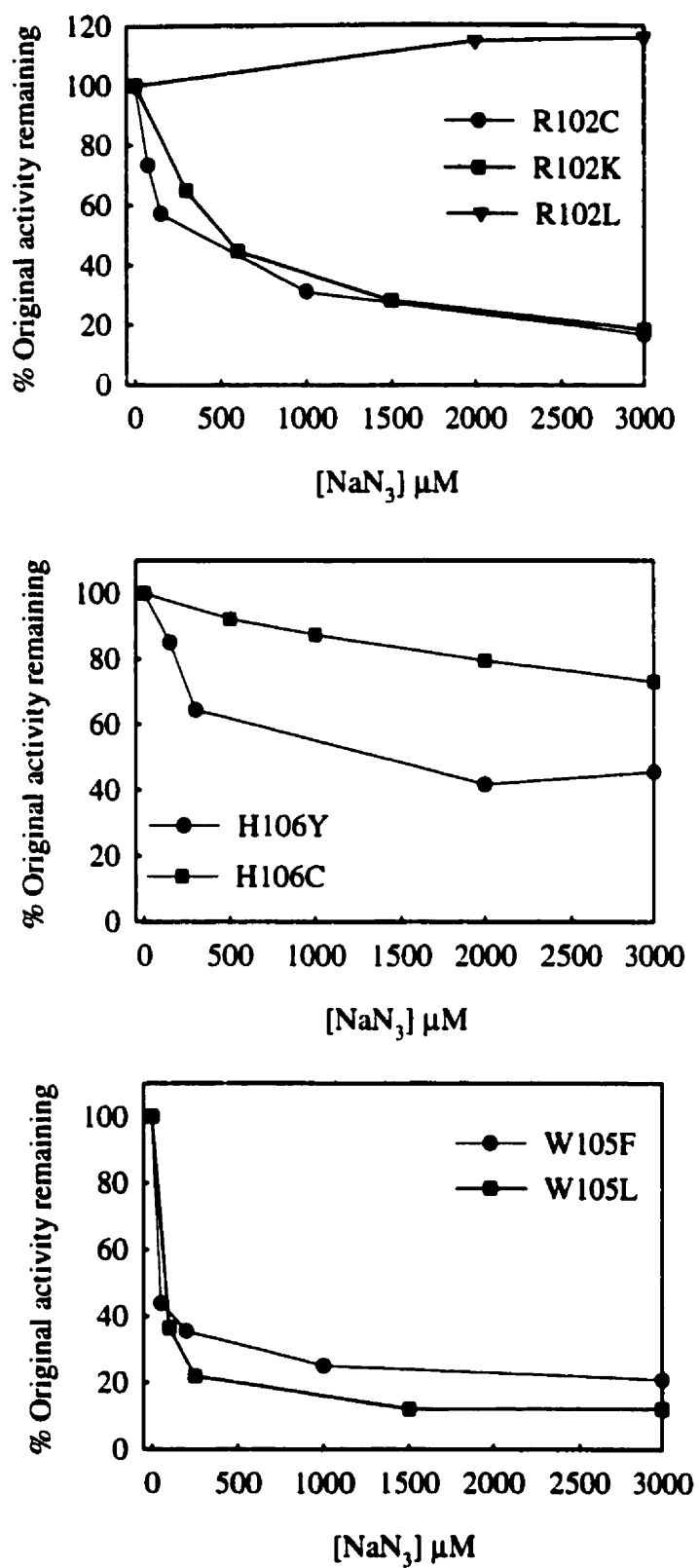


Figure 3.4.10B

was not tested for peroxidase inhibition due to the requirement for extremely large concentrations of enzyme in order to achieve reaction rates high enough to study the effects of inhibitor action. Both KCN and  $\text{NaN}_3$  showed similar inhibition patterns for catalase activities for most of the mutants tested. H106Y however, showed lower endpoint inhibition by both inhibitors for this activity, while R102K and W105F showed slightly lower susceptibilities to catalase inhibition by KCN and  $\text{NaN}_3$ , respectively. Results for inhibition of the mutants' peroxidase activities were less consistent. Both H106 mutants showed decreased susceptibility to peroxidase inhibition by KCN and  $\text{NaN}_3$ , with only about 20% inhibition of H106Y observed in the presence of 3 mM  $\text{NaN}_3$ . Conversely, the W105 mutants showed apparently enhanced sensitivity to KCN as a peroxidase inhibitor, showing almost complete inactivation at only 75  $\mu\text{M}$  KCN. Of the R102 mutants, R102C showed lower susceptibility to KCN compared to the other R102 mutants, and no inhibition of peroxidase activity by  $\text{NaN}_3$  at concentrations up to 3mM. Lack of susceptibility of some mutants to peroxidase inhibition by KCN or  $\text{NaN}_3$  may be rationalized as being partially due to the initial inhibition of compound I formation, the first step in the catalytic reaction cycle in which  $\text{H}_2\text{O}_2$  reacts with the heme iron, which is a common step to both catalase and peroxidase. Secondly, steric and charge effects probably also play a role in inhibition of both activities, but more so in the case of peroxidase, as the larger azide molecule is apparently much less an effective inhibitor in several cases compared to cyanide (Fig 3.4.10).

### **3.4.3c. Effect of KCN on EcHPI mutants as a heme ligand**

EcHPI mutants were titrated with increasing amounts of KCN, and the resultant spectral shifts, indicating formation of low-spin EcHPI-cyanide complexes, were followed spectrophotometrically at appropriate wavelengths in the Sorêt region, as was previously done for EcHPI and MtHPI wild type enzymes. The H267Y mutant was not titrated, as the heme/protein ratio was so low that large amounts of protein would have

been required. Changes in absorbance of the difference spectra maxima and minima in the Sorêt region were then plotted as a function of KCN concentration, as shown in Figure 3.4.11. Linear regression on the double reciprocal plots of these data was done and the estimated equilibrium dissociation constants of cyanide binding to the mutants are summarized in Table 3.4.5. R102L, R102C, and H106C mutants all showed increases in estimated  $K_d$  compared to wild type EcHPI, indicating a much lower affinity for HCN binding at the active sites of these mutants. Conversely, the remaining mutants all showed slight increases in apparent cyanide binding affinity of their active sites compared to EcHPI wild type. H106Y and the W105 mutants had estimated  $K_d$  values similar to that determined for MtHPI (7  $\mu$ M). A slight increase in binding affinity could be rationalized in the case of R102K, as this modification results in no net change in charge in the active site. Increased cyanide binding by the H106Y and W105 mutants may be as a result of substantial restructuring of side chain conformations and/or changes in hydrogen bonding interactions in the active site, as it appears that steric constraints in the vicinity of the heme alone are not sole determinants of cyanide binding affinity.

#### **3.4.3d. Determination of sulfhydryl groups in H106C and R102C mutants**

Free sulfhydryl groups were quantitated for the cysteine replacement mutants H106C and R102C. H106C, when reacted with DTNB, indicated a sulfhydryl/subunit ratio of  $0.06 \pm 0.02$ . Similarly, R102C, when reacted with DTNB, indicated a sulfhydryl/subunit ratio of  $0.35 \pm 0.19$ . The same ratio for the EcHPI wild type enzyme was  $0.12 \pm 0.12$ . Based on these data, it may be assumed that cysteine residues introduced into the active site of EcHPI are either not reactive with DTNB, which may not be able to penetrate to the active site due to steric constraints, or that such cysteine residues have oxidized side chains.

**Figure 3.4.11** Primary plots of equilibrium spectrophotometric cyanide binding titrations of EcHPI mutants.

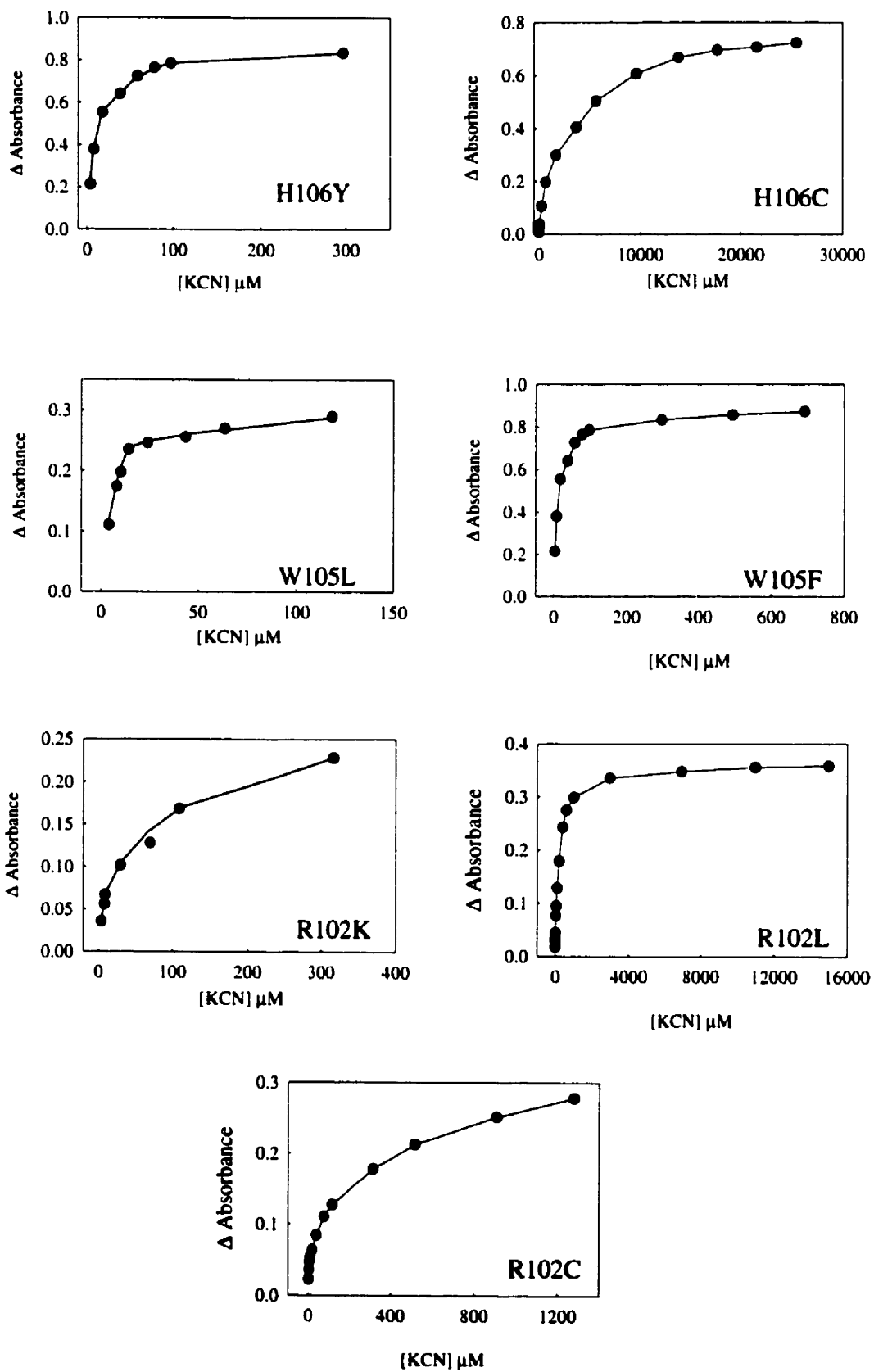


**Table 3.4.5.** Estimated equilibrium dissociation constants for EcHPI mutant-cyanide complexes.

<b>Mutant</b>	<b><math>K_d</math> (<math>\mu\text{M}</math>)</b>
<b>Wild type</b>	<b>50</b>
R102K	16
R102L	100
R102C	>180
H106Y	12.5
H106C	1,000
W105F	12.3
W105L	7.1

#### 3.4.4. Further characterization of W105 mutants

The observation that the W105 mutants are essentially inactive as catalases, but retain the full peroxidase activities of, and are kinetically similar to, wild type EcHPI, merited their further investigation with regard to their similarity to canonical peroxidase enzymes. Peroxidases react with  $H_2O_2$  to form a very stable peroxide-enzyme complex known as compound I, characterized as an oxoferryl species in which one electron from  $H_2O_2$  contributes to the oxygen-heme iron double bond, while a second electron contributes to form a  $\pi$ -cation radical delocalized on the porphyrin ring (Dolphin *et al.*, 1971). Compound I species of peroxidases have optical absorbance spectra distinct from that of the ferriprotoporphyrin forms of the enzymes (resting enzymes), characterized by a slight red shifting and reduced intensity of their Sorêt bands. Figure 3.4.12 compares the spectra of EcHPI, W105F, W105L, and commercial horseradish peroxidase, in the presence of glucose oxidase and glucose, which provides constant generation of low levels of  $H_2O_2$ . EcHPI wild type enzyme shows very little perturbation of the original spectrum during a 15 min incubation in the presence of  $H_2O_2$ , apart from a slight red shift of the leading edge of the Sorêt band (Fig 3.4.12A). In comparison, W105F, W105L, and commercial horseradish peroxidase showed red-shifting and significant declines in absorbance intensities of their Sorêt bands, as well as increases in absorbance intensity in the visible regions of the spectrum between 500 and 700 nm (Fig 3.4.12 B,C, and D). Subsequent incubations of W105F, W105L, or horseradish peroxidase with  $H_2O_2$  (from the glucose oxidase/glucose system) at room temperature, resulted in no further change of the spectra for periods of up to 24h. These data indicate that the W105 mutants form stable compound I-like species similar to those of canonical peroxidases.

During incubation of W105 mutants with glucose oxidase/glucose, the capacity for the compound I formed to react with the peroxidatic substrate ABTS was also evaluated, as is shown in figure 3.4.13. Under these conditions, ABTS oxidation was

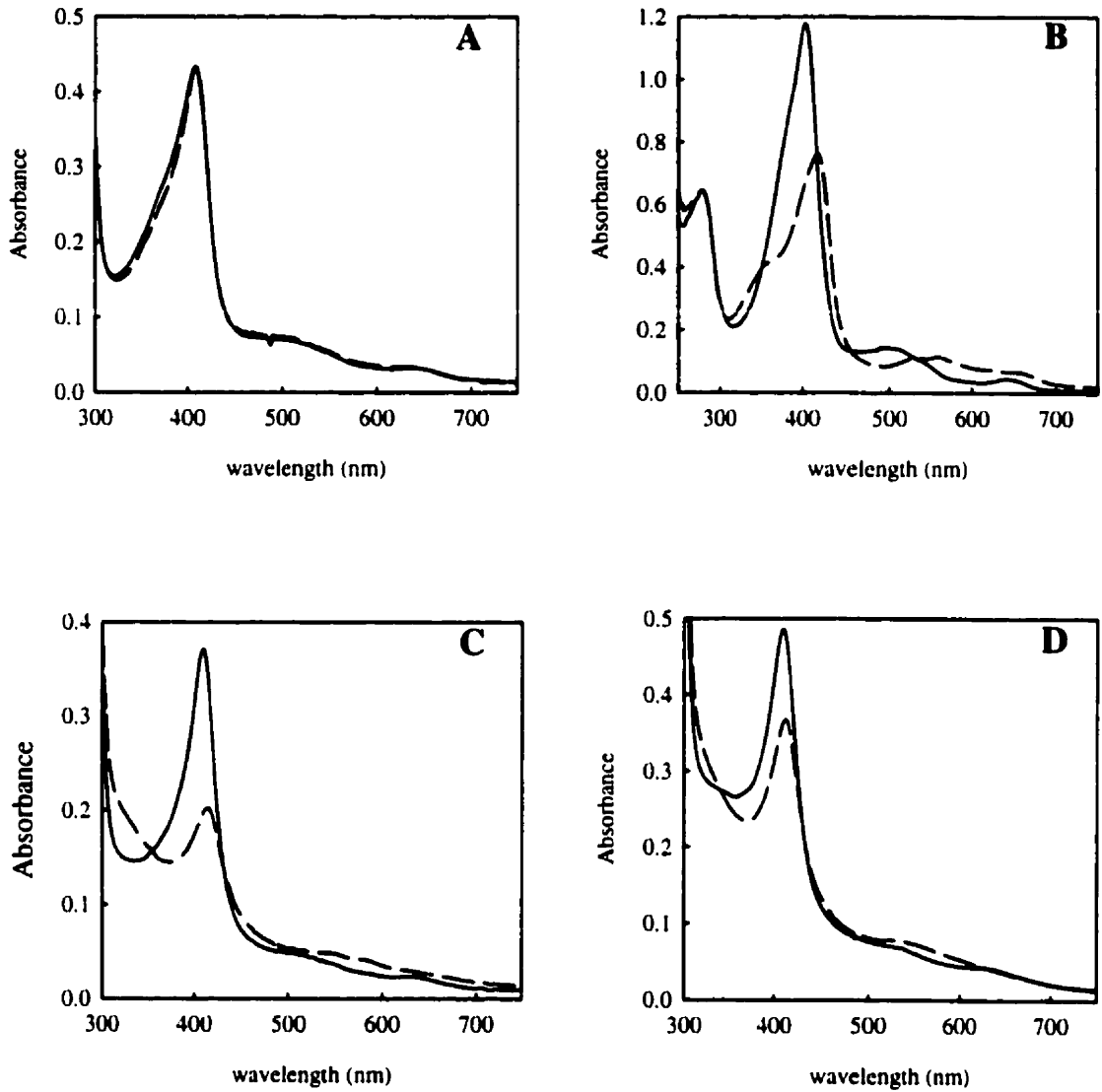


**Figure 3.4.12.** Effect of  $\text{H}_2\text{O}_2$  on the spectra of EchPI, horseradish peroxidase, and W105 mutants. Spectra of purified EchPI (A), commercial horseradish peroxidase (B), W105F (C), and W105L (D) in the absence (solid lines) or presence (broken lines) of  $\text{H}_2\text{O}_2$  following 15 min of constant generation from glucose oxidase/ glucose.

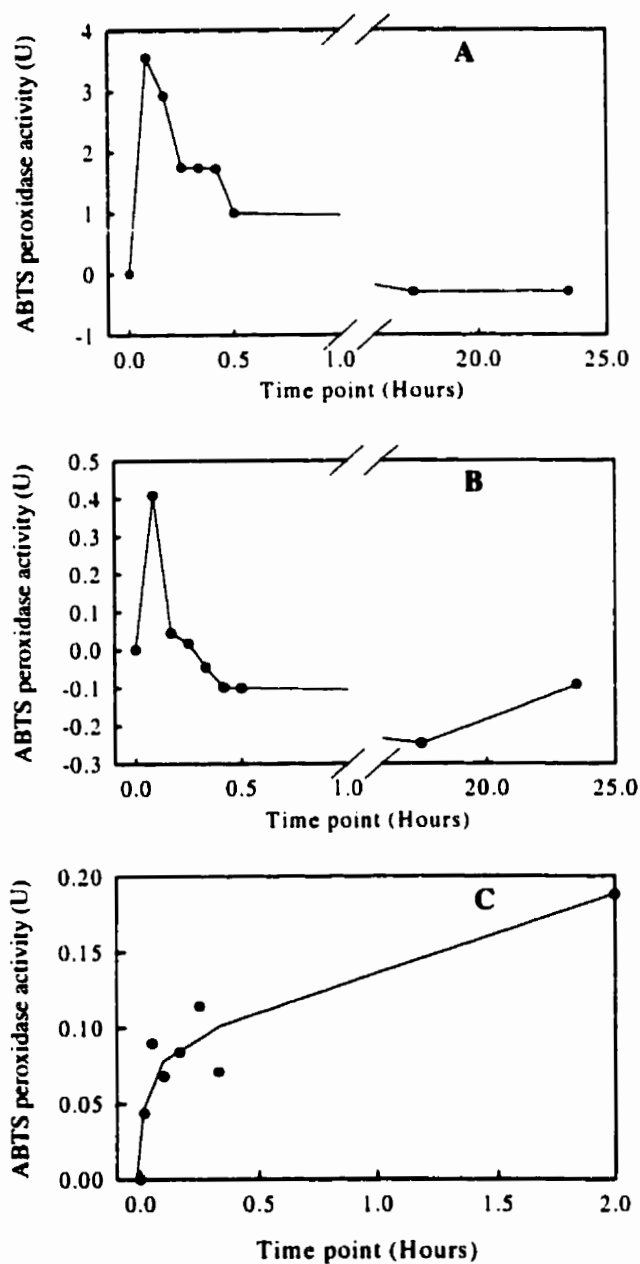


**Figure 3.4.13.** ABTS peroxidase activity of W105 mutants primed by  $H_2O_2$ . Purified W105F(A), W105L(B), or horseradish peroxidase (C) (1-3 mg) were incubated with glucose oxidase/ glucose in 1 ml final volumes, and 20  $\mu$ l aliquots of the reaction mixtures were withdrawn at indicated time points and assayed for ABTS peroxidase activity in 1 ml potassium phosphate buffer, pH 6.0, 05 mM ABTS. Estimated line of best fit for (C) was drawn manually.

maximal for both W105F and W105L between 0- 5 minutes of initiating the reaction with glucose, following which, the initial ABTS oxidation rate declined continuously, and eventually reached baseline values after about 30 min. This result could be due to some inactivation of the mutant enzymes by the generated peroxide, or due to the decay of a radical component of the putative compound I species, such as a porphyrin radical or possibly a radical localized on a side chain in the vicinity of the heme. When the W105 mutants were preincubated with increasing concentrations of H<sub>2</sub>O<sub>2</sub> and subsequently assayed for ABTS peroxidase activity, as shown in Figure 3.4.14, enzyme activity increased steadily after the H<sub>2</sub>O<sub>2</sub> concentration had surpassed about 50 μM, and continued to increase as a function of [H<sub>2</sub>O<sub>2</sub>] to a concentration of about 1 mM, at which point maximum activity had been reached. ABTS oxidation by the W105 mutants is thus [H<sub>2</sub>O<sub>2</sub>] dependent, and can be carried out by W105F or W105L initially primed with H<sub>2</sub>O<sub>2</sub> alone.

### **3.5. Construction and characterization of other EcHPI variants**

#### **3.5.1. Introduction**

In addition to the mutants constructed and purified, two further EcHPI variants were constructed. A region in the *E. coli katG* gene encoding amino acids 197-226 has no corresponding region of alignment with the coding sequence of cytochrome *c* peroxidase, and as such, may be an extraneous loop structure in the EcHPI enzyme. To test whether there is a structural requirement for this putative loop in EcHPI, the sequence coding for amino acids 197-226 was deleted by digestion with the restriction endonuclease *Hpa* I, in subclone I (pAH2) of the *E. coli katG* gene, and subsequently religated and recloned to construct the *E. coli katG* loop deletion variant.

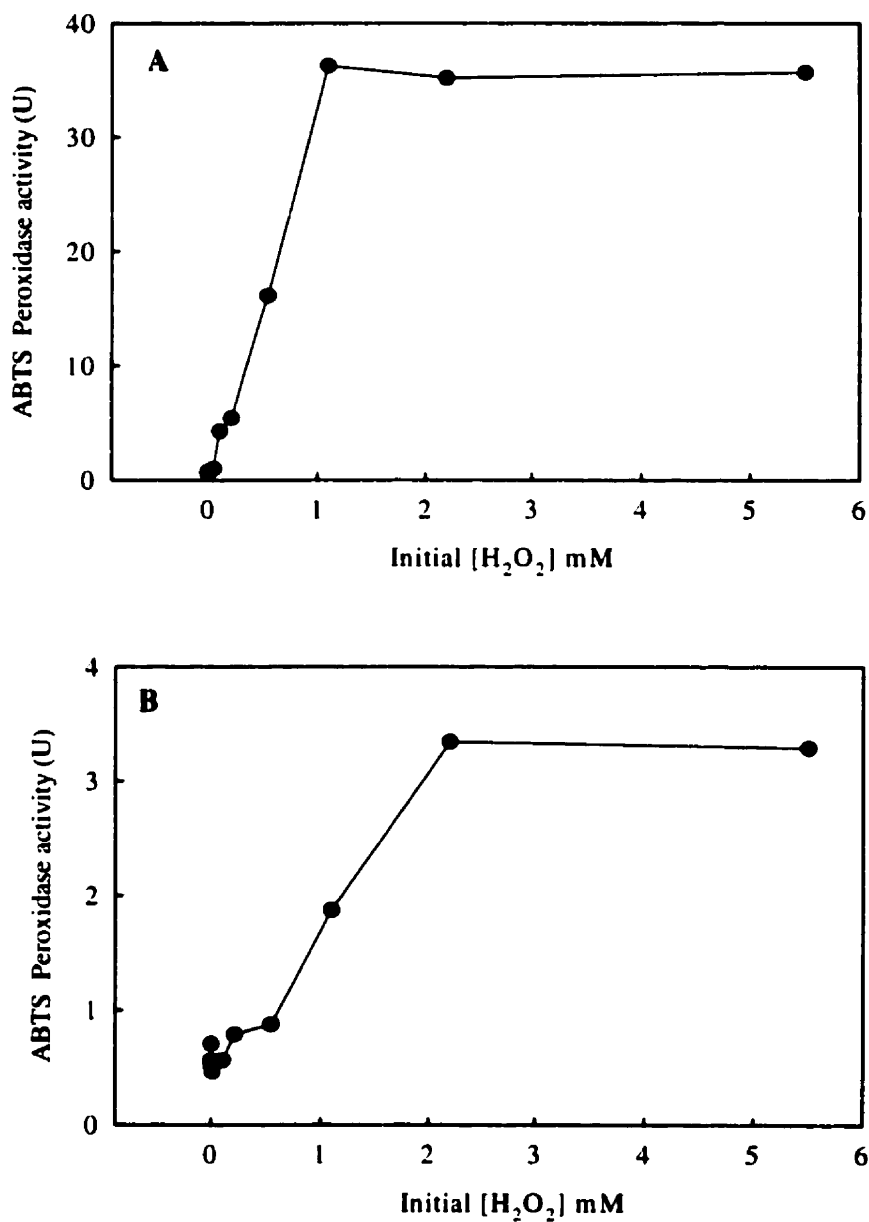


**Figure 3.4.14.** Effect of  $H_2O_2$  preincubation on the ABTS peroxidase activity of W105 mutants. Purified W105F(A) or W105L(B) samples (1-3 mg) were preincubated ( $\approx 1$  min) with increasing  $H_2O_2$  concentrations in 50mM potassium phosphate buffer, pH 7.0, and then assayed for ABTS peroxidase activity by removing 20  $\mu$ l aliquots of the preincubation mixture to the peroxidase assay mixture.

Simplifying protein purification procedures has been achieved by various techniques, but more recent approaches have introduced the initial step of modifying the coding sequences of proteins in order to make the gene product itself easier to purify. One such approach is to append a short DNA sequence to the ends of the gene encoding either the amino or carboxyl terminal ends of the protein of interest, which (for the amino terminal ends) codes for a start codon and a short sequence including six adjacent histidine residues in the same reading frame as for the rest of the coding sequence. This polyhistidine "tag" allows the protein to specifically chelate  $\text{Ni}^{2+}$  ions, which may be linked to a column chromatographic support matrix, in order to effect purification. In an attempt both to simplify the purification of EcHPI, and to produce more homogeneous preparations of the enzyme, a polyhistidine-tagged variant of the *E. coli katG* gene was constructed. To introduce the in-frame sequence encoding the start codon and the polyhistidine tag, the *E. coli katG* gene was first mutagenized in subclone III (pAH300) to create a *Pst* I restriction endonuclease site *de novo* near the start codon of the *E. coli katG* gene. This site was then used to insert the polyhistidine encoding DNA fragment on commercial plasmid vector pQE11 into the amino terminal coding end of the *katG* gene. Expression problems with the pQE11 vector necessitated the sequential recloning of the His-tag *katG* gene to plasmid vector pBAD18 (Guzman *et al.*, 1995), and finally back to the original plasmid vector pSK+ as plasmid pAH6-H. The polyhistidine tag sequence introduced 12 additional amino acids, and changed the first four amino terminal residues of the EcHPI protein, leading to an increase in the predicted pI of the protein from 5.06 to 5.55.

### **3.5.2. Characterization of the EcHPI variants**

The overexpression and purification of the putative loop deletion variant was achieved without additional purification problems, despite encoding an EcHPI protein lacking 30 internal amino acids. Overexpression and trial purification of the His-tag

**EcHPI variant was also achieved on a small scale, using a nickel linked resin (NiTA) and eluting the bound protein using a step gradient of imidazole. SDS-PAGE analysis of the purified EcHPI loop deletion variant and the His-tag variant is shown in Figure 3.5.1(B,C). Non-denaturing PAGE analysis for the purified loop deletion variant is also shown in the figure (Fig 3.5.1C). The EcHPI loop deletion variant migrates as one main band with an estimated size of about 77 kDa for SDS-PAGE, and as three distinct bands during non-denaturing PAGE, presumably three different charge isoforms, with different mobilities compared to wild type EcHPI. The smaller apparent subunit size of the loop deletion variant band in SDS-PAGE is consistent with the lack of 30 amino acid residues. The His-tag variant migrates as one main band with an estimated size of only 70 kDa in SDS-PAGE. This aberrant migration pattern may be the result of the introduction of the six histidine residues into the protein subunit, which would all be ionized at the running pH of 8.0, thus increasing the effective electronegativity of the protein molecules. Unfortunately, these results also show that there are a number of contaminating protein species present in the purified His-tag variant sample, especially those of smaller molecular weights, which suggests that purification by this method is not better than that achieved by the usual larger scale protocol employed for wild type EcHPI purifications.**

**Specific activities for catalase of both EcHPI variants were extremely low. The loop deletion variant had a specific catalase activity of  $1.57 \pm 0.25$  U/mg, while that of the His-tag variant was  $114 \pm 11$  U/mg. The loop deletion variant had peroxidase activities of 0.18 U/mg,  $1.3 \times 10^{-3}$  U/mg, and 0.07 U/mg for ABTS, o-dianisidine, and INH substrates, respectively. The optical absorbance spectrum of the purified loop deletion variant is shown in Figure 3.5.2. The quality of the spectra obtained for the loop deletion variant was poor, as the heme/protein ratio of the purified protein was found to be only 0.027, only 5% of that expected for EcHPI wild type (0.51).**

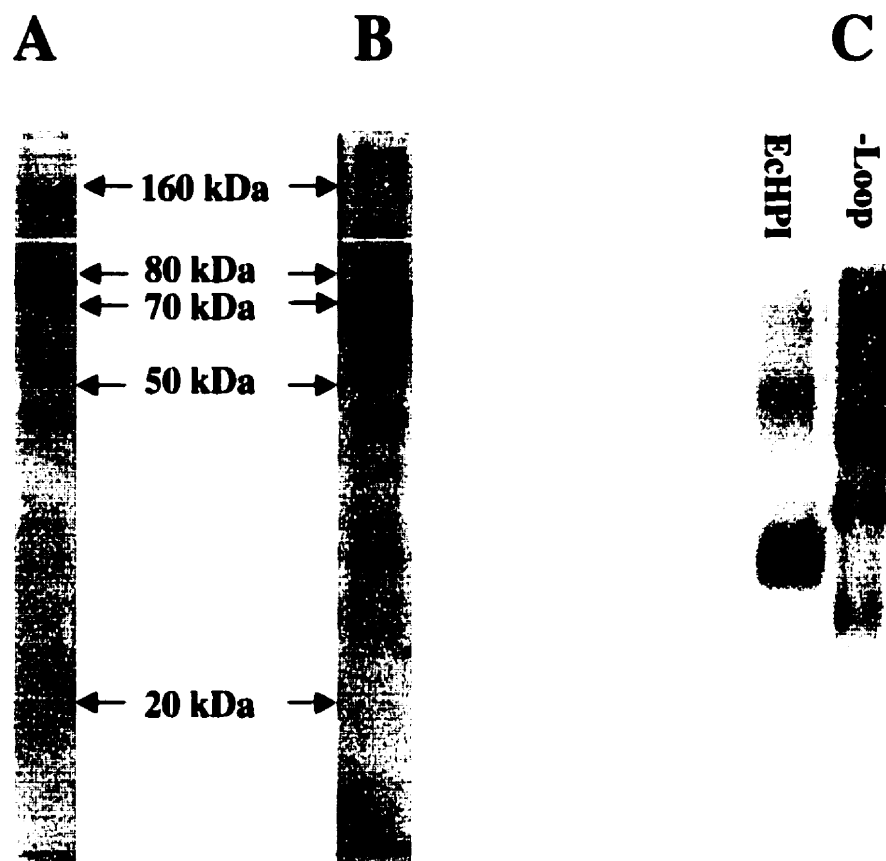


**Figure 3.5.1** A. SDS-polyacrylamide gel electrophoresis analysis of purified EchPI loop deletion variant. B. SDS-polyacrylamide gel electrophoresis analysis of purified EchPI- polyhistidine tagged variant. C. Non-denaturing polyacrylamide gel electrophoresis analysis of purified EchPI loop deletion variant with comparison to EchPI wild type. Samples of approximately 7.5  $\mu\text{g}$  were electrophoresed on 8% gels and stained with Coomassie Brilliant Blue.

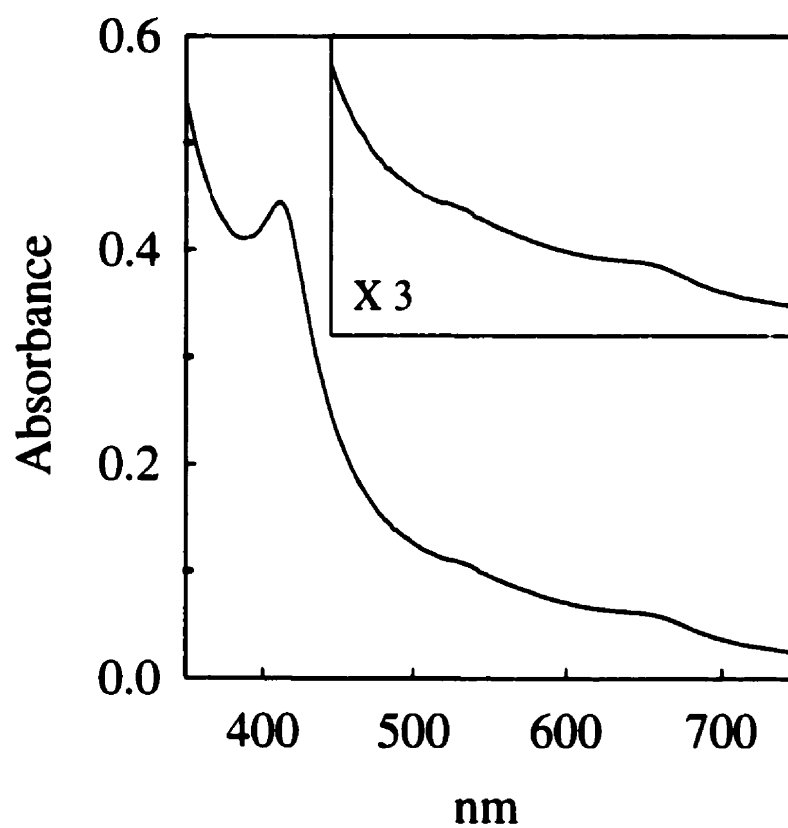


**Figure 3.5.2.** Optical absorbance spectrum of purified EcHPI loop deletion variant. The spectrum between 450-750nm is shown in the inset, expanded by the factor shown.

Despite this, the spectrum for the loop deletion variant shows a Sorêt band at  $\approx 407\text{nm}$  and a clear charge transfer band at  $\approx 660\text{nm}$ , indicating the presence of some heme in the enzyme. Further characterization of the purified His-tag EcHPI variant was not carried out, as the enzyme was less pure and had significantly lower catalase activity than wild type enzyme, thereby negating the point of the construction.

## 4. DISCUSSION

### 4.1. Purification of MtHPI

Overexpression and purification of recombinant MtHPI were achieved from *E. coli* cells harbouring an expression vector. The purification procedure followed was essentially that used for previous purifications of recombinant EcHPI. Other reports detailing purification of recombinant MtHPI have appeared in the recent literature, subsequent to publication of the one described here, and that by Nagy *et al.* (1995). Including the heme precursors ALA and iron in the form of  $\text{FeCl}_3$  was found to increase yields of MtHPI catalase enzyme activity in test cultures, and allowed for consistent quality in yields of MtHPI from larger batch cultures of *E. coli* cells used to prepare purified MtHPI. Similar findings reported by Johnsson *et al.* (1997), in which  $\text{Fe}(\text{NH}_4)_2(\text{SO}_4)_2$  was used to supplement the growth medium, concluded that the addition of iron allowed recovery of MtHPI with a higher proportion of bound heme (heme/protein ratio  $\{A_{407/280}\}$  of 0.67). Interestingly, only addition of  $\text{FeCl}_3$  to the growth medium was found to marginally increase EcHPI catalase activity levels in the test cultures. The results reported may be an indication that the *E. coli* cells have a lower intracellular level of free heme than is optimal for MtHPI assembly in the absence of exogenously added heme precursors, although this level is sufficient for EcHPI assembly. Recent demonstration that a ferric uptake regulon (*fur*) homolog may be involved in regulation of HPI expression in both *E. coli* and *M. tuberculosis* (Pagán-Ramos *et al.*, 1998) could also therefore explain how increasing iron concentration in the medium might result in higher heme content or higher catalase levels in cells.

### 4.2. Biochemical and structural comparison between EcHPI and MtHPI

EcHPI and MtHPI have many similar physico-chemical properties. Both enzymes have nearly identical subunit sizes of about 80 kDa, based on both SDS-PAGE results and from data obtained by ESI-TOF mass spectrometry. Optical absorption spectra for

both purified enzymes show characteristics consistent with high spin, pentacoordinated hemes in the active sites. Kinetic data shows that both enzymes have similar substrate affinities for both  $\text{H}_2\text{O}_2$  and the peroxidase substrate, ABTS. Investigation of inhibition by both KCN and  $\text{NaN}_3$  also shows similar susceptibility of the two enzymes.

Despite the overall similarities of EcHPI and MtHPI, several notable differences between the two enzymes were observed. ESI-TOF mass spectrometry shows that the EcHPI holoenzyme maintains a tetrameric form even while a proportion of the hemes occurring in the molecules are ionized off at higher declustering potentials. This is in contrast MtHPI, which maintains a dimeric form while hemes are ionized off at higher declustering voltages. The results suggest that the EcHPI holoenzyme is either more stable than that of MtHPI, or that EcHPI is functional as a tetrameric enzyme while MtHPI is functional as a dimer.

Despite similar substrate affinities for both catalase and peroxidase activities, MtHPI showed consistently lower maximal reaction rates and turnover rates for both activities; significantly higher specific activities for peroxidase activity using either ABTS or o-dianisidine as substrate, and significantly lower specific activities for catalase activity. It must be borne in mind that both enzymes are highly active catalases, which will influence the effective  $\text{H}_2\text{O}_2$  concentration present during peroxidatic turnover. As EcHPI has a higher catalytic turnover number than MtHPI, one can assume that MtHPI will have a smaller steady state concentration of the  $\text{H}_2\text{O}_2$ -enzyme (compound I) intermediate, and consequently, the peroxidatic kinetic parameters for MtHPI may be underestimated. This may also explain why MtHPI has higher peroxidase specific activities than EcHPI.

EcHPI was shown to have lower binding affinity for cyanide ( $K_d = 55\mu\text{M}$ ), while MtHPI had a binding affinity ( $K_d = 7\mu\text{M}$ ) very similar to those reported for a previous MtHPI purification (Saint-Joanis *et al.*, 1999) and that reported for bovine liver catalase (Nicholls and Schonbaum, 1963). The possibility that access of cyanide to the heme as a

ligand is partially occluded due to steric constraints in the active site is a possibility that would be consistent with the specific activities and kinetics of both enzymes. Both cyanide and  $H_2O_2$  require direct access to the active site in order to coordinate with the heme iron, while evidence exists that peroxidatic substrates may bind some distance from the heme prior to being oxidized (Veitch, 1995).

#### **4.3. Inhomogeneity of EchPI and MthPI preparations**

Non-denaturing PAGE and ESI-TOF analysis of purified EchPI and MthPI samples suggests that typical preparations of the enzymes are inhomogeneous mixtures. EchPI shows two predominant bands or isoforms on non-denaturing PAGE, while MthPI shows three. Interestingly, this pattern is maintained when the samples are analyzed by ESI-TOF mass spectrometry, where the mass spectra at declustering potentials  $\geq 200V$  show EchPI to have two major size components, while that of MthPI shows three. In both cases, the populations of molecular species differ by masses closely corresponding to the mass of a heme or a porphyrin. These data suggest that both HPI preparations are actually inhomogeneous mixtures of dimeric or tetrameric holoenzymes containing either two hemes, one heme, or no hemes, per dimer. These observations may also serve to explain why no HPI enzyme has yet been crystallized, as the formation of protein crystals requires samples of both high concentration and homogeneity (Jones and Stuart, 1992).

#### **4.4. Differential oxidation and binding of isoniazid by EchPI and MthPI**

While expression of *E. coli katG* in *M. tuberculosis* cells has been shown to confer low level susceptibility to INH (Zhang *et al.*, 1993), overexpression of *M. tuberculosis katG* in *E. coli* also leads to low level susceptibility to INH (Zhang *et al.*, 1992). In the latter case, however, cognate target(s) of INH activated by HPI oxidation, such as *M. tuberculosis* InhA enoyl reductase, are absent. While there is some evidence

that suggests that the enoyl reductase of *E. coli* may also bind activated INH (Baldock *et al.*, 1996), it is also possible that differences between EcHPI and MtHPI oxidation of INH to its active form could play a role in exerting cytotoxic effects.

The results of the current study indicate that 1) MtHPI is capable of oxidizing INH to produce free radicals at a significantly higher rate than EcHPI and 2) that MtHPI apparently binds INH with higher affinity than EcHPI. The first observation is based on the results of the INH-NBT reduction assay under conditions of constant peroxide flux. Preliminary kinetic analysis of this reaction for both enzymes showed that MtHPI has similar substrate affinity for, but several times higher turnover, of INH in comparison to EcHPI. NBT reduction coupled with INH oxidation was also demonstrated to be applicable to staining of non-denaturing polyacrylamide activity gels for HPI enzymes, especially MtHPI.

MtHPI was shown to have higher binding affinity for INH than EcHPI by equilibrium spectral titrations with increasing concentrations of INH. This technique had previously been used to compare INH binding affinities for MtHPI and the INH resistant MtHPI mutant S315T (Wengenack *et al.*, 1998). Contrary to that report, the results obtained in this work show no evidence of a sigmoidal binding curve or assumed cooperativity in INH binding to either EcHPI or MtHPI. The estimated dissociation constants for the INH-EcHPI complex at 130  $\mu\text{M}$ , was almost ten times that for the MtHPI enzyme (17  $\mu\text{M}$ ). These data suggest that the EcHPI and MtHPI enzymes have substantially different binding sites for aromatic donor molecules like INH, and provides further evidence that subtle differences between EcHPI and MtHPI are at least partially responsible for MtHPI supporting higher levels of INH oxidation

#### **4.5. EcHPI is predominantly cytoplasmic**

Prior to this study, EcHPI had been localized to the periplasm of *E. coli* cells (Heimberger and Eisenstark, 1988), though more recent evidence suggested that EcHPI

may be primarily cytoplasmic (Brunner *et al.*, 1996). Using known cytoplasmic and periplasmic markers following spheroplasting, glucose-6-phosphate dehydrogenase and alkaline phosphatase, respectively, for comparison, both *E. coli* catalases were found to have distribution patterns typical of a cytoplasmic enzyme. Immunogold labeling *in situ* confirmed an even distribution of the enzyme throughout the cytoplasm. While EcHPI and the monofunctional catalase HPII of *E. coli* are not periplasmic, enterohemorrhagic *E. coli* strain O157:H7 produces a plasmid-encoded catalase as a periplasmic enzyme (Brunner *et al.*, 1996). Other bacteria producing periplasmic and extracellular catalases include phytopathogenic *Pseudomonas syringae* (Klotz and Hutcheson, 1992; Klotz *et al.*, 1995), *Vibrio fischeri* (Visick and Ruby, 1998); *Brucella abortus* (Sha *et al.*, 1994); *Bacillus subtilis* (Naclerio *et al.*, 1995); and *Caulobacter crescentus* (Schnell and Steinman, 1995).

While the intrinsic resistance of *E. coli* cells to INH compared to *M. tuberculosis* may be explained by EcHPI being less efficient in INH oxidation than MtHPI, the cytoplasmic location of EcHPI may also be partially responsible. The drug must pass through both the cell wall and two membranes before coming into contact with a relatively low concentration of the enzyme. A periplasmic or membrane associated localization would provide the enzyme with a greater chance of coming in contact with the drug. Determination of the intracellular location of MtHPI in *M. tuberculosis* is required to help ascertain whether this in fact the case.

#### **4.6. Identification of amino acid residues critical to catalysis of EcHPI**

Various workers have carried out extensive studies on the role of individual amino acid residues in the active sites of common peroxidases, including cytochrome *c* peroxidase (Vitello *et al.*, 1993; Erman *et al.*, 1993) and horseradish peroxidase (Howes *et al.*, 1997; Gilfoyle *et al.*, 1996; Nagano *et al.*, 1996; Newmyer *et al.*, 1996). The high resolution crystal structure for CCP was solved fifteen years ago (Finzel *et al.*, 1984),

while that for HRP only became available recently (Gajhede *et al.*, 1997). Structure-function, as well as biochemical and spectroscopic data, based on the studies of CCP, HRP, and other heme-containing peroxidases, indicates that all share certain fundamental characteristics, including the identities of their key catalytic residues and the axial ligand(s) to the heme iron (Welinder, 1992).

Modifications of the His106, Arg102, and His267 residues of EcHPI were carried out via site-directed mutagenesis to confirm their putative roles as catalytically important (H106,R102) or as proximal heme ligand(H267), based on the alignment of the EcHPI sequence with that of CCP. Variants with H106 changes had reaction rates that were  $10^5$  fold lower than that of wild type EcHPI for catalase, and some 300 times lower than that of wild type EcHPI for peroxidase activity with ABTS as substrate. In comparison, mutation of the analogous His52 of CCP to leucine has been characterized to have its reaction rate reduced by  $10^5$  fold compared to the parent enzyme, essentially abolishing the ability of the enzyme to produce CCP compound I(Erman *et al.*, 1993), and the equivalent mutation in MtHPI (His108Leu) also results in drastic declines in catalase and peroxidase activities (Rouse *et al.*, 1996). Data from these studies thus suggest that H106Y and H106C are effectively inactivated as catalases and have significantly lower peroxidase activities than wild type EcHPI, which is consistent with the role of H106 being the residue involved in initiating base catalysis to form compound I in EcHPI.

EcHPI variants with R102 alterations had reaction rates reduced about two orders of magnitude compared to the wild type enzyme for the catalase reaction, but only about 4-10 fold compared to the wild type for the peroxidase reaction (depending on the peroxidatic substrate tested). In comparison, mutation of the analogous residue Arg48 of CCP to leucine resulted in a decline in rate for the O-O bond scission step of the enzyme during  $H_2O_2$ -compound I formation of an estimated two orders of magnitude (Vitello *et al.*, 1993), while mutation to a lysine residue reduced the rate by only twofold (Erman *et al.*, 1993). Data from the present study suggests that the mutations in EcHPI cause

similar changes in properties as analogous mutations in CCP and MtHPI. One exception is the modification of R102 to lysine in EcHPI which caused reduction of the overall catalytic reaction rate similar to that observed for other R102 mutants and the equivalent variant of MtHPI (Rouse *et al.*, 1996), whereas the R48K variant of CCP is much less affected. The proposed role of R102, like that of R48 in CCP, is the stabilization of compound I (Poulos and Kraut, 1980; Vitello *et al.*, 1993), and modification of the residue to either leucine or cysteine, which are structurally and functionally different, probably limits compound I formation at the O-O bond scission step. The R102K mutant, unlike its CCP analog, seems to be incapable of stabilizing compound I, though it would be expected to be functionally similar to the arginine residue it replaces. Some evidence suggests that a conformational gating step involving movement of positively charged side chains out of the peroxide binding site may be associated with entry of hydrogen peroxide (Vitello *et al.*, 1993). Such a mechanism would make the hydrogen-bonding pattern in R102 mutants important factors in compound I stabilization. The fact that modifications of R102 did not elicit reductions in peroxidatic activity similar to those in catalytic activity indicates that such mutations probably affect formation of compound I, since the rate of peroxidatic oxidation is slow compared to the rate of compound I formation.

The His267Tyr variant of EcHPI was  $10^4$ - $10^5$  fold less active than wild type EcHPI for both catalase and peroxidase activities. This was not unexpected because the H267 is analogous to the proximal heme ligand residue in CCP, H175. Compared to the other active site mutants, His267Tyr also had extremely low levels of heme suggesting that the modification either prevents assembly of the enzyme with heme, or results in an unstable protein structure, making heme loss more likely. A previous study in which random mutations resulting in amino acid substitutions were made in EcHPI, but outside the putative active site, also resulted in the variants having significantly lower levels of heme (Loewen *et al.*, 1990). The absorption spectrum of the His267Tyr variant at high concentrations reveals a small amount of heme with a spectrum similar to wild type

EcHPI, suggesting that heme may still be coordinated by the Tyr side chain, albeit poorly. For all purposes, however, H267Y may be considered to be an inactivated catalase and peroxidase.

#### **4.7. Modulation of catalase versus peroxidase activities in W105 mutants**

The use of site-directed mutagenesis has been instrumental in furthering our understanding of structure-functional relationships in proteins. The understanding of molecular mechanisms of catalysis has been one area in particular in which studies of mutants have been useful in rational redesign of enzymes to either change or modulate enzymatic specificities (Gerlt, 1994). Successes in this regard have included the rational modification of the active site of the bacterial serine protease, subtilisin BPN', into subtiligase, which efficiently ligates esterified peptides in aqueous solutions (Jackson *et al.*, 1994), as well as modification of the ribulose-1,5-bisphosphate carboxylases (RUBISCOs) from *Rhodospirillum rubrum* and *Synechococcus* in which carboxylation activities were greatly reduced at the expense of the oxygenation activities (Gutteridge *et al.*, 1993; Lee *et al.*, 1993). Similar modifications have also been carried out in CCP, in which site-directed mutagenesis allowed the creation of a de novo cation binding site on the periphery of the heme ring, decreasing reactivity of the enzyme toward ferrocyanochrome c, while increasing reactivity toward small molecule substrates (Bonagura *et al.*, 1996)

A significant modulation of enzyme specificity was achieved in EcHPI by modification of Trp105, located in the putative distal heme pocket of the enzyme, to either Phe or Leu. Both mutations essentially abolished catalase activity in the enzyme (at least  $10^3$  fold reduction compared to wild type EcHPI) while the peroxidase activity remained at wild type levels or was increased in the case of the Trp105Phe variant. Reaction of both Trp105Phe and Trp105Leu with  $H_2O_2$  produced a stable compound I species as determined by the absorption spectra. The compound I species was capable of

oxidizing the peroxidase substrate ABTS, with no further  $\text{H}_2\text{O}_2$  addition, suggesting that the W105 mutant variants behave as peroxidases. A variant of CCP analogous to the Trp105Phe variant of EcHPI had a  $k_{\text{cat}}$  decreased by only 2 to 4 fold and a  $K_m$  increased for substrate by the same magnitude (Finzel *et al.*, 1987); similar qualitative effects to those seen for the EcHPI variant. The opposite Phe41Trp mutation of HRP, which would make the HRP active site resemble HPI, however, caused reduction in peroxidatic activity to 5% of wild type levels (Smulevich *et al.*, 1994). Unlike the Trp105 mutant variants of EcHPI however, the analogous CCP mutant also forms a compound I-like, spectrophotometrically observable species, which decays back to the spectrum of resting enzyme very rapidly. The Trp105 mutant variants differ from this enzyme variant in that they exhibit very stable spectra resembling compound I, which are apparently inactive peroxidatically, and perhaps similar to the inactive compound II species of catalases.

The question of how modifying the Trp105 residue in EcHPI leads to the remarkable change in enzymatic specificity obviously must also be addressed. Comparison of the active site structures of CCP and HRP as analogs to wild type EcHPI and the Trp105Phe mutant, respectively, can provide some information. In this regard, analysis of the active sites indicates that the F41 phenyl ring in HRP is both coplanar and occupies the same space as the indole ring of W51 in CCP. This modification could account for the 2 to 3 fold increase in peroxidase activity of the EcHPI variant, perhaps by increasing facility of substrate binding. Changing Trp105 is also conservative enough such that reaction of the enzyme with  $\text{H}_2\text{O}_2$  to form compound I is not greatly affected, which is apparent from the spectral evidence, and suggests that the Trp105 indole ring may therefore have a role in the catalytic reduction of compound I. This also directly implies that catalase-peroxidase enzymes carry out the overall catalytic reaction via a mechanism different from that proposed for monofunctional catalases (Fita and Rossmann, 1985)

Modelling the active site of EcHPI on the known structure of CCP has allowed the proposal of a novel catalytic mechanism for catalase-peroxidases (Fig. 4.1). The formation of catalase-peroxidase compound I proceeds according the steps of 1)  $\text{H}_2\text{O}_2$  entrance and preorientation in the active site, 2) followed by scission of the O-O bond and release of  $\text{H}_2\text{O}$  as has been previously described (Poulos and Kraut, 1980; Fita and Rossmann, 1985). Whereas catalases possess a histidine-asparagine couple that allows for preorientation and reaction with  $\text{H}_2\text{O}_2$ , in catalase-peroxidases this is accomplished by a histidine and an arginine in the same relative positions. The reduction of compound I then proceeds by 3) orientation of the hydrogen peroxide such that hydrogen bonding interactions occur via the imidazole ring of the distal catalytic histidine and the tryptophan indole ring, and 4) abstraction of the hydrogens and an electron from the  $\text{H}_2\text{O}_2$  molecule to reduce the oxoferryl heme, producing one molecule of  $\text{H}_2\text{O}$  and one molecule of  $\text{O}_2$ . Step 3) of the mechanism described above is thus the principal point whereby the catalytic mechanism differs for catalase-peroxidase versus monofunctional catalases. In the former, the His-Trp pair mediates reduction of compound I by  $\text{H}_2\text{O}_2$ , whereas in the latter, a His-Asn pair both mediates oxidation by  $\text{H}_2\text{O}_2$  of the enzyme, and its reduction by  $\text{H}_2\text{O}_2$ .

#### **4.8. Failure in improving purification and homogeneity by His-tag EcHPI**

Modification of EcHPI to include a polyhistidine tag was unsuccessful in achieving the production of a more homogeneous EcHPI protein variant, and did not lead to an improvement in the purity of the enzyme, as was originally intended. Possible reasons for this result include the higher potential for unrelated, untagged proteins to interact with the nickel chromatography resin under native rather than denaturing conditions (Qiagen Inc., 1997), and that the introduction of the polyhistidine tag onto such a large and multimeric protein as EcHPI may partially disrupt quaternary interactions as well as affect the tertiary structure of the protein subunits in the region of

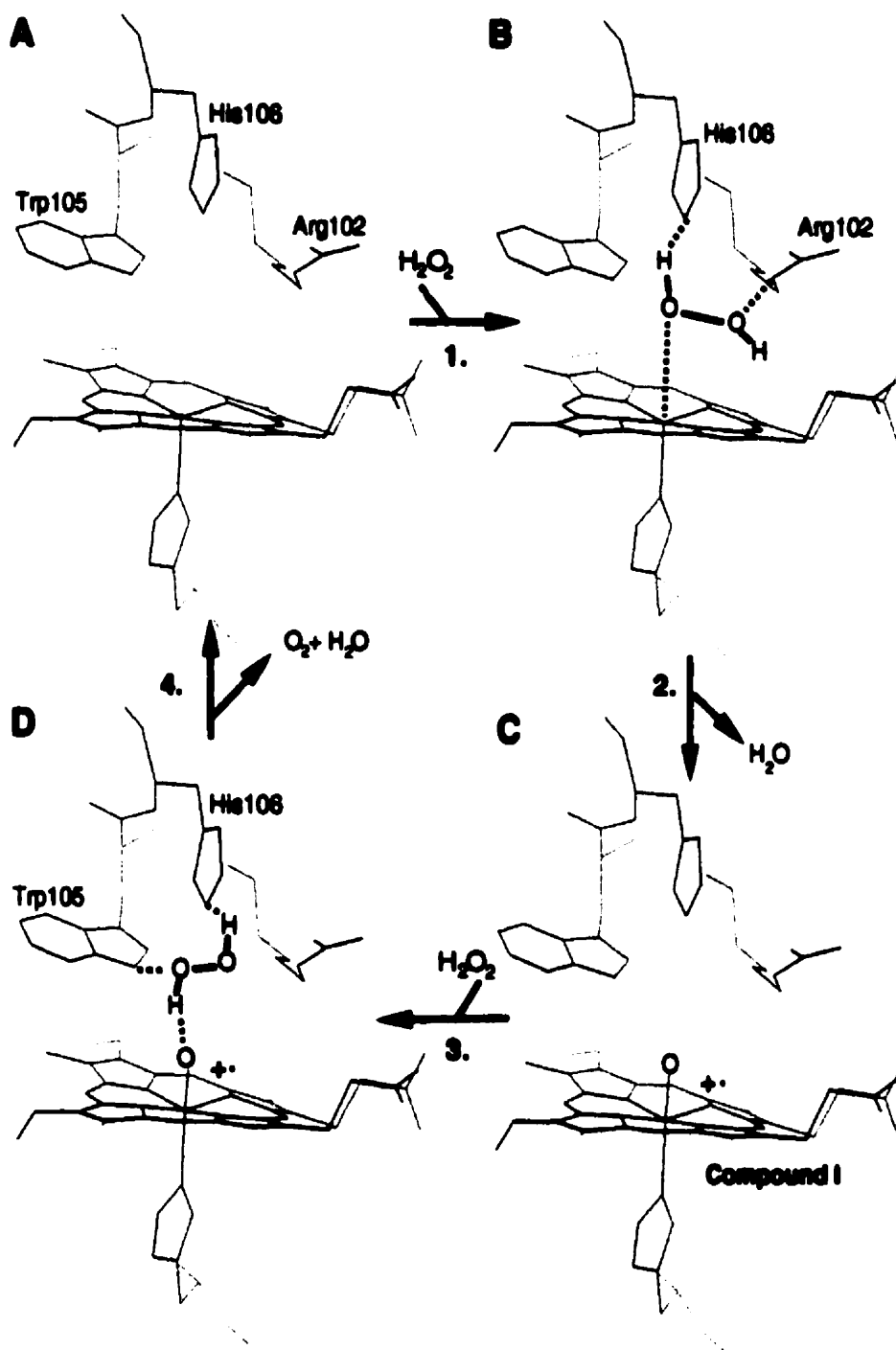


**Figure 4.1** Hypothetical scheme for the mechanism of compound I formation and reduction during the catalytic turnover of catalase-peroxidases. Details are discussed in the text.

the amino terminus. Purifications of higher quality may be achieved using this system if the stringency of the binding and elution conditions are further explored to minimize non-specific binding.

#### **4.9. Future directions**

Several possibilities exist for further experimentation proceeding from the work presented here. More detailed kinetic evaluation of EcHPI and MtHPI should be done in order to establish what the relative rates of compound I formation and decomposition are for both enzymes, as this should help clarify how MtHPI is capable of oxidizing peroxidatic substrates better than EcHPI. A rational site-directed mutagenesis study of MtHPI should also be undertaken in an attempt to target possible aromatic residues that may be in the vicinity of the heme periphery, such as phenylalanines, which have been suggested to play key roles in binding peroxidatic substrates in HRP (Gajhede *et al.*, 1997). The intracellular localization of MtHPI in *M. tuberculosis* cells should also be investigated, in order to determine whether the location of the enzyme may play a role in INH cytotoxicity compared to EcHPI in *E. coli*. The W105 mutant variants should be further investigated to determine how the mutations introduced modulate the enzymatic activities. Studies by electron paramagnetic resonance spectroscopy, Resonance Raman spectroscopy, and other methodologies, should be helpful in providing added evidence for, and information about, the formation of the compound I like species which is long lived in these mutants. Kinetic experiments may also be designed using these and other potential W105 variants in the future, as these variant can readily form the compound I upon reaction with hydrogen peroxide, a feat which has until recently only been possible with catalase-peroxidases using peracetic acid (Regelsberger *et al.*, 1999). Lastly, the utility of certain mutants and variants of EcHPI, such as the putative loop deletion variant, and certain other mutants that are largely devoid of heme, may be realized in the future. These purified proteins may be homogeneous (despite lacking hemes) enough to

provide solutions that could yield protein crystals. Alternatively, expression and purification of EcHPI or MtHPI under conditions in which the heme content of the enzymes is maximized and heme loss is prevented, perhaps by introduction of a heme-protein cross-link, could also be explored as a way to achieve more homogeneous enzyme samples amenable to producing crystals for X-ray diffraction analysis.

## 5. REFERENCES

**Altamirano, M., Marostenmaki, J., Wong, A., FitzGerald, M., Black, W.A., and Smith, J.A.** (1994) Mutations in the catalase-peroxidase gene from isoniazid-resistant *Mycobacterium tuberculosis*. *J. Infect. Dis.* **169**: 1162-1165.

**Ames, B.N.** (1983) Dietary carcinogens and anticarcinogens. *Science* **221**:1256-1264.

**Ames, B.N. and Shigenaga, M.K.** (1992) DNA damage by endogenous oxidants and mitogenesis as causes of aging and cancer. In *Molecular biology of free radical scavenging systems*. (Scandalios, J.G. ed.) pp. 1-22. Cold Spring Harbour Press. New York.

**Auclair, C. and Voisin, E.** (1985) Nitroblue tetrazolium reduction. In *CRC Handbook of Methods for Oxygen Radical Research*. (Greenwald, R.A. ed.) pp.123-132. CRC Press. Boca Raton.

**Ausubel, F.M., Brent, R., Kingston, R.E., Moore, D.D., Seidman, J.G., Smith, J.A., and Struhl, K.** (1989) *Current Protocols in Molecular Biology*. Green Publishing-Wiley Interscience. New York.

**Babior, B.M.** (1981) Oxygen as a weapon: how neutrophils use oxygen to kill bacteria. In *Oxygen and Life: Second BOC Priestley Conference*. Royal Society of Chemistry Special Publication 39. pp.101-108. Royal Society of Chemistry. London.

**Baldock, C., Rafferty, J.B., Sedelnikova, S.E., Baker, P.J., Stuitje, A.R., Slabas, A.R., Hawkes, T.R., and Rice, D.W.** (1996) A mechanism of drug action revealed by structural studies of enoyl reductase. *Science* **274**: 2107-2110.

**Banerjee, A., Dubnau, E., Quemard, A., Balasubramanian, V., Sun Um, K., Wilson, T., Collins, D., de Lisle, G., and Jacobs, W.R. Jr.** (1994) *inhA*, a gene encoding a target for isoniazid and ethionamide in *Mycobacterium tuberculosis*. *Science* **263**: 227-230.

**Bardou, F., Raynaud, C., Ramos, C., Lan elle, M.A., and Lan elle, G.** (1998) Mechanism of isoniazid uptake in *Mycobacterium tuberculosis*. *Microbiology* **144**: 2539-2544.

**Battistoni, A. and Rotillo, G.** (1995) Isolation of an active and heat-stable monomeric form of Cu, Zn superoxide dismutase from the periplasmic space of *Escherichia coli*. *FEBS Lett.* **374**: 199-202.

**Baynton, K.J., Bewtra, J.K., Biswas, N., and Taylor, K.E.** (1994) Inactivation of horseradish peroxidase by phenol and hydrogen peroxide: a kinetic investigation. *Biochim. Biophys. Acta.* **1206**: 272-278.

- Blanchard, J.S.** (1996) Molecular mechanisms of drug resistance in *Mycobacterium tuberculosis*. *Ann. Rev. Biochem.* **65**: 215-239.
- Blattner, F.R., Plunkett, G. III., Bloch, C.A., Perna, N.T., Burland, V., Riley, M., Collado-Vides, J., Glasner, J.D., Rode, C.K., Mayhew, G.F., Gregor, J., Davis, N.W., Kirkpatrick, H.A., Goeden, M.A., Rose, D.J., Mau, B., Shao, Y.** (1997) The complete genome sequence of *Escherichia coli* K-12. *Science* **277**: 1453-74
- Bloom, B.R. and Murray, C.J.L.** (1992) Tuberculosis: Commentary on a reemerging killer. *Nature*(London) **257**: 1055-1063.
- Boguski, M.S., Ostell, J., and States, D.J.** (1992) Molecular sequence data-bases and their uses. In *Protein engineering- a practical approach*. (Rees, A.R., Sternberg, M.J.E., and Wetzel, R. eds.) pp. 57-88. Oxford University Press, New York.
- Bonagura, C.A., Sundaramoorthy, M., Pappa, H.S., Patterson, W.R., and Poulos, T.L.** (1996) An engineered cation site in cytochrome *c* peroxidase alters the reactivity of the redox active tryptophan. *Biochemistry* **35**: 6107-6115.
- Bosshard, H.R., Anni, H., and Yonetani, T.** (1991) Yeast cytochrome *c* peroxidase. In *Peroxidase in chemistry and biology*, Vol. 2. (Everse, J., Everse, K.E., Grisham, M.B. eds.) pp 51-84. CRC Press. Boca Raton.
- Bravo, J., Verdaguer, N., Tormo, J., Betzel, C., Switala, J., Loewen, P.C., and Fita, I.** (1995) Crystal structure of catalase HPII from *Escherichia coli*. *Structure* **3**: 491-502.
- Bravo, J., Mate, M.J., Schneider, T., Switala, J., Wilson, K., Loewen, P.C., and Fita, I.** (1999) Structure of catalase HPII from *Escherichia coli* at 1.9Å resolution. *Proteins* **34**: 155-166.
- Brimnes, J., Mjørner, H., Anthoni, U., Bruun, L., and Houen, G.** (1999) Reactions of N-N and N-O compounds with horseradish peroxidase and peroxidases from *Mycobacterium tuberculosis*. *APMIS* **107**: 555-565.
- Brunder, W., Schmidt, H., and Karch, H.** (1996) KatP, a novel catalase-peroxidase encoded by the large plasmid of enterohaemorrhagic *Escherichia coli* O157:H7. *Microbiology* **142**: 3305-3315.
- Cadenas, E. and Sies, H.** (1984) Singlet molecular oxygen in lipid peroxidation as detected by low-level chemiluminescence in *Oxidative damage and related enzymes*, Life Chemistry Reports Supplement 2 (Rotilio, G. and Bannister, J.V. eds.) pp. 111-120. Harwood Academic Publishers, London.

- Cerutti, P.A.** (1991) Oxidant stress and carcinogenesis. *Eur. J. clin. Invest.* **21**:1-5.
- Chance, B., Sies, H., and Boveris, A.** (1979) Hydroperoxide metabolism in mammalian organs. *Physiol. Rev.* **59**: 527-605.
- Chance, B.** (1950) The reactions of catalase in the presence of the notatin system. *Biochem. J.* **46**: 387-402.
- Chang, J.Y. and Schroeder, W.A.** (1972) Reaction of 3-amino-1,2,4 triazole with bovine liver catalase and human erythrocyte catalase. *Arch. Biochem. Biophys.* **148**: 505-508.
- Chernushevich, I.V., Ens, W., and Standing, K.G.** (1997) Electrospray ionization time-of-flight mass spectrometry. In *Electrospray Ionization Mass Spectrometry*. (Cole, R.B. ed.) pp. 203-234. John Wiley and Sons, Inc. New York.
- Choi, H.J., Kang, S.W., Yang, C.H., Rhee, S.G., and Ryu, S.E.** (1998) Crystal structure of a novel human peroxidase enzyme at 2.0Å resolution. *Nat. Struct. Biol.* **5**: 400-406.
- Christman, M., Morgan, R., and Ames, B.N.** (1989) OxyR, a positive regulator of hydrogen peroxide inducible genes in *Escherichia coli* and *Salmonella typhimurium*, is homologous to a new family of bacterial regulatory proteins. *Proc. Natl. Acad. Sci U.S.A.* **86**: 3484-3488.
- Chung, C.T., Niemala, S.L., and Miller, R.H.** (1989) One-step preparation of competent *Escherichia coli*: transformation and storage of bacterial cells in the same solution. *Proc. Natl. Acad. Sci U.S.A.* **86**: 2172-2175.
- Claiborne, A., Malinowski, D.P., and Fridovich, I.** (1979) Purification and characterization of hydroperoxidase II of *Escherichia coli* B. *J. Biol. Chem.* **254**: 11664-11668.
- Claiborne, A. and Fridovich, I.** (1979) Purification of the o-dianisidine peroxidase from *Escherichia coli* B. *J. Biol. Chem.* **254**: 4245-4252.
- Clare, D.A., Blum, J., and Fridovich, I.** (1984) A hybrid superoxide dismutase containing both functional iron and manganese. *J. Biol. Chem.* **259**: 5932-5936.
- Clare, D.A., Duong, M.N., Darr, D., Archibald, F., and Fridovich, I.** (1984) Effects of molecular oxygen on detection of superoxide radical with nitroblue tetrazolium and on activity stains for catalase. *Anal. Biochem.* **140**: 532-537.
- Cymerman-Craig, J., Rubbo, S.D., Willis, D., and Edgar, J.** (1955) Mode of action of isonicotinic hydrazide. *Nature*(London) **176**: 34-35.

- Davis, B.J.** (1964) Disc electrophoresis II: method and application to human serum proteins. *Ann. N.Y. Acad. Sci.* **121**: 404-427.
- DeLuca, D.C., Dennis, R., and Smith, W.G.** (1995) Inactivation of an animal and a fungal catalase by hydrogen peroxide. *Arch. Biochem. Biophys.* **320**: 129-134.
- Deretic, V., Philipp, W., Dhandayuthapani, S., Mudd, M.H., Curcic, R., Garbe, T., Heym, B., Via, L.E., and Cole, S.T.** (1995) *Mycobacterium tuberculosis* is a natural mutant with an inactivated oxidative-stress regulatory gene: implications for sensitivity to isoniazid. *Mol. Microbiol.* **17**: 889-900.
- DeSandro, V., Dupuy, C., Kaniewski, J., Ohayon, R., Dème, D., Virion, A., and Pommier, J.** (1991) Mechanism of NADPH oxidation catalyzed by horse-radish peroxidase and 2,4-diacetyl-[<sup>2</sup>H]heme-substituted horse-radish peroxidase. *Eur. J. Biochem.* **201**: 507-513.
- Dessen, A., Quémard, A., Blanchard, J.S., Jacobs, W.R.Jr., and Sacchettini, J.C.** (1995) Crystal structure and function of the isoniazid target of *Mycobacterium tuberculosis*. *Science* **267**: 1638-1641.
- Diaz, G.A. and Wayne, L.G.** (1974) Isolation and characterization of catalase produced by *Mycobacterium tuberculosis*. *Am. Rev. Resp. Dis.* **110**: 312-319.
- Dionisi, O., Galeotti, T., Terranova, A.A.** (1975) Superoxide radicals and hydrogen peroxide formation in mitochondria from normal and neoplastic tissues. *Biochim. Biophys. Acta.* **403**: 292-300.
- Dolphin, D., Forman, A., Borg, D.C., Fajer, J., and Felton, R.H.** (1971) Compounds I of catalase and horse radish peroxidase:  $\pi$ - cation radicals. *Proc. Natl. Acad. Sci. U.S.A.* **68**: 614-618.
- Dunford, H.B.** (1991) Horseradish peroxidase: structure and kinetic properties. In *Peroxidase in chemistry and biology, Vol. 2.* (Everse, J., Everse, K.E., Grisham, M.B. eds.) pp 1-24. CRC Press. Boca Raton.
- Ellman, G.L.** (1959) Tissue sulfhydryl groups. *Arch. Biochem. Biophys.* **82**: 70-77.
- Erman, J.E., Vitello, L.B., Miller, M.A., Shaw, A., Brown, K.A., and Kraut, J.** (1993) Histidine 52 is a critical residue for rapid formation of cytochrome c peroxidase compound I. *Biochemistry* **32**: 9798-9806.
- Farr, S.B. and Kogoma, T.** (1991) Oxidative stress responses in *Escherichia coli* and *Salmonella typhimurium*. *Microbiol. Rev.* **55**: 561-585.

**Finzel, B.C., Poulos, T.L., and Kraut, J.** (1984) Crystal structure of yeast cytochrome *c* peroxidase refined at 1.7Å. *J. Biol. Chem.* **259**: 13027-13036.

**Fishel, L.A., Villafranca, J.E., Mauro, J.M., and Kraut, J.** (1987) Yeast cytochrome *c* peroxidase: mutagenesis and expression in *Escherichia coli* show tryptophan-51 is not the radical site in compound I. *Biochemistry* **26**: 351-360.

**Fita, I. and Rossmann, M.G.** (1985) The active center of catalase. *J. Mol. Biol.* **185**: 21-37.

**Fraaije, M.W., Roubroeks, H.P., Hagen, W.R., and Van Berkel, W.J.H.** (1996) Purification and characterization of an intracellular catalase-peroxidase from *Penicillium simplicissimum*. *Eur. J. Biochem.* **235**: 192-198.

**Frei, B., Stocker, R., and Ames, B.N.** (1992) Small molecule antioxidant defenses in human extracellular fluids. In *Molecular biology of free radical scavenging systems*. (Scandalios, J.G. ed.) pp. 23-45. Cold Spring Harbour Press. New York.

**Fülöp, V., Ridout, C.J., Greenwood, C., and Hajdu, J.** (1995) Crystal structure of the di-haem cytochrome *c* peroxidase from *Pseudomonas aeruginosa*. *Structure* **3**: 1225-1233.

**Gajhede, M., Schuller, D.J., Henriksen, A., Smith, A.T., and Poulos, T.L.** (1997) Crystal structure of horseradish peroxidase C at 2.15Å resolution. *Nat. Struct. Biol.* **4**: 1032-1038.

**Gardner, P.R. and Fridovich, I.** (1991) Superoxide sensitivity of the *Escherichia coli* 6-phosphogluconate dehydratase. *J. Biol. Chem.* **266**: 1478-1483.

**Gayathri Devi, B., Shaila, M.S., Ramakrishnan, T., Gopinathan, K.P.** (1978) The purification and properties of peroxidase in *Mycobacterium tuberculosis* H37Rv and its possible role in the mechanism of action of isonicotinic acid hydrazide. *Biochem. J.* **149**: 187-197.

**Gerlt, J.A.** (1994) Protein engineering to study enzyme catalytic mechanisms. *Curr. Opin. Struct. Biol.* **4**: 593-600.

**Gilfoyle, D.J., Rodriguez-Lopez, J.N., and Smith, A.T.** (1996) Probing the aromatic donor-binding site of horseradish peroxidase using site-directed mutagenesis and the suicide substrate phenylhydrazine. *Eur. J. Biochem.* **236**: 714-722.

**Gouet, P., Jouve, H-M., and Didelberg, O.** (1995) Crystal structure of *Proteus mirabilis* catalase with and without bound NADPH. *J. Mol. Biol.* **249**: 933-954.

**Gregory, E.M. and Fridovich, I.** (1974) Visualization of catalase on acrylamide gels. *Anal. Biochem.* **58**: 57-62.

**Grisham, M.B.** (1992) *Reactive Metabolites of Oxygen and Nitrogen in Biology and Medicine*. R.G. Landes Co., Austin.

**Gutteridge, S., Rhoades, D.F., Herrmann, C.** (1993) Site-specific mutations in a loop region of the C-terminal domain of the large subunit of ribulose biphosphate carboxylase/ oxygenase that influence substrate partitioning. *J. Biol. Chem.* **268**: 7818-7824.

**Guzman, L-M., Belin, D., Carson, M.J., and Beckwith, J.** (1995) Tight regulation, modulation, and high-level expression by vectors containing the arabinose P<sub>BAD</sub> promoter. *J. Bacteriol.* **177**: 4121-4130.

**Halliwell, B., and Gutteridge, J.M.C.** (1986) Oxygen free radicals and iron in relation to biology and medicine: some problems and concepts. *Arch. Biochem. Biophys.* **246**: 501-514.

**Halliwell, B.** (1978) Lignin synthesis: the generation of hydrogen peroxide and superoxide by horseradish peroxidase and its stimulation by manganese (II) and phenols. *Planta* **140**: 81-88.

**Heimberger, A. and Eisenstark, A.** (1988) Compartmentalization of catalases in *Escherichia coli*. *Biochem. Biophys. Res. Comm.* **154**: 392-397.  
heme. *J. Biol. Chem.* **265**:13335-43.

**Heym, B., Honoré, N., Truffot-Pernod, C., Banerjee, A., Schurra, C., Jacobs, W.R. Jr., van Embden, J.D.A., Grosset, J.H., and Cole, S.T.** (1994) Implications of multidrug resistance for the future of short-course chemotherapy of tuberculosis: a molecular study. *Lancet* **344**: 293-298.

**Hillar, A., Nicholls, P., Switala, J., and Loewen, P.C.** (1994) NADPH binding and control of catalase compound II formation: comparison of bovine, yeast, and *Escherichia coli* enzymes. *Biochem. J.* **300**: 531-539.

**Hillar, A. and Nicholls, P.** (1992) A mechanism for NADPH inhibition of catalase compound II formation. *FEBS Lett.* **314**: 179-182.

**Howes, B.D., Rodriguez-Lopez, J.N., Smith, A.T., and Smulevich, G.** (1997) Mutation of distal residues of horseradish peroxidase: influence on substrate binding and cavity properties. *Biochemistry* **36**: 1532-1543.

- Ivancich, A., Jouve, H.M., Sartor, B., and Gaillard, J.** (1997) EPR investigation of compound I in *Proteus mirabilis* and bovine liver catalases: formation of porphyrin and tyrosyl radical intermediates. *Biochemistry* **36**: 9356-9364.
- Ivanova, A., Miller, C., Glinsky, G., and Eisenstark, A.** (1994) Role of Rpo (katF) in *oxyR*-dependent regulation of hydroperoxidase I in *Escherichia coli*. *Mol. Microbiol.* **12**: 571-578.
- Jackson, D.Y., Burnier, J., Quan, C., Stanley, M., Tom, J., Wells, J.A.** (1994) A designed peptide ligase for total synthesis of ribonuclease A with unnatural catalytic residues. *Science* **266**: 243-247.
- Jacobson, F., Morgan, R., Christman, M.F., and Ames, B.N.** (1989) An alkyl hydroperoxidase reductase from *Salmonella typhimurium* involved in the defence of DNA against oxidative damage. *J. Biol. Chem.* **264**: 1488-1496.
- Johnsson, K., Froland, W.A., and Schultz, P.G.** (1997) Overexpression, purification, and characterization of the catalase-peroxidase KatG from *Mycobacterium tuberculosis*. *J. Biol. Chem.* **272**: 2834-2840.
- Johnsson, K. and Schultz, P.G.** (1994) Mechanistic studies of the oxidation of isoniazid by the catalase-peroxidase from *Mycobacterium tuberculosis*. *J. Am. Chem. Soc.* **116**: 7425-7426.
- Johnsson, K., King, D.S., and Schultz, P.G.** (1995) Studies on the mechanism of action of isoniazid and ethionamide in the chemotherapy of tuberculosis. *J. Am. Chem. Soc.* **117**: 5009-5010.
- Jones, P. and Wilson, I.** (1978) Catalases and iron complexes with catalase-like properties. In *Metal ions in biological systems* (Sigel, H. ed.) pp. 185-239. Marcel Dekker Inc. New York.
- Jones, E.Y. and Stuart, D.I.** (1992) Methods of structural analysis of proteins. Part 1-protein crystallography in *Protein engineering- a practical approach*. (Rees, A.R., Sternberg, M.J.E., and Wetzel, R. eds.) pp. 3-32. Oxford University Press, New York.
- Keele, B.B., McCord, J.M. Jr., and Fridovich, I.** (1970) Superoxide dismutase from *Escherichia coli* B. A new manganese containing enzyme. *J. Biol. Chem.* **245**: 6176-6181.
- Keilin, D. and Hartree, E.F.** (1955) Catalase, peroxidase, and metmyoglobin as catalysts of coupled peroxidatic reactions. *Biochem. J.* **60**: 310-325.
- Kirkman, H.N. and Gaetani, G.F.** (1984) Catalase: a tetrameric enzyme with four tightly bound molecules of NADPH. *Proc. Natl. Acad. Sci. U.S.A.* **81**: 4343-4348.

- Kirkman, H.N., Galiano, S., and Gaetani, G.F.** (1987) The function of catalase-bound NADPH. *J. Biol. Chem.* **262**: 660-666.
- Kirkman, H.N., Rolfo, M., Ferraris, A.M., Gaetani, G.F.** (1999) Mechanisms of protection of catalase by NADPH: kinetics and stoichiometry. *J. Biol. Chem.* **274**: 13908-13914.
- Klotz, M.G. and Hutcheson, S.W.** (1992) Multiple periplasmic catalases in phytopathogenic strains of *Pseudomonas syringae*. *Appl. Environ. Microbiol.* **58**: 2468-2473.
- Klotz, M.G., Kim, Y.C., Katsuwon, J., and Anderson, A.J.** (1995) Cloning, characterization and phenotypic expression in *Escherichia coli* of *catF*, which encodes the catalytic subunit of catalase isozyme CatF of *Pseudomonas syringae*. *Appl. Microbiol. Biotechnol.* **43**: 656-666.
- Kono, Y. and Fridovich, I** (1982) Superoxide radical inhibits catalase. *J. Biol. Chem.* **257**: 5751-5754.
- Koster, J.F., Slee, R.G., Essed, C.E., and Stam H.** (1984) Lipid peroxidation in the perfused heart in *Oxidative Damage and Related Enzymes*, Life Chemistry Reports Supplement 2 (Rotilio, G. and Bannister, J.V. eds.) pp.121-126 Harwood Academic Publishers, London.
- Kritski, A.L., de Jesus, L.S.R., Andrade, M.K., Werneck-Barroso, E., Vieira, M.A.M.S., Haffner, A, and Riley, L.W.** (1997) Retreatment tuberculosis cases: Factors associated with drug resistance and adverse outcomes. *Chest* **111**: 1162-1167.
- Kunkel, T.A., Roberts, J.D., and Zakour, R.A.** (1987) Rapid and efficient site-specific mutagenesis without phenotypic selection. *Methods Enzymol.* **154**: 367-382.
- Kyte, J. and Doolittle, R.F.** (1982) A simple method for displaying the hydrophobic character of a protein. *J. Mol. Biol.* **157**: 105-32.
- Layne, E.** (1957) Spectrophotometric and turbidometric methods for measuring protein concentrations. *Methods Enzymol.* **3**: 447-454.
- Lee, E.H., Harpel, M.R., Chen, Y.R., and Hartman, F.C.** (1993) Perturbation of reaction-intermediate partitioning by a site-directed mutant of ribulose-bisphosphate carboxylase/ oxygenase. *J. Biol. Chem.* **268**: 26583-26591.
- Levy, E., Eyal, Z., and Hochman, A.** (1992) Purification and characterization of a catalase-peroxidase from the fungus *Septoria tritici*. *Arch. Biochem. Biophys.* **296**: 321-327.

- Liochev, S.I., and Fridovich, I.** (1992) Superoxide radical in *Escherichia coli*. In *Molecular biology of free radical scavenging systems*. (Scandalios, J.G. ed.) pp. 213-229. Cold Spring Harbour Press. New York.
- Loewen, P.C.** (1997) Bacterial catalases. In *Oxidative stress and the molecular biology of antioxidant defenses*. (Scandalios, J.G. ed.) pp. 273-307. Cold Spring Harbour Press. New York.
- Loewen, P.C. and Switala, J.** (1986) Purification and characterization of catalase HPII in *Escherichia coli*.K12. *Biochem. Cell Biol.* **64**: 638-646.
- Loewen, P.C., Triggs, B.L., Klassen, G.R., and Weiner, J.H.** (1983) Identification and physical characterization of a Col E1 hybrid plasmid containing a catalase gene of *Escherichia coli*. *Can. J. Biochem. Cell Biol.* **61**: 1315-1321.
- Loewen, P.C., Switala, J., Smolenski, M., and Triggs-Raine, B.L.** (1990) Molecular characterization of three mutations in *katG* affecting the activity of hydroperoxidase I of *Escherichia coli*. *Biochem. Cell Biol.* **68**: 1037-1044.
- Loewen, P.C., Switala, J., and Triggs-Raine, B.L.** (1985) Catalases HPI and HPII in *Escherichia coli* are induced independently. *Arch. Biochem. Biophys.* **243**: 144-149.
- Loewen, P.C. and Triggs, B.L.** (1984) Genetic mapping of *katF*, a locus that with *katE* affects the synthesis of a second catalase species in *Escherichia coli*. *J. Bacteriol.* **160**: 668-675.
- Maeda, Y., Trautwein, A., Gonser, U., Yoshida, K., Kikiuchi-Tori, K., Homma, T. and Ogura, Y.** (1973) Mössbauer effect in bacterial catalase. *Biochim. Biophys. Acta.* **303**: 230-236.
- Magliozzo, R.S. and Marcinkeviciene, J.A.** (1997) The role of Mn(II)-peroxidase activity of mycobacterial catalase-peroxidase in activation of the antibiotic isoniazid. *J. Biol. Chem.* **272**: 8867-8870.
- Magliozzo, R.S. and Marcinkeviciene, J.A.** (1996) Evidence for isoniazid oxidation by oxyferrous mycobacterial catalase-peroxidase. *J. Am. Chem. Soc.* **118**: 11303-11304.
- Maj, M., Nicholls, P., Obinger, C., Hillar, A., and Loewen, P.C.** (1996) Reaction of *E. coli* catalase HPII with cyanide as ligand and as inhibitor. *Biochim. Biophys. Acta.* **1298**: 241- 249.

- Marcinkeviciene, J.A., Magliozzo, R.S., and Blanchard, J.S.** (1995) Purification and characterization of the *Mycobacterium smegmatis* catalase-peroxidase involved in isoniazid activation. *J. Biol. Chem.* **270**: 22290-22295.
- Markesbery, W.R. and Carney, J.M.** (1999) Oxidative alterations in Alzheimer's disease. *Brain Pathol.* **9**(1): 133-46.
- Mason, R.P.** (1992) Free radical metabolites of toxic chemicals and drugs as sources of oxidative stress. In *Biological consequences of oxidative stress: Implications for cardiovascular disease and carcinogenesis.* (Spatz, L. and Bloom, A.D. eds.) pp. 23-49. Oxford University Press. New York.
- Mdluli, K., Sherman, D.R., Hickey, M.J., Kreiswirth, B.N., Morris, S., Stover, C.K., and Barry, C.E.III.** (1996) Biochemical and genetic data suggest that InhA is not the primary target for activated isoniazid in *Mycobacterium tuberculosis*. *J. Infect. Dis.* **174**: 1085-1090.
- Mdluli, K., Slayden, R.A., Zhu, Y., Ramaswamy, S., Pan, X., Mead, D., Crane, D.D., Musser, J.M., and Barry, C.E. III.** (1998) Inhibition of a *Mycobacterium tuberculosis* beta-ketoacyl ACP synthase by isoniazid. *Science* **280**: 1607-1610.
- Mead, D.A., Skorupa, E.S., Kemper, B.** (1985) Single-stranded DNA SP6 promoter plasmids for engineering mutant RNAs and proteins: synthesis of a 'stretched' preparathyroid hormone. *Nucl. Acids. Res.* **13**: 1103-1118.
- Merchante, R., Pooley, H.M., and Karamata, D.** (1995) A periplasm in *Bacillus subtilis*. *J. Bacteriol.* **177**: 6176-6183.
- Messerschmidt, A. and Wever, R.** (1996) X-ray structure of a vanadium-containing enzyme: chloroperoxidase from the fungus *Curvularia inaequalis*. *Proc. Natl. Acad. Sci U.S.A.* **93**: 392-396.
- Miller, M.A.** (1996) A complete mechanism for steady-state oxidation of yeast cytochrome *c* by yeast cytochrome *c* peroxidase. *Biochemistry* **35**: 15791-15799.
- Morris, S.L., Nair, J., and Rouse, D.A.** (1992) The catalase-peroxidase of *Mycobacterium intracellulare*: nucleotide sequence analysis and expression in *Escherichia coli*. *J. Gen. Microbiol.* **138**: 2363-70.
- Murshudov, G.N., Melik-Adamyanyan, W.R., Grebenko, A.I., Barynin, V.V., Vagin, A.A., Vainshtein, B.K., Dauter, Z., and Wilson, K.S.** (1992) Three dimensional structure of catalase from *Micrococcus lysodeikticus* at 1.5Å resolution. *FEBS Lett.* **312**: 127-131.

- Murthy, M.R.N., Reid, T.J.III, Sicignano, A., Tanaka, N., and Rossmann, M.G.** (1981) Structure of beef liver catalase. *J. Mol. Biol.* **152**: 465-499.
- Naclerio, G., Bacciagalupi, L., Caruso, C., De Felice, M., and Ricca, E.** (1995) *Bacillus subtilis* vegetative catalase is an extracellular enzyme. *Appl. Environ. Microbiol.* **61**: 4471-4473.
- Nagano, S., Tanaka, M., Ishimori, K., Watanabe, Y., and Morishima, I.** (1996) Catalytic roles of the distal site asparagine-histidine couple in peroxidases. *Biochemistry* **35**: 14251-14258.
- Nagy, J.M., Cass, A.E., and Brown, K.A.** (1995) Progress in the characterization of catalase-peroxidase from *Mycobacterium tuberculosis*. *Biochem. Soc. Trans.* **23**: 152S
- Nagy, J.M., Cass, A.E.G., and Brown, K.A.** (1997a) Purification and characterization of recombinant catalase-peroxidase, which confers isoniazid sensitivity in *Mycobacterium tuberculosis*. *J. Biol. Chem.* **272**: 31265-31271.
- Nagy, J.M., Svergun, D., Koch, M.H.J., Cass, A.E.G., and Brown, K.A.** (1997b) Structural characterization of recombinant catalase-peroxidase from *Mycobacterium tuberculosis*. *Biochem. Soc. Trans.* **25**: S617.
- Nakajima, R. and Yamazaki, I.** (1987) The mechanism of oxyperoxidase formation from ferryl peroxidase and hydrogen peroxide. *J. Biol. Chem.* **262**: 2576-2581.
- Newmyer, S.L., Sun, J., Loehr, T.M., and Ortiz de Montellano, P.R.** (1996) Rescue of the horseradish peroxidase His-170→Ala mutant activity by imidazole: importance of proximal ligand tethering. *Biochemistry* **35**: 12788-12795.
- Nicholls, P. and Schonbaum, G.R.** (1963) Catalases. In *The Enzymes, Vol. 8*, 2nd edit., (Lardy, H., Boyer, P.D., and Myrback, K. eds.) pp. 147-225. Academic Press, New York.
- Oakes, J.** (1986) <sup>1</sup>H and <sup>19</sup>F nuclear magnetic resonance investigation of the active site of catalase. *J. Chem. Soc., Faraday Trans.* **82**: 2079-2087.
- Ohlsson, P.I., Yonetani, T., and Wold, S.** (1986) The formation of ES of cytochrome-c peroxidase: a comparison with lactoperoxidase and horseradish peroxidase. *Biochim. Biophys. Acta.* **874**:160-166.
- Pagán-Ramos, E., Song, J., McFalone, M., Mudd, M.H., and Deretic, V.** (1998) Oxidative stress response and characterization of the *oxyR-ahpC* and *furA-katG* loci in *Mycobacterium marinum*. *J. Bacteriol.* **180**: 4856-4864.
- Pearson, M.L.** (1972) The role of adenosine-3',5'-cyclic monophosphate in the growth of bacteriophage lambda. *Virology* **49**: 605-609.

- Pichorner, H., Jessner, G., and Ebermann, R.** (1993) t-BOOH acts as a suicide substrate for catalase. *Arch. Biochem. Biophys.* **300**: 258-264.
- Poitier, N., Donald, L.J., Chernushevich, I., Ayed, A., Ens, W., Arrowsmith, C.A., Standing, K.G., and Duckworth, H.W.** (1998) Study of a noncovalent trp repressor: DNA operator complex by electrospray ionization time of flight mass spectrometry. *Prot. Sci.* **7**: 1388-1395.
- Poulos, T.L., Freer, S.T., Alden, R.A., Edwards, S.L., Skogland, U., Takio, K., Eriksson, B., Xuong, N., Yonetani, T., and Kraut, J.** (1980) The crystal structure of cytochrome c peroxidase. *J. Biol. Chem.* **255**: 575-580.
- Poulos, T.L. and Kraut, J.** (1980) The stereochemistry of peroxidase catalysis. *J. Biol. Chem.* **255**: 8199-8205.
- Qiagen Inc.** (1997) *The QIAexpressionist: A handbook for high-level expression and purification of 6xHis-tagged proteins.* Qiagen Inc. Valencia, California.
- Quemard, A., Dessen, A., Sugantino, M., Jacobs, W.R.Jr., Sacchettini, J.C., and Blanchard, J.S.** (1996) Binding of catalase-peroxidase-activated isoniazid to wild-type and mutant *Mycobacterium tuberculosis* enoyl-ACP reductases. *J. Am. Chem. Soc.* **118**: 1561-1562.
- Rafli, F., Lunsford, P., Hehman, G., and Cerniglia, C.E.** (1999) Detection and purification of a catalase-peroxidase from *Mycobacterium sp.* Pyr-1 *FEMS Microbiol. Lett.* **173**: 285-290.
- Regelsberger, G., Jakopitsch, C., Englender, M., Ruker, F., Peschek, G.A., Obinger, C.** (1999) Spectral and kinetic studies of the oxidation of monosubstituted phenols and anilines by recombinant synechocystis catalase-peroxidase compound I. *Biochemistry* **38**: 10480-10488.
- Reid, T.J.III., Murthy, M.R.N., Sicignano, A., Tanaka, N., Musick, W.D.L., and Rossmann, M.G.** (1981) Structure and heme environment of beef liver catalase at 2.5Å resolution. *Proc. Natl. Acad. Sci. U.S.A.* **78**: 4767-4771.
- Ren, B., Huang, W., Akesson, B., and Ladenstein, R.** (1997) The crystal structure of seleno-glutathione peroxidase from human plasma at 2.9Å resolution. *J. Mol. Biol.* **268**: 869-885.
- Reynolds, E.S.** (1963) The use of lead citrate at high pH as an electron-opaque stain in electron microscopy. *J. Cell Biol.* **17**: 208-212.

- Ritacco, V., Di Lonardo, M., Reneiro, A., Ambroggi, M., Barrera, L., Dambrosi, A., Lopez, B., Isola, N., de Kantor, I.N.** (1997) Nosocomial spread of human immunodeficiency virus-related multidrug resistant tuberculosis in Buenos Aires. *J. Infect. Dis.* **176**: 637-642.
- Rørth, M. and Jensen, P.K.** (1967) Determination of catalase activity by means of the Clark oxygen electrode. *Biochim. Biophys. Acta.* **139**: 171-173.
- Rouse, D.A., DeVito, J.A., Li, Z., Byer, H., Morris, S.L.** (1996) Site-directed mutagenesis of the katG gene of *Mycobacterium tuberculosis*: effects on catalase-peroxidase activities and isoniazid resistance. *Mol. Microbiol.* **22**: 583-92.
- Rozwarski, D.A., Grant, G.A., Barton, D.H.R., Jacobs, W.R.Jr., Sacchettini, J.C.** (1998) Modification of the NADH of the isoniazid target (InhA) from *Mycobacterium tuberculosis*. *Science* **279**:98-102.
- Saikumar, P., Swaroop, A., Ramakrishna Kurup, C.K., and Ramasarma, T.** (1994) Competing peroxidase and oxidase reactions in scopoletin-dependent H<sub>2</sub>O<sub>2</sub>-initiated oxidation of NADH by horseradish peroxidase. *Biochim. Biophys. Acta.* **1204**: 117-123.
- Saint-Joanis, B., Souchon, H., Wilming, M., Johnsson, K., Alzari, P., and Cole, S.T.** (1999) Use of site-directed mutagenesis to probe the structure, function and isoniazid activation of the catalase/peroxidase, KatG, from *Mycobacterium tuberculosis*. *Biochem. J.* **338**: 753-760.
- Sambrook, J., Fritsch, E.F., and Maniatis, T.** (1989) *Molecular Cloning: A Laboratory Manual*. Cold Spring Harbour Laboratory. Cold Spring Harbour Press. New York.
- Sanger, F.S., Nicklen, S., and Coulson, A.R.** (1977) DNA sequencing with chain terminating inhibitors. *Proc. Natl. Acad. Sci. U.S.A.* **74**: 5463-6467.
- Sbarbaro, J.A.** (1997) 'Multidrug'-resistant tuberculosis: It is time to focus on the private sector of medicine. *Chest* **111**: 1149-1151.
- Schnell, S. and Steinman, H.M.** (1995) Function and stationary-phase induction of periplasmic copper-zinc superoxide dismutase and catalase/peroxidase in *Caulobacter crescentus*. *J. Bacteriol.* **177**: 5924-5929.
- Schonbaum, G.R. and Chance, B.** (1976) Catalase. In *The Enzymes, Vol. 13*, 3rd edit., (Boyer, P.D. ed.) pp. 363-408. Academic Press, New York.
- Sevinc, M.S., Maté, M.J., Switala, J., Fita, I., and Loewen, P.C.** (1999) Role of the lateral channel in catalase HPII of *Escherichia coli*. *Protein Sci.* **8**: 490-498.

- Sha, Z., Stabel, T.J., and Mayfield, J.E.** (1994) *Brucella abortus* catalase is a periplasmic protein lacking a standard signal sequence. *J. Bacteriol.* **176**: 7375-7377.
- Sherman, D.R., Mdluli, K., Hickey, M.J., Arain, T.M., Morris, S.L., Barry, C.E.III., and Stover, C.K.** (1996) Compensatory *ahpC* gene expression in isoniazid-resistant *Mycobacterium tuberculosis*. *Science* **272**: 1641-1643.
- Sherman, D.R., Sabo, P.J., Hickey, M.J., Arain, T.M., Mahairas, G.G., Yuan, Y., Barry C.E. III, Stover, C.K.** (1995) Disparate responses to oxidative stress in saprophytic and pathogenic mycobacteria. *Proc. Natl. Acad. Sci. U. S. A.* **92**: 6625-6629.
- Shoeb, H.A., Bowman, B.U. Jr., Ottolenghi, A.C., and Merola, A.J.** (1985) Peroxidase-mediated oxidation of isoniazid. *Antimicrob. Agents Chemother.* **27**: 399-403.
- Sichak, S.P. and Dounce, A.L.** (1986) Analysis of the peroxidatic mode of action of catalase. *Arch. Biochem. Biophys.* **249**: 286-295.
- Sivaraja, M., Goodin D.B., Smith, M., and Hoffman, B.M.** (1989) Identification by ENDOR of Trp191 as the free-radical site in cytochrome *c* peroxidase compound ES. *Science* **245**:738-740.
- Smith, J. and Schrift, A.** (1979) Phylogenic distribution of glutathione peroxidase. *Comp. Biochem. Physiol.* **638**: 39-44.
- Smith, A.T., Du, P., and Loew, G.H.** (1995) Homology modeling of horseradish peroxidase. In *Nuclear magnetic resonance of paramagnetic macromolecules*. (La Mar, G.N. ed) pp. 75-93. Kluwer Academic Publishers. Amsterdam.
- Smith, H.S.** (1977) *Antibiotics in clinical practice, 3rd Edition*. Pitman Medical Publishing Co., Tunbridge Wells, U.K.
- Smith, A.T., Santama, N., Dacey, S., Edwards, M., Bray, R.C., Thorneley, R.N., Burke J.F.** (1990) Expression of a synthetic gene for horseradish peroxidase C in *Escherichia coli* and folding and activation of the recombinant enzyme with Ca<sup>2+</sup> and heme. *J. Biol. Chem.* **265**: 13335-13343.
- Smulevich, G., Paoli, M., Burke, J.F., Sanders, S.A., Thorneley, R.N.F., and Smith, A.T.** (1994) Characterization of recombinant horseradish peroxidase C and three site-directed mutants, F41V, F41W, and R38K, by Resonance Raman spectroscopy. *Biochemistry* **33**: 7398-7407.

**Stadtman, E.R. and Berlett, B.S.** (1998) Reactive oxygen-mediated protein oxidation in aging and disease. *Drug Metab. Rev.* 30(2): 225-43.

**Stallings, W.C., Bull, C., Fee, J.A., Lah, M.S., and Ludwig, M.L.** (1992) Iron and manganese superoxide dismutases: catalytic inferences from the structures. In *Molecular biology of free radical scavenging systems*. (Scandalios, J.G. ed.) pp. 193-211. Cold Spring Harbour Press. New York.

**Stehle, T., Ahmed, S.A., Claiborne, A., and Schulz, G.E.** (1991) Structure of NADH peroxidase from *Streptococcus faecalis* 10C1 refined at 2.16Å resolution. *J. Mol. Biol.* 221: 1325-1344.

**Stern, K.G.** (1936) The constitution of the prosthetic group of catalase. *J. Biol. Chem.* 112: 661-669.

**Storz, G. and Tartaglia, L.A.** (1992) OxyR: A regulator of antioxidant genes. *J. Nutr.* 122(3S): 627-630.

**Switala, J., O'Neil, J.O., and Loewen, P.C.** (1999) Catalase HPII from *Escherichia coli* exhibits enhanced resistance to denaturation. *Biochemistry* 38: 3895-3901.

**Takeda, A., Miyahara, T., Hachimori, A., and Samejima, T.** (1980) The interaction of thiol compounds with porcine erythrocyte catalase. *J. Biochem.* 87: 429-439.

**Tanford, C. and Lovrien, R.** (1962) Dissociation of catalase into subunits. *J. Am. Chem. Soc.* 84: 1892-1896.

**Torriani, A.** (1968) Alkaline phosphatase of *Escherichia coli*. *Methods Enzymol.* 12B:212-218.

**Triggs-Raine, B.L., Doble, B.W., Mulvey, M.R., Sorbey, P.A., and Loewen, P.C.** (1988) Nucleotide sequence of *katG* encoding catalase HPI of *Escherichia coli*. *J. Bacteriol.* 170: 4415-4419.

**Triggs-Raine, B.L. and Loewen, P.C.** (1987) Physical characterization of *katG*, encoding catalase HPI of *Escherichia coli*. *Gene* 52: 121-128.

**Vainshtein, B.K., Melik-Adamyanyan, W.R., Barynin, V.V., Vagin, A.A., Grebenko, A.I., Borisov, V.V., Bartels, K.S., Fita, I., and Rossmann, M.G.** (1986) Three-dimensional structure of the catalase from *Penicillium vitale* at 2.0Å resolution. *J. Mol. Biol.* 188: 49-61.

**van der Walt, B.J., van Zyl, J.M., and Kriegler, A.** (1994) Different oxidative pathways of isonicotinic acid hydrazide and its meta-isomer, nicotinic acid hydrazide. *Int. J. Biochem.* 26: 1081-1093.

- Veitch, N.C.** (1995) Aromatic donor molecule binding sites of haem peroxidases. *Biochem. Soc. Trans.* **23**: 232-40.
- Verentchikov, A.N., Ens, W., Standing, K.G.** (1994) Reflecting time-of-flight mass spectrometer with an electrospray ion source and orthogonal extraction. *Anal. Chem.* **66**: 126-133.
- Vieira, J. and Messing, J.** (1987) Production of single-stranded plasmid DNA. *Methods Enzymol.* **153**: 3-11.
- Visick, K.L. and Ruby, E.G.** (1998) The periplasmic, group III catalase of *Vibrio fischeri* is required for normal symbiotic competence and is induced both by oxidative stress and by approach to stationary phase. *J. Bacteriol.* **180**: 2087-2092.
- Vitello, L.B., Erman, J.E., Miller, M.A., Wang, J., and Kraut, J.** (1993) Effect of arginine-48 replacement on the reaction between cytochrome *c* peroxidase and hydrogen peroxide. *Biochemistry* **32**: 9807-9818.
- Weber, K., Pringle, J.R., and Osborn, M.** (1972) Measurement of molecular weights by electrophoresis on SDS-acrylamide gels. *Methods Enzymol.* **26**: 3-27.
- Weis, S.E., Slocum, P.C., Blais, F.X., King, B., Nunn, M., Matney, G.B., Gomez, E., and Foresman, B.H.** (1994) The effect of directly observed therapy on the rates of drug resistance and relapse in tuberculosis. *N. Engl. J. Med.* **330**: 1179-1183.
- Welinder, K.G.** (1992) Superfamily of plant, fungal, and bacterial peroxidases. *Curr. Opin. Struct. Biol.* **2**: 388-393.
- Welinder, K.G., Mauro, J.M., and Norskov-Lauritsen, L.** (1992) Structure of plant and fungal peroxidases. *Biochem. Soc. Trans.* **20**: 337-340.
- Wengenack, N.L., Uhl, J.R., St. Amand, A.L., Tomlinson, A.J., Benson, L.M., Naylor, S., Kline, B.C., Cockerill III, F.R., and Rusnak, F.** (1997) Recombinant *Mycobacterium tuberculosis* KatG(S315T) is a competent catalase-peroxidase with reduced activity toward isoniazid. *J. Infect. Dis.* **176**: 722-727.
- Wengenack, N.L., Todorovic, S., Yu, L., and Rusnak, F.** (1998) Evidence for differential binding of isoniazid by *Mycobacterium tuberculosis* KatG and the isoniazid-resistant mutant KatG(S315T). *Biochemistry* **37**: 15825-15834.
- Weser, U.** (1984) Oxidation of sulphur containing amino acid residues in some biologically important proteins in *Oxidative damage and related enzymes*, Life Chemistry Reports Supplement 2 (Rotilio, G. and Bannister, J.V. eds.) pp. 87-94. Harwood Academic Publishers, London.

**Winder, F.G.** (1982) Mode of action of the antimycobacterial agents and associated aspects of the molecular biology of mycobacteria. In *The biology of the Mycobacteria*. (Ratledge, C. and Stanford, J. eds.) pp. 353-438. Academic Press. New York.

**Winder, F.G.** (1964) The antibacterial action of streptomycin, isoniazid, and PAS. In *Chemotherapy of tuberculosis*. (Barry, V.C. ed.) pp111-149. Butterworths. London.

**Winder, F.G. and Denneny, J.M.** (1959) Metal-catalyzed auto-oxidation of isoniazid. *Biochem. J.* **73**: 500-507.

**Worthington Enzyme Catalog** (1968) *Peroxidase (Horseradish)*. p 4-69. Worthington Biochemical Corp., Freehold, New Jersey.

**Yanisch-Perron, C., Vietra, J., and Messing, J.** (1985) Improved M13 phage cloning vectors and host strains: nucleotide sequence of the M13mp18 and pUC19 vectors. *Gene* **33**: 103-119.

**Yonetani, T. and Ray, G.S.** (1966) Studies on cytochrome *c* peroxidase. III. Kinetics of the peroxidatic oxidation of ferrocytochrome *c* catalyzed by cytochrome *c* peroxidase. *J. Biol. Chem.* **241**: 700-706.

**Yost, F.J. and Fridovich, I.** (1973) An iron-containing superoxide dismutase from *Escherichia coli*. *J. Biol. Chem.* **248**: 4905-4908.

**Yusifov, E.F., Grebenko, A.I., Barynin, V.V., Murshudov, G.N., Vagin, A.A., Melik-Adamyan, W.R., and Vainshtein, B.K.** (1989) Three-dimensional structure of catalase from *Micrococcus lysodeikticus* at a resolution of 3.0Å. *Sov. Phys. Crystallogr.* **34**: 870-874.

**Zabinski, R.F. and Blanchard, J.S.** (1997) The requirement for manganese and oxygen in the isoniazid-dependent inactivation of *Mycobacterium tuberculosis* enoyl reductase. *J. Am. Chem. Soc.* **119**: 2331-2332.

**Zhang, Y., Heym, B., Allen, B., Young, D., and Cole, S.T.** (1992) The catalase-peroxidase gene and isoniazid resistance of *Mycobacterium tuberculosis*. *Nature*(London) **358**: 591-593.

**Zhang, Y., Garbe, T., and Young, D.** (1993) Transformation with *katG* restores isoniazid-sensitivity in *Mycobacterium tuberculosis* isolates resistant to a range of drug concentrations. *Mol. Microbiol.* **8**: 521-524.

**Zinner, K., Vidigal, C.C.C., Durán, N., and Cilento, G.** (1977) Oxidation of isonicotinic acid hydrazide by the peroxidase system. *Arch. Biochem. Biophys.* **180**: 452-458.

## 6. APPENDIX

**Figure 6.1.** Alignment of amino acid sequences or deduced amino acid sequences of *E. coli* HPI catalase-peroxidase (1), *M. tuberculosis* KatG (HPI) catalase-peroxidase (2), *Saccharomyces cerevisiae* cytochrome c peroxidase (3), and horseradish peroxidase isoenzyme C (4). Residues occurring in 3 or more sequences are identified by letter and placed above the sequences. The alignment is a composite of that of Loewen, 1997 and Welinder, 1992, with further minor refinements done by eye. The numbering is consecutive throughout the sequence starting from the amino-terminal residue of the *S. cerevisiae* cytochrome c peroxidase sequence.

```

1. -----MSTSDDIHNTTATGKCPFHQGGHDQSAGAGTTTRDWWPNQLRVDLLNQHSNRS 60
2. --MPEQHPPITETTTGAASNG-CPVVGHMKYPVEG--GGNQDWWPNRLNLKVLHQNPAVA
3. MTTAVRLLPSLGRTAHKRSLYLFSAAAAAAAAAATFAYSQSQRSSSSPGGGSNHGWNNWG
4. -----

                                     R AWH 120
1. NPLGED---FDYRKEFSKLDYYGLKKDLKALLTESQ---PWWPADWGSYAGLFIRMAWHG
2. DPMGAA---FDYAAEVATIDVDALTRDIEEVMTTSQ---PWWPADYGHYGPLFIRMAWHA
3. KAAALASTTPLVHVASVEKGRSYEDFQKVYNALALKLREDDEYDNYIGYGPVLVRLAWHT
4. -----MQLTPTFYDNSCP NVSNIVRDTIVNELRSD-----PRIAASILRLHFHD

      GT   D  GG   G  RF           P  NA  L           L  P  K           S  ADL   G  180
1. AGTYRSIDGRGGAGRGQRFAPLNSWPDNVSLDKARLLWPIKQKYGQKISWADLFILAG
2. AGTYRIHDGRGGAGGGMQRFAPLNSWPDNASLDKARLLWPKKKYGGKLSWADLIVFAG
3. SGTWDKHDNTGGSYGGTYRFKKEFNDFPSNAGLQNGFKFLEPIHKEFPWISSG-DLFSLGG
4. CFVNGCDASILLDN--TTSFRTEKDAFGNANSARGFPVIDRMKAAVESACPRTVSCADLL

      A           G  G  D  E                                     240
1. NVALENSGFRFTFGFGAGREDVWEPDLVDVNWGDEKAWLTHR-----HPEALAKAPLGATE
2. NCALESMSGFKTFGFGFRVDQWEPDEVYWGKEATWLGDER-----YSGKRDLLENPLAAVQ
3. VTAVQEMQGPKIPWRCGRVDTPEDTT-----PDN-----
4. TIAAQSVTLAGGPSWRVPLGRRDSLQAFLLDLANAN-----

                                     M           VAL  GGHT  GKTH  300
1. MGLIYVNPEGPDHSGEPLS--AAAAIRATFGNMGMNDEETVALIAGGHTLGKTHGAGPTS
2. MGLIYVNPEAPNGNPDMA--AAVDIRETFRMAMNDVETAALIVGGHTFGKTHGAGPAD
3. -----GRLPDADKDADYVRTFFQRLNMNDREV--VALM-GAHALGKTHLK-----
4. -----LPAPFFTLPQLKDSFRNVGLNRSDDLVAL-SGGHTFGKNQCRFIMD

                                     SG  E  WT  P           NF  L  W  360
1. NVGPDPEAAPIEEQGLGWASTYGSVGADAITSGLEVWVWVTPPTQWSNYFFENLFKYEWV
2. LVGPEPEAAPLEQMGLGWKSSYGTGTGKDAITSGIEVWVWVNTPTKWDNSFLEILYGYEWE
3. -----NSGYEGPWGAANNVFTNEFYLNLLNEDWK
4. RLYNF-----SNTGLPDPTLNTTYLQTLRGLCP

      L   A   Q           P                                     R  F  420
1. QTRSPAGAIQFEAVDAP--EII PDPFDPSPKRRKPTMLVTDLTLRFDPEFEKISRRLNDP
2. LTKSPAGAWQYTAKDGAGAGTIPDPFGGGRSPTMLATDLSLRVDPIYERITRWLEHPE
3. LEKNDANNEQWDSKSGY--MMLPTDYSLIQDPKYLIVKEYANDQDKFFKDFSKAFKLL
4. LNGNLSALVDFDLRTPITFDNKYYVNL EEQKGLIQSDQELFSSPNATDTIPLVRSFANST

      A
1. QAFNEAFARAWFKLTHRDMGPKSRYIGPEVPKEDLIWQDPLPQPIYNPTE-QDIIDLKFA 480
2. ELADEFK-AWYKLIHRDMGPVARYLGLPLVPKQTLWQDPVPAVSHDLVGEAEIASLKSQ
3. ENGITFPKDAPSPFIFKTL EEQGL-----
4. QTFNFAFVEAMDRMGNITPLTGTQGQIRLNCRVVNSNS-----

```

## Figure 6.1 (continued)

1. IADSGLSVSELVSVAWASASTFRGGDKRGGANGARLALMPQRDWDVN--AAAVRALPVLE 540  
 2. IRASGLTVSQLVSTAWAAAASSFRGSDKRGGANGGRIRLQPQVGWEVNDPDGDLRKVIRTL  
 3. -----  
 4. -----

1. KIQKESGK-----ASLADIIVLAGVVGVEKAASAAGLSIHVPFAPGRVDARQDQTDI 600  
 2. EEIQESFNSAAPGNIKVSFADLVVLGGCAAIEKAACAAGHNITVPFTPGRTDASQEQTDV  
 3. -----  
 4. -----

1. EMFELLEPIADGFRNYRARLDVSTTESLLIDKAQQLTLTAPEMTALVGGMRVLGANFDGS 660  
 2. ESFAVLEPKADGFRNYLGKGNPLPAEYMLLDKANLLTSAPEMTVLVGGRLVGLGANYKRL  
 3. -----  
 4. -----

1. KNGVFTDRVGVLSNDFVNLDMRYEWKATDESKELFEGRDRETGEVKFTASRADLVFGS 720  
 2. PLGVFTEASESLTNDFFVNLDMGITWEPSPADDGTYQGDGS-GKVKWTGSRVDLVFGS  
 3. -----  
 4. -----

1. NSVLRAVAEYVASSDAHEKFKDFVAAWVKVMNLDRFDLL  
 2. NSELRALVEVYGADDAQPKFVQDFVAAWDKVMNLDRFDVR  
 3. -----  
 4. -----